2021

Development of a Method to Model an Enclosed, Coaxial Carbon Nanotube Speaker with Experimental Validation

Suraj Prabhu
Michigan Technological University, smprabhu@mtu.edu

DEVELOPMENT OF A METHOD TO MODEL AN ENCLOSED, COAXIAL CARBON NANOTUBE SPEAKER WITH EXPERIMENTAL VALIDATION

By

Suraj Madhav Prabhu

A DISSERTATION

Submitted in partial fulfillment of the requirements for the degree of

DOCTOR OF PHILOSOPHY

In Mechanical Engineering-Engineering Mechanics

MICHIGAN TECHNOLOGICAL UNIVERSITY

2021

This dissertation has been approved in partial fulfillment of the requirements for the Degree of DOCTOR OF PHILOSOPHY in Mechanical Engineering-Engineering Mechanics.

Department of Mechanical Engineering – Engineering Mechanics

Dissertation Advisor: *Dr. Andrew Barnard*

Committee Member: *Dr. Jason Blough*

Committee Member: *Dr. Sriram Malladi*

Committee Member: *Dr. Scott Wagner*

Department Chair: *Dr. William W. Predebon*

Table of Contents

List of Figures

Acknowledgements

The success achieved by an individual is never achieved by him alone. It involves hard work from the individual, his family, his mentors, people who have worked before him and luck. It is the same in my case.

Thank you to my parents for cultivating the ethics of hard work and sincerity in me. Thank you, mom, for working hard to support my dreams and ambitions as well as to support our family. Thank you, dad, for teaching me to be bold and never to be afraid of any new challenges in life. Both of you have sacrificed everything for me and I feel the luckiest kid in the world to have you as my parents. I love you 3000! (credits: Tony Stark)

Thank you to my wife. You left your job and agreed to be my partner for life when I was still studying. It takes a lot of courage to do so for someone you knew only for few months. You sacrificed time you could have spent with me because I was always working. I thank you for your love, faith, sacrifice, and support. I love you 3000! (credits: Tony Stark)

Thank you to my advisor. You have been the rock support in my research journey away from home. You guided me to think creatively, motivated me not to give up and cared about me when I was feeling down. Your contribution of time, effort and talent towards my research is the reason I am here today. You are the best advisor a student could have, and I am lucky to be your student. Thank you, Dr. B!!

Thank you to Faurecia, Mr. Jim Egan, and Mr. Charles Shappell. You provided me with an opportunity to apply my knowledge in the actual world and provided me with a platform to build my career successfully. The guidance you provided inculcated in me confidence, maturity and taught me to approach every new challenge with positivity and new outlook. I am grateful for the opportunity to work with you at Faurecia.

Last but not the least, thank you to all my friends, additional family, and my cat who, in their own way have been supporting me and my eccentricities. I love you all!

Abstract

Carbon nanotube (CNT) speakers operate on heat as compared to conventional loudspeakers that operate on vibration. CNT speakers are extremely lightweight, stretchable, flexible and have high operating temperatures. Due to these advantages, CNT speakers are being considered as a viable replacement option for conventional loudspeakers. One such application is the automotive exhaust noise control. The goal of this research is to design an enclosed, coaxial CNT speaker and to develop a modeling method to model this speaker using COMSOL Multiphysics.

As part of this research, an enclosed, coaxial CNT speaker was designed and manufactured for automotive exhaust noise control. The first prototype was a proof of concept that the design is feasible, and the speaker works. Two additional prototypes have been developed to improve the manufacturing feasibility and performance.

The first task undertaken during the modeling method development has been to create COMSOL models that simulated the CNT film temperature oscillation and the corresponding SPL. The simulation results have been compared with a MATLAB model for a planar CNT speaker. In addition, the SPL generated by the coaxial speaker has been compared with the simulated SPL generated by the CNT speaker. In addition, the performance of the coaxial speaker has been simulated in the presence of flow. Generally, good correlation has been observed between the experimental SPL and simulated SPL. The models can be improved with future development of improved material properties.

1 Introduction

1.1 Problem Definition

Sound is a vibration that travels through a transmission medium, such as solid, liquid or gas in the form of pressure disturbances. Sound as music, is pleasing to the listener. However, sound that is irritating or unwanted is termed as noise. Prolonged exposure to noise, even at low volume is harmful to the listener. Also, noise in the vicinity of public buildings such as hospitals causes discomfort. So, it is very important to control and/or attenuate noise.

Noise can be generated by a variety of sources. One of the common noise sources is exhaust noise. We encounter exhaust noise multiple times during our daily life. One source of exhaust noise is automotive exhaust (fig.1(a)). When fuel is combusted in the engine, it releases high temperature gases. Pressure pulsations are introduced in the gases due to alternate intake and combustion of fuel process in the engine. These gases are released into the atmosphere through the tailpipe, known as exhaust gases. The pressure pulsations and flow of the exhaust gases generates exhaust noise in automobiles. The exhaust noise sound pressure profile depends on parameters such as the engine operating condition, quantity of exhaust gases generated, tailpipe design, etc. Comparing with the source-path-receiver paradigm, the sources in this case are the engine and the tailpipe which radiates noise, path is air-borne through the pipe while the receiver are the people around the automobile as well as those driving. Another example of noise in our life is duct noise (fig. 1(b)). Duct can be a HVAC outlet in homes, kitchen, and bathroom vents, etc. In case of duct noise,

source is the duct outlet which again acts as a radiator of sound, path is air-borne through the HVAC pipe, and the receiver are the people in homes and offices. Both these noise sources are extremely irritating and harmful as people spend their day in homes, offices and travelling. Control and attenuation of exhaust and duct noise is done by applying various noise control techniques.

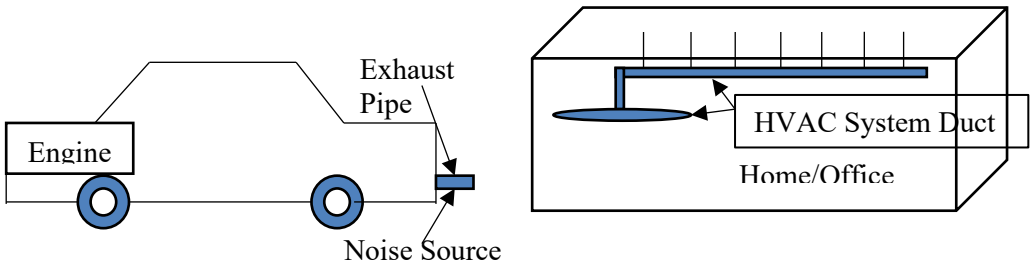

Figure 1: Schematic of automotive exhaust noise source(a). It shows the engine and the exhaust pipe (tailpipe) that are the two major sources of automotive exhaust noise. Schematic of duct noise source present in homes and offices(b). HVAC ducts are the main source of duct noise present in homes and offices due to the flow of air.

Noise control techniques are available to control/attenuate noise present at source, path and receiver. However, in the case of automotive exhaust noise and duct noise, there are certain limitations as to where noise control techniques can be applied in the source-path-receiver paradigm. Automobile engines are designed, manufactured, and fitted based on the type of car, its purpose (everyday use, luxury, supercar, etc.). The engine's location and operating conditions are fixed. Also, the engines run very hot and because of their design, it is very difficult to apply noise control techniques at the engine. With respect to the end of the tailpipe, if the application of any noise control solution obstructs the flow of exhaust gases

into the atmosphere, it creates a backpressure. Backpressure is harmful, especially to the engine and its operation. With respect to the second source, i.e., ducts, noise is radiated from the outlet and the control of this radiated noise with standard noise control techniques has limited potential. The effective use of noise control techniques would be at the travel path of the noise. In both cases, noise is carried to the radiating end by pipes and so, it is very important to focus on pipe acoustics to understand the behavior of acoustic waves inside the pipe. The next sections the current systems in use for control of automotive exhaust noise, carbon nanotube (CNT) speakers, modeling methods used to design and analyze the control systems and CNT speakers, the motivation behind the research and explanation of further chapters.

1.2 Current Noise Control Solutions

1.2.1 Passive Systems

1.2.1.1 Noise Cancellation Mechanisms

Two mechanisms used to attenuation/cancellation of sound are destructive interference and absorption. Expansion and contraction of air results in the generation of sound waves in the form of sine waves. These waves contain positive and negative displacements of the air particles. When the positive displacement of one wave interacts with the negative displacement of the second wave, they are cancelled out by each other. This process is known as destructive interference and the result is wave of zero amplitude (figure 2a). One important condition of this process is that the waves should be out-of-phase with each other, i.e., their phases should differ by 180^{o}.

Sound waves moving through a medium contain energy. These waves interact with the molecules of any medium they travel through. Attenuation of sound using the absorption mechanism makes use of this principle. When sound travels through some dense mediums such as glass wool, fibers, foam, etc., the molecules of the medium absorb the energy of the sound waves. This energy reduction results in the reduction of the sound pressure level (figure 2b). When the energy of the sound is absorbed by the medium, some form of the energy is released as heat.

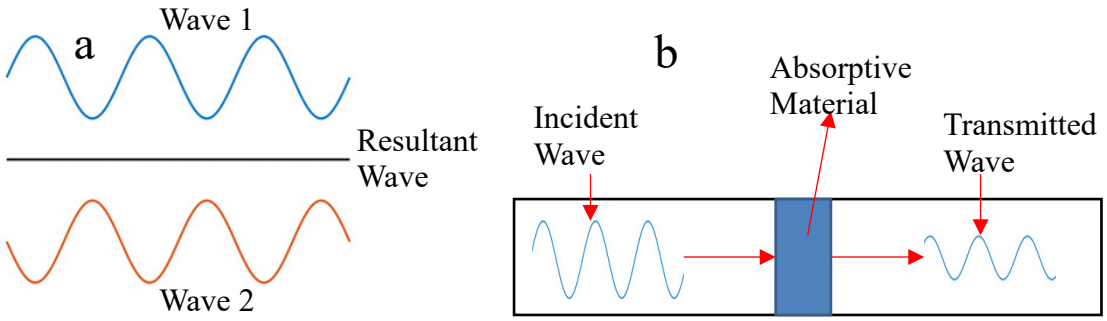

Figure 2: Schematic of destructive interference principle(a). Interaction of two wave of equal amplitude and opposite phase result in a wave of zero amplitude. Schematic of sound attenuation using an absorptive material(b). Energy of sound wave is absorbed, resulting in reduction of sound pressure level.

A passive process does not involve the generation of sound for cancelling the target noise. Both these mechanisms are effective in attenuation/cancellation of noise and can be passive in nature. When noise is reflected onto the original noise, the interaction of the two waves results in noise cancellation. This interaction is based on the destructive interference principle. Noise attenuation using absorptive material does not involve any sound generation by the absorptive material. So, these two mechanisms form the basis of passive noise control units used for automotive exhaust noise control. Expansion chamber,

perforated pipes and mufflers are the main passive control units widely used in automobiles.

1.2.1.2 Expansion Chamber

The effect of changing cross-sectional area and the reflection of sound waves from this area was first documented by Miles in 1944[1] by determining the reflection coefficient due to the discontinuity. Based on this idea, the simplest device used for passive control of noise is an expansion chamber[2]. The design of an expansion chamber consists of sections of different cross-sectional area (figure 3). When sound travels through an expansion chamber, it encounters this sudden change in cross-sectional area of the pipe. The sound waves are reflected from the junction point of this changed area back in the path of the incoming wave. The reflected waves are ideally 180^{o} out-of-phase with the incoming sound wave and attenuates the target sound. Another advantage of the reflected wave is that less sound is transmitted through the expansion chamber on the outlet side. This also reduces the sound pressure level coming through the expansion chamber.

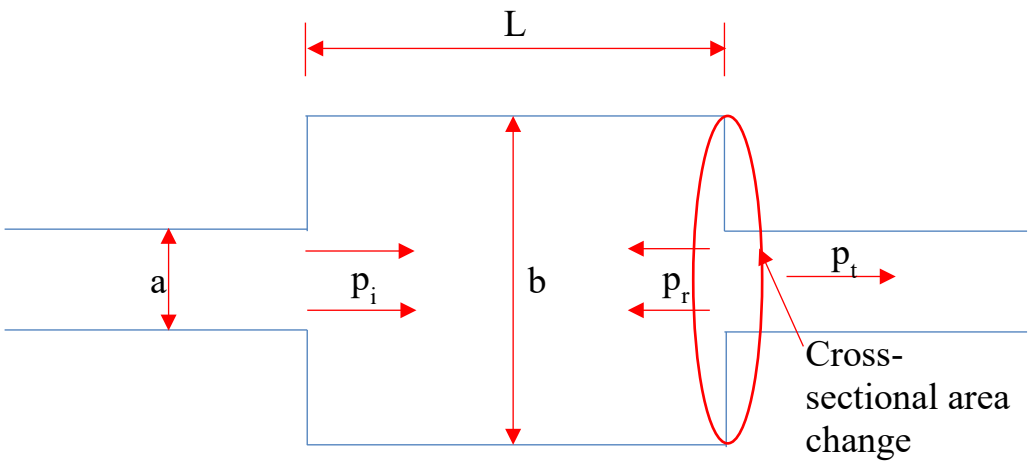

Figure 3: Expansion chamber block diagram. The incoming sound wave is reflected from the section of the chamber that has a change in cross-sectional area back into the chamber.

As shown in the above figure, L is the length of the expansion chamber, a is the diameter of the inlet pipe, b is the diameter of the expansion chamber, p_i is the incoming sound wave, p_r is the reflected sound wave, p_t is the transmitted sound wave. Ideally, performance of an expansion chamber is identified with a term known as transmission loss. Transmission loss in general, describes the reduction in the energy of the sound when it passes through an element travelling from a sound source[2]. Transmission loss of an expansion chamber can be expressed analytically as[153]:

$$TL = 10log_{10}\left\{1 + \frac{1}{4}(m - \frac{1}{m})^2\right\} sin^2 kl_c \quad (1)$$

In the above equation, $m = S_c/S_i$, S_c is the cross-sectional area of the central chamber, S_i is the cross-sectional area of the inlet pipe (when inlet and outlet pipes are same diameter) and l_c is the length of the expansion central chamber.

In case of expansion chambers, the source can be considered as the inlet of the expansion chamber, the element as the expansion chamber with area change and the outlet will be the opposite end of the expansion chamber pipe. The transmission loss of an expansion chamber consists of alternate regions of peaks and rapid falls of the sound pressure level transmitted through the chamber[3]. The nature of the peaks and falls depends on various factors such as length of the chamber, amount of change in the cross-sectional area, length of the pipe before and after the expansion chamber[4]. Several studies have been performed to characterize the transmission loss of expansion chambers[5-9].

Expansion chambers are very effective at low frequencies. At high frequencies, their attenuation performance drops, particularly when the cross-axis chamber dimension is about 82% of the wavelength of the sound[2]. In addition, there is a limitation on the maximum transmission loss that the expansion chamber can achieve while maintaining a small size of the chamber. Design of the expansion chamber is done to achieve broadband attenuation response[2] and the transmission loss characteristics is fixed. So, the unit cannot respond well to any changes in the sound field, affecting its performance. To overcome these shortcomings, another passive control unit used in tandem with expansion chambers, is a perforated pipe.

1.2.1.3 Perforated Pipes

Expansion chambers, as mentioned earlier are more effective at low frequencies and their performance reduces at high frequencies. To improve the transmission loss at high frequencies, perforated pipes are used in tandem with the expansion chambers[10]. The simplest form of the perforated pipe and expansion chamber combination is when the

perforated pipe extends through the expansion chamber (figure 4). This type of a unit is known as a concentric tube resonator (CTR). The transmission loss of a CTR is calculated using the following formula[154]:

$$TL = 20log_{10}\left(\frac{p_1+\rho c v_1}{2p_2}\right) + 10log_{10}\left(\frac{S_o}{S_i}\right) \quad (2)$$

In the above equation, ρc is the characteristic impedance of the medium, p_1 is the sound pressure at the inlet pipe of the CTR, p_2 is the sound pressure at the outlet pipe end of the CTR, S_o *and* S_i are the cross-sectional area of the outlet and inlet pipes respectively.

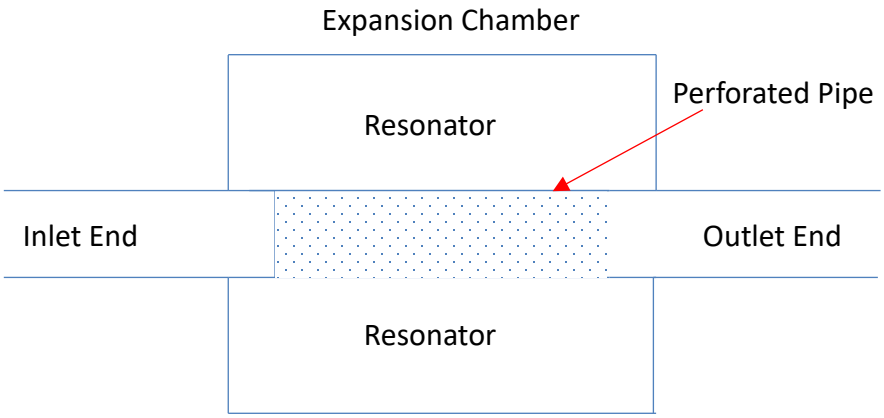

Figure 4: Block diagram of perforated pipe and expansion chamber combination. The inlet pipe extends through the expansion chamber and has perforations in the section inside the expansion chamber.

As shown in above block diagram, the inlet pipe extends through the length of the expansion chamber and comes out of the other side as outlet pipe end. The pipe section inside the expansion chamber has perforations along its length for some predetermined area. The main effect of having a perforated pipe through the expansion chamber is to split

the expansion chamber into two parts. Each part acts as a resonator for the sound traveling through the inlet[10]. The perforations in the pipe provide a path for the sound to travel into the two resonators. The sound in the resonators is then reflected onto the target sound traveling through the interior pipe. The interaction between the reflected sound and target sound results in attenuation of the target sound and the transmission loss is better at high frequencies. Introduction of perforations in pipe of the expansion chamber alters its transmission loss characteristics. For a simple expansion chamber without a pipe extending through it, the transmission loss is a combination of alternate peaks and valleys[3]. However, with the presence of the perforated pipe section, the peaks in the transmission loss rise at certain frequencies while the valleys become more pronounced at higher frequencies[11], which is desirable. The rise in the peaks, which indicate more transmission of sound is not significant compared to the transmission values for a simple expansion chamber[3,11].

The performance of CTRs is highly dependent on the dimensions of the perforate section, namely the diameter of the holes (*d)* and the length of the perforate section (*L*). Neihguk and Prasad performed a study to understand the relation between the perforate dimensions and the acoustic performance of CTRs[11]. They performed simulations on the model of different CTRs in COMSOL Multiphysics by altering the length and perforate hole diameters and validated the simulation results experimentally. The results showed that with increasing L/d ratio and increasing porosity of the perforate section, the transmission loss increased at high frequencies. Many studies have been performed to characterize the acoustic performance of the CTRs, mainly its transmission loss performance[12-17].

Despite the benefit of improved attenuation performance at high frequencies, CTRs face a major problem: backpressure. Whenever there is an obstruction or an alternate path to the flow of exhaust gases in an automobile, backpressure is generated. This backpressure has negative effect on the engine operation. Higher backpressure puts extra load on the engine to push the exhaust gases out into the atmosphere through the tailpipe. So, it becomes crucial to have little-to-zero backpressure due to the introduction of CTRs in the tailpipe. Studies have been conducted to understand the backpressure generated due to different CTR designs[14,17,18]. These studies show that even with design changes, backpressure is generated with the use of CTRs in automobiles. Another disadvantage of CTRs is the limited attenuation performance. The resonator chambers generated are fixed in dimensions and so they provide attenuation in only a fixed frequency range. With any change in the exhaust sound frequency spectrum, the performance of the CTRs drops heavily. So, to make the frequency range of these CTRs more broadband and to reduce the generated backpressure, a combination of perforated pipes and resonant chambers are used. The multiple chamber arrangement is also combined with absorption material to further improve attenuation performance. These two units are collectively known as mufflers or passive systems used for automotive exhaust noise attenuation.

1.2.1.4 Reactive Mufflers

Reactive mufflers primarily use the destructive interference phenomenon to attenuate the exhaust noise in automobiles (figure 5). The reactive muffler consists of multiple chambers which act as resonators and expansion chambers. These dimensions of these chambers are designed to target noise attenuation in a broad frequency range. The inlet and outlet pipes

are generally offset to the longitudinal axis of the dissipative muffler[19]. In addition, the inner pipes of the muffler are perforated to allow exhaust noise to enter the chambers formed inside the shell of the muffler[19]. Having the above design ensures that the exhaust noise is scattered in all possible directions and maximum destructive interference is obtained.

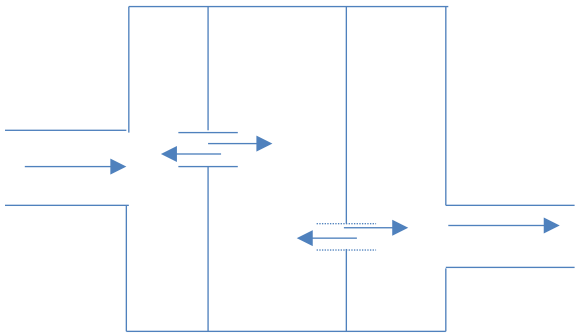

Figure 5: Block diagram of reactive muffler(a)[20]. The inlet and the outlet pipes are set at offset to the longitudinal axis of the muffler. Chambers are created in the muffler shell with baffles and perforated pipes are used to scatter the exhaust noise inside the muffler.

Reactive mufflers are categorized into two types based on the direction of mean flow of the exhaust gases through them: straight-through mufflers and reverse flow mufflers[21]. Straight through mufflers have the exhaust gas flow entering from the inlet and exiting through the outlet on opposite side of the muffler. Reversed flow mufflers have the inlet and outlet pipes on the same side of the muffler[22]. Based on the operational requirements, engine type, exhaust gas profile, either type muffler is used.

The design of a reactive muffler is a precise process as the dimensions set during design are fixed and they determine the working frequency as well as the performance of the

muffler. Achieving destructive interference in a reactive muffler is essential and so, the location of the chambers, its number, the location of the perforate pipes is very important. The chambers and perforated pipes scatter the exhaust noise coming from the engine[21]. The chambers and the perforated pipes redirect the low frequency waves to interact with the target exhaust noise and cancels or attenuates it. So, the primary design parameter is the length of the chamber, which includes the main shell as well as the sub-chambers inside it. The chamber length is designed based on the wavelength of exhaust noise to be cancelled and the varying exhaust gas temperatures[21]. The design of the perforate pipes in the mufflers depend on the length (L) to diameter (d) ratio of the perforate section[11]. Selecting a proper L/d ratio helps to have a high transmission loss for the frequencies of interest as well as broaden the frequency range of operation.

Parameters considered to determine the muffler effectiveness are: insertion loss, transmission loss, size, backpressure and durability[19]. Insertion loss is the reduction in the SPL due to the attachment of the muffler in the tailpipe. A rule of thumb used for insertion loss is that more the number of area discontinuities, higher is the insertion loss[19,30]. The transmission loss of the reactive muffler is an extension of that of a simple expansion chamber. Suitable positioning of the interior chambers and the perforated pipes increases the transmission loss of the muffler. Size of the muffler is a very crucial parameter. There is a limitation of space available in the exhaust system of all automobiles. Adding more components such as mufflers requires precise design and positioning of the components. Further, larger the muffler, heavier it is, and it requires additional supports to hold it in place. These points make it important to have a balance between the muffler size

and its attenuation performance[19]. Reactive mufflers generally tend to be large in size for cancellation of low frequencies and have weak performance at high frequencies.

Backpressure is probably the most important parameter to be considered for the performance of the muffler. Having a high backpressure is undesirable as it adds extra load on the engine, due to creation of static pressure[19]. It is observed that higher the attenuation performance of the reactive muffler, higher is the backpressure generated. If the exhaust gas is forced to change its flow direction more number of times, more backpressure is generated[19]. Several CFD studies have been performed to understand the backpressure generated by the reactive muffler and its relation to the muffler design[23-29]. Reactive mufflers traditionally have high backpressure for the desired high attenuation performance.

To overcome some of above-mentioned disadvantages of the reactive mufflers, a second type of muffler is used known as an absorptive muffler.

1.2.1.5 Absorptive Mufflers

The second type of muffler is known as an absorptive muffler. This muffler makes use of the absorption principle to reduce the energy of the exhaust noise. An absorptive material is used, and exhaust noise is passed through it. The molecules of the material absorb the sound energy, reducing the SPL. The general design of the absorptive muffler is like a reactive muffler. Various chambers are present in the absorptive muffler. The perforated pipes in these chambers are enclosed in a larger steel housing[19]. In between the

perforated pipe and the housing, absorptive material is placed. The sound through the perforations passes through the absorptive material and experiences a reduction in energy.

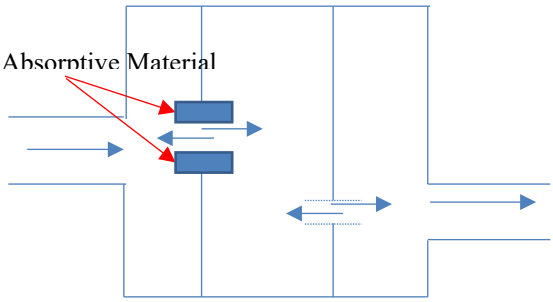

Figure 6: Block diagram of absorptive muffler(a)[20]. The perforated pipes are covered with absorptive material lining to absorb energy from the incoming exhaust noise. The absorptive material is sandwiched between the perforated pipe and external housing.

The major component of an absorptive muffler is the absorptive material used to line the walls of the perforated pipe. Several materials are available for use in the absorptive muffler. One major requirement of the absorptive material is that it allows sound to pass through it while absorbing its energy. This means that the material requires to have some degree of acoustic transparency, possibly a very low value. Second requirement of the absorptive material is that it does not allow the exhaust gases to flow through it relatively easily. Further, as the absorptive material is placed inside the muffler, it absorbs the pressure waves while reflecting a very small amount back[33]. Common types of absorptive materials used are fibres, glass wool, woven glass fiber, porous absorbing materials, porous fibrous materials and advanced metals and ceramics[33-39]. Each of

these materials have some advantages for noise attenuation while having disadvantages related to their durability and environmental impact.

Absorptive mufflers perform better at mid to high frequencies[40,41]. One major advantage of absorptive mufflers over reactive mufflers in the backpressure generated. In absorptive mufflers, the absorptive material provides a straight path for the exhaust gases to flow into and out of the muffler. So, there is very little change in the direction of flow of the exhaust gases and hence very little backpressure. Number of studies have been conducted for determining the backpressure generated in an absorptive muffler[42-47].

In an exhaust system, a combination type muffler is used for passive noise attenuation. In the combination muffler, attenuation is performed using destructive interference and absorption. These processes are done in the same muffler. The muffler has chambers that act as resonators and some perforated pipes are lined with absorptive materials. The advantage of using a combination muffler is improved performance at low, mid and high frequencies. This helps to avoid using separate reactive and absorptive mufflers to broaden the operational frequency range. Also, using a combination muffler helps to reduce the backpressure as the number of direction changes for the exhaust gas flow is reduced.

1.2.1.6 Need for Alternate Noise Control System

Passive noise control systems, though simple in installation and operation have some disadvantages. For reactive mufflers to be effective, multiple chambers and perforated pipes are required. Their presence provides multiple paths to the exhaust gas to change its flow direction. This generates large amount of backpressure, affecting the engine

performance. Also, the reactive muffler has weak performance at high frequencies. The resonant and expansion chamber volumes are frequency dependent. Lower the frequency of target sound, larger is the volume required. This makes the reactive muffler bulky and heavy.

Absorptive mufflers have less backpressure compared to a reactive muffler. However, the prolonged contact of the absorptive material with the exhaust gas causes accumulation of the soot, dust particles, and other particulates on it. Over time, it clogs the pores of the absorptive material, blocking the paths through which sound travels through the absorptive material. A rule of thumb for efficient absorption of sound by a material requires that the thickness of the absorptive material be at least $1/6^{th}$ of the wavelength of the target frequency. For low frequencies, the wavelength of sound is very large. This makes it necessary that the thickness of the absorptive material be large. This increases the size of the muffler, making it bulky and heavy.

Another disadvantage of mufflers is that they are inflexible with respect to the operational frequency. When mufflers are designed, their dimensions decide the frequency range of operation. Any changes in the exhaust noise spectrum, particularly the frequency reduces the attenuation performance of the mufflers. With these disadvantages in mind, active noise control units are used for exhaust noise cancellation.

1.2.2 Active Systems

1.2.2.1 Noise Control Mechanisms

The main working principle of active noise cancellation systems is destructive interference. As mentioned in the passive systems section, destructive interference occurs when two sound waves of equal amplitude, but opposite phase (180^{o}) interact with each other. The positive and negative displacements of the waves cancel each other, and the resultant wave has zero amplitude. The major difference between the passive and active systems is manner in which destructive interference is achieved. Passive systems rely on the reflection of sound from the shell of the mufflers back onto the target noise wave. Active systems utilize a loudspeaker to generate a sound wave that has equal amplitude, but opposite phase compared to the target wave (figure 7). The sound generated by the loudspeaker can be pure tones or broadband (white noise) in nature.

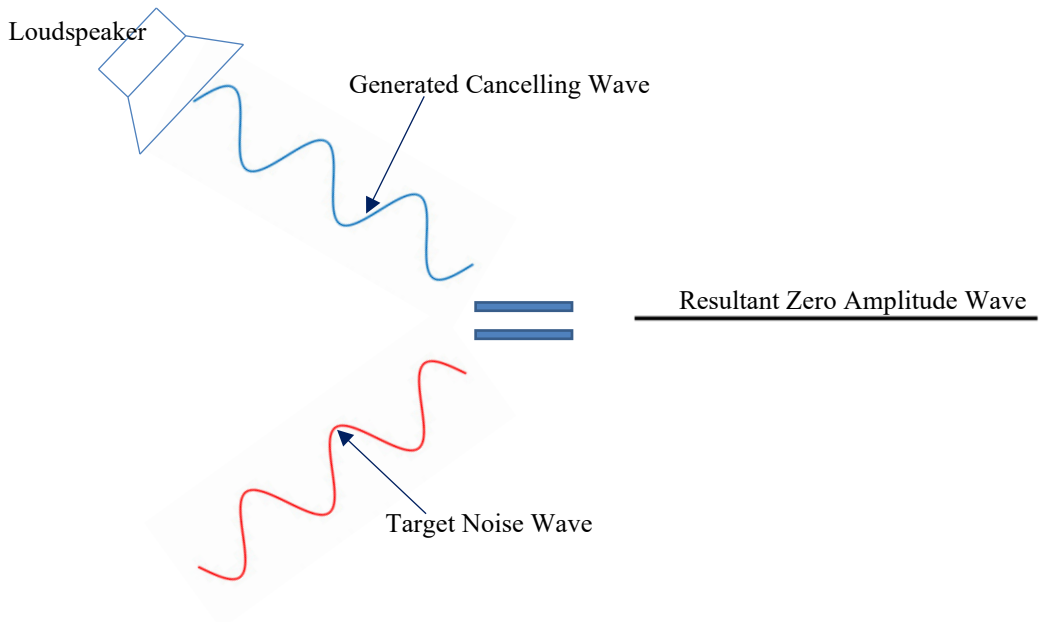

Figure 7: Schematic of destructive interference used in active control systems. A loudspeaker generates sound that has equal amplitude, but opposite phase compared to the target noise.

Two main conditions for destructive interference to happen successfully are: equal amplitude and opposite phase. Achieving these two conditions is very important. If the amplitude of the wave generated by the loudspeaker does not match that of the target wave, the resultant wave might have higher amplitude than intended. In addition, if the generated wave is not completely out-of-phase with the target wave, the positive displacement of one wave will not align with the negative displacement of the other wave. Addition of two such waves will result in some constructive interference, increasing the amplitude of the target wave. So, to make sure that the two waves have the same amplitude and opposite phase, a control unit is used to provide input to the loudspeaker. The control unit runs on an algorithm which are of several different types and are known as active control algorithms.

1.2.2.2 Active Control Systems

Active control algorithms are divided into two broad types: feedforward algorithms and feedback algorithms[48]. Both feedforward and feedback algorithms are closed loop systems.

1.2.2.3 Feedforward Systems

Feedforward control systems do not generate output until all the necessary computations are completed that take into account only the input parameters or the environmental factors[49] (figure 8). The control signal generated is based on the evaluation of the state of the current system and the inputs considered. The control signal is fixed and cannot be altered once it passes the evaluation stage[49]. So, the main property of a feedforward control is that the present output of the system has no influence on the future output of the system. Due to this property, feedforward systems have fast reaction to any changes in the surrounding input parameters and so are used for high speed output systems[50].

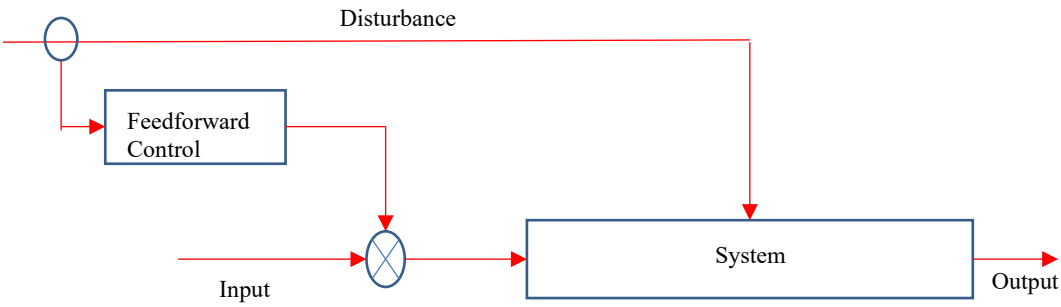

Figure 8: Schematic of feedforward control system[51]. The disturbances coming into the system are sensed by the feedback control and its output is provided the inputs of the system. Output of feedforward control unit is independent of the output of the system.

Based on this principle of operation, feedforward ANC algorithms are used to control the output of the loudspeaker and in turn, cancel automotive exhaust noise (figure 9). In the feedforward control system for automotive exhaust, a single reference sensor (e.g. microphone), a secondary source (loudspeaker) and a single error sensor (e.g. microphone) are used[48]. The output of the reference sensor is used to create the driving signal for the secondary source. The error sensor output is used to evaluate the performance of the ANC system. This type of arrangement is used for broadband control of exhaust noise[48].

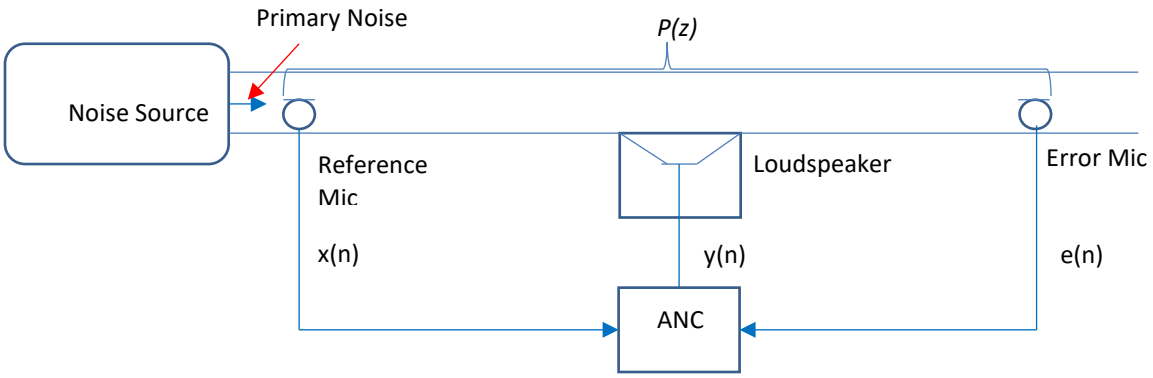

Figure 9: Schematic of broadband feedforward ANC system[48]. The reference sensor measures the primary noise and is used an input to the ANC. The error sensor measures the output of the system after the application of the signal by the loudspeaker.

The ANC unit consists of an adaptive filter *W(z)* which is used to estimate the unknown system that is being controlled. This estimate is done using a function known as plant function *P(z)*. *P(z)* which is also known as primary path, consists of the acoustic response of the path between the reference mic and error mic. The sound traveling through this path is the target sound that must be cancelled. *P(z)* also keeps track of any changes in the system and dynamically adapts to provide the appropriate control signal to the loudspeaker. The main function of the adaptive filter *W(z)* is to the minimize the residual signal *e(n)*. Initially, when the primary noise is introduced in the system, the residual signal *e(n)* is maximum. Also, there is no signal generated from the loudspeaker to cancel this noise. The adaptive filter adjusts its weights *W(z)* for every iteration and provides signal to the loudspeaker, which is *y(n)*. The value of *e(n)* is reduced due to the destructive interference between the primary noise and the sound generated by the loudspeaker. This process is continued till the residual signal *e(n)* is reduced to a minimum value set in the ANC[48].

The most commonly used algorithm in active control of noise is known as Least Mean Square (LMS)[48]. The LMS algorithm was first introduced by Widrow and Hoff in 1959[53]. They showed that LMS algorithm is an adaptive algorithm, and it adjusts its output based on the inputs and the error signal of the system. The LMS algorithm adapts its output based on the principle of method of steepest descent[54]. The method is simply an optimization algorithm that finds the local minimum of a function based on its negative gradient[55]. So, the LMS algorithm iterates the weight vector of a Weiner filter in the negative direction of the gradient vector till the mean square error is minimized. Multiple variants of LMS algorithms such as Filtered-X LMS (FXLMS), Normalized LMS (NLMS), variable step size LMS, Recursive LMS (RLS) are used based on the type of system, its acoustic response, the speed of computations and stability[56-61].

1.2.2.4 Feedback Systems

A feedback system generates output which is provided to the loudspeaker based on the output of the system[49] (figure 10). The output state is identified using an appropriate sensor and the signal from the sensor is fed back to the control unit at the beginning of the closed loop. The control unit compares this feedback signal value with the desired output (already preset) and updates the signal to the loudspeaker so as to maintain or achieve the desired system output. So, in a feedback system, the previous output has maximum influence on future system outputs. Because of the time taken to relay the output state back to the controller, feedback systems are relatively slower compared to feedforward systems.

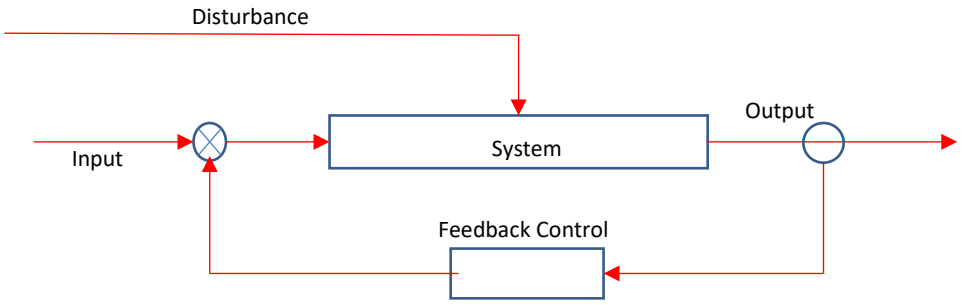

Figure 10: Schematic of feedback control system[51]. The output of the system is fed back using sensors to the inputs of the system. Output of feedback control system depends on the system output.

Like feedforward control, a reference sensor, a secondary source, and an error sensor are used in feedback control. The major difference is the arrangement of the loudspeaker with respect to the error sensor (figure 11). In feedback control system, the loudspeaker is placed after the error sensor and generates sound into the pipe/duct. The error sensor output is fed back into the control unit and processed by comparing with the desired output. The control unit then generates a signal as input to the loudspeaker, which is the secondary signal. Feedback control systems can be both adaptive as well as nonadaptive in nature[48].

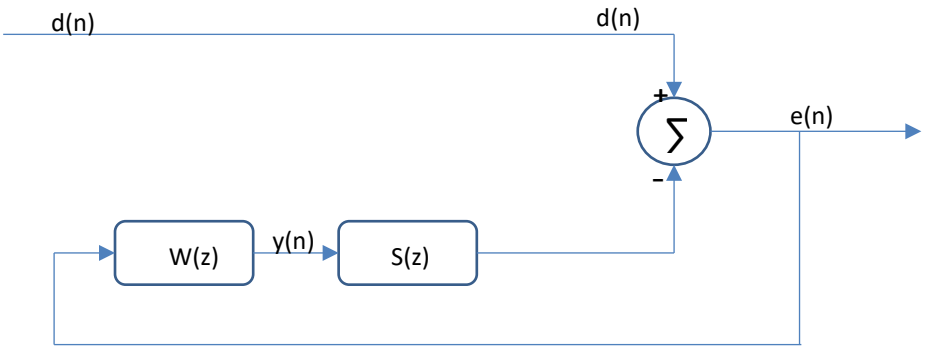

Figure 11: Schematic of feedback ANC system[52]. The error sensor signal is fed back to the control unit and the output signal of the control unit depends on the difference between the desired output and the error signal.

Feedback ANC systems also use the LMS algorithm to iterate the Weiner filter based on the difference in the values of the desired and achieved system outputs. The LMS algorithm uses the method of steepest descent to minimize the mean square error in feedback systems. The major difference in the implementation of the feedback algorithm is the noise source. In feedback systems, the reference signal *y(n)* used by the controller is generated using an external source such as a loudspeaker[62]. Alternatively, the reference signal to the controller can also be generated by the addition of the system output and the error signal. In feedback systems, FXLMS algorithm is the most preferred due to its stability and adaptability[48]. Several studies have been performed to improve the functionality, speed, stability and robustness of the feedback algorithms[62-71].

1.2.2.5 Active Exhaust Noise Control System

Based on the feedforward and feedback algorithm principles, the active system used for control of automotive exhaust noise is designed and operated. All active control systems

include a reference sensor, a secondary error sensor and a source to generate the cancelling sound (figure 9,11). The reference senor identifies the exhaust noise moving through the tailpipe. The error sensor determines the exhaust noise after destructive interference has been applied to it, i.e., after it passes the loudspeaker section. The loudspeaker generates the cancelling tone which is controlled by the algorithm in use.

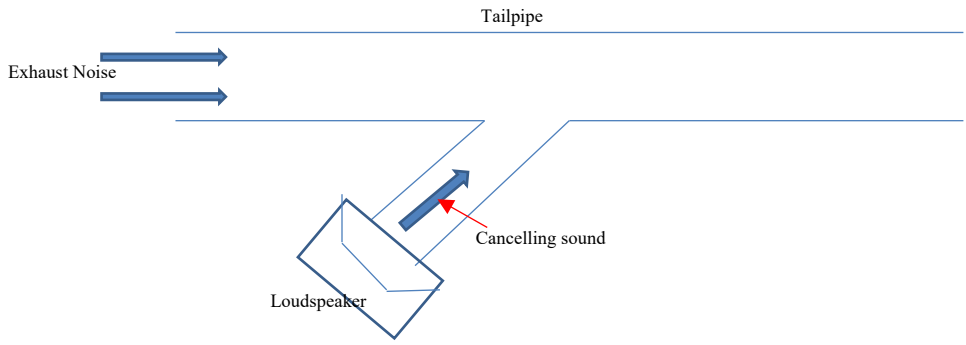

Figure 12: Active control system arrangements for automotive exhaust noise control. Loudspeakers are generally mounted on a side branch attached to the tailpipe.

As shown in figure 12, loudspeakers are generally mounted on the end of a straight pipe. This straight pipe is then connected to the tailpipe at a particular distance from the inlet. This arrangement is different compared to a passive muffler, which is connected in-line with the tailpipe. The main reason for this arrangement is the temperature of exhaust gases. Combustion of fuel in engines result in generation of exhaust gases along with exhaust noise. These exhaust gases travel through the tailpipe and have very high temperatures, more than 600^{o}C. Standard loudspeakers have very low operating temperatures compared to exhaust gas temperatures. So, any contact with the exhaust gases will damage the speakers. The side branch on which the speakers are mounted allows the exhaust gases to

sufficiently cool down before they meet the speakers. This ensures that the speakers are not damaged, and the active control system works without any disruptions.

It is not customary to use a single loudspeaker for active cancellation of exhaust noise. Multiple configurations of loudspeakers can be arranged around the tailpipe. One popular method of the loudspeaker arrangement is to have a concentric array of loudspeakers around the tailpipe[73]. The loudspeakers are arranged in between the inner tailpipe and an outer casing (figure 13).

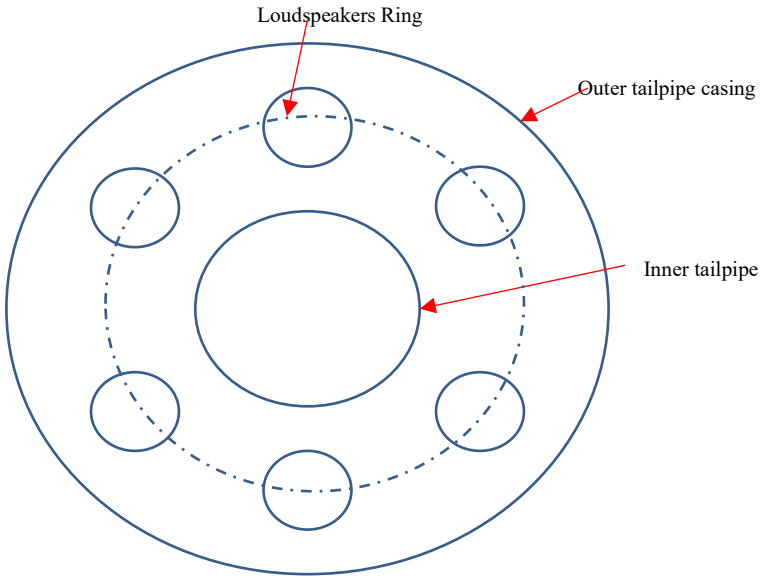

Figure 13: Schematic of concentric ring of loudspeakers around the tailpipe. The loudspeakers are encased between the inner tailpipe and outer pipe casing[73].

The main difference between the concentric arrangement and side branch arrangement is the way in which the cancelling noise is generated. In the concentric arrangement, the cancelling noise is generated radially inwards into the tailpipe. It is possible to activate the radial modes of the tailpipe in this arrangement. When the loudspeaker is connected using

a side branch, the plane waves generated are along the length of the pipe, i.e., along the longitudinal pipe axis. In this case, the axial modes of the tailpipe can be activated. As seen in the pipe acoustics section, proper tuning of the tailpipe dimensions and activating the right modes can result in increase in the SPL of the cancelling wave. This is highly beneficial as it would reduce the amount of power needed to produce the required SPL for effective cancellation of the exhaust noise.

Li Keqiang et. al. studied the active control system for vehicle exhaust noise, particularly for diesel trucks[74]. They studied the performance of the system based on the variable time synchronized FXLMS algorithm during the vehicle's acceleration. The algorithm was able to efficiently reduce the exhaust noise and was stable. F Buganza et. al. performed the acoustic analysis of the active control system on a HIL test bench[75]. They analyzed the system for its weight and volume reduction compared to passive systems, generated backpressure and sound profile of exhaust after cancellation. The results showed that the active system did not need a dual tailpipe design, had a 33% weight and 54% volume reduction and the exhaust sound could be tuned to sound like a sports car exhaust. Several studies have been performed in addition to design, characterize and improve the performance and stability of active noise control systems[76-91].

1.2.3 Need for an alternative noise cancellation source

Active noise control systems offer significant advantages over the passive control systems. First, the cancelling noise is generated by a loudspeaker. So, this makes it possible to control the frequency range of the cancelling noise being generated. Due to this, the active control system is more suited to adapt to changes in the exhaust noise spectrum, both in

terms of frequency and SPL. Mufflers require 10L of exhaust volume for every liter of engine size as a rule of thumb. This rule makes it necessary to have large mufflers for large sized engines, making them heavy, bulky and also affect the space limitations in the exhaust system. Active control systems, on the other hand, have no such requirement and this makes the active systems less heavy and bulky compared to passive systems. Most times, a combination of mufflers is required to attenuate the exhaust noise over a broad frequency range. This disadvantage is overcome in an active control system as a single system (with one or multiple loudspeakers) can efficiently attenuate the exhaust noise over a broad frequency range.

Despite all these advantages, the use of loudspeakers has its own limitations. The primary limitation is the operating temperature of the loudspeaker. Compared to the automotive exhaust gas temperatures which are over 600^{o}C, loudspeakers have very low operating temperatures. So, inline arrangement of the active control system is not possible. Any contact with the high temperature exhaust gases will damage the loudspeaker and make active system lose its functionality. So, for this reason, the loudspeakers are mounted on a side branch connected to the tailpipe. This arrangement severely affects the space limitation of the automotive exhaust tailpipe. In addition, the side branch dimensions (diameter and length) have to be designed carefully to make sure that plane waves are generated along the side branch and at the point of cancellation. If plane waves are not generated, the complexity of the ANC algorithm increases due to generation of cross modes in the tailpipe. The side branch also results in increase in the backpressure and exerts extra load on the engine.

To overcome these shortcomings, an alternative for the loudspeakers is considered in the form of carbon nanotube (CNT) loudspeakers.

1.2.4 Carbon Nanotube (CNT) Speakers

1.2.4.1 Introduction

Carbon nanotubes are structures of carbon grown as vertical forests on silicon wafers using chemical vapor deposition (CVD). When they are stretched along the length, these forests collapse, interlock with each other and then can be drawn as thin, long films. The films are extremely lightweight, flexible, and highly stretchable. When the films are stretched across two electrodes, they act as thin conductors. This configuration forms a planar CNT speaker. The sound generation principle of CNT speakers is known as thermoacoustic effect.

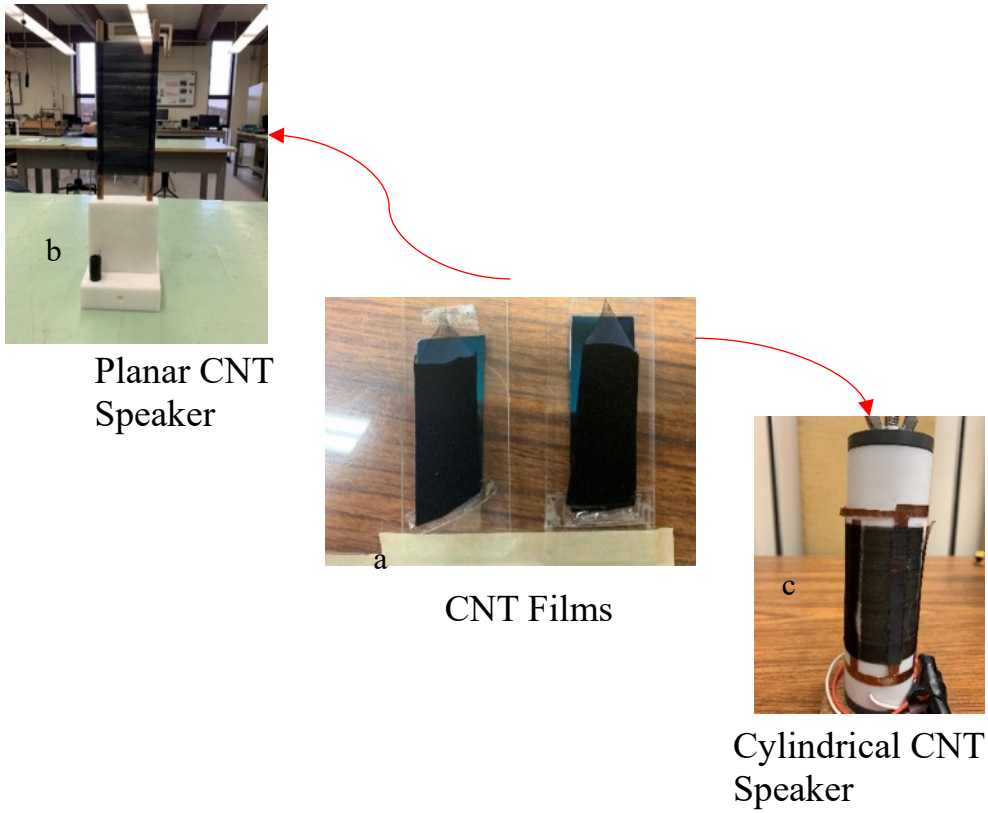

Figure 14: CNT forests grown on silicon wafers by CVD (a). Planar (b) and cylindrical (c) CNT speakers manufactured by stretching the CNT film across electrodes.

1.2.4.2 Working Principle

Thermoacoustic effect is the generation of sound through heat. When electric current is passed through a thin conductor, it heats and cools rapidly, i.e., its surface temperature oscillates. This rapid temperature oscillation expands and contracts the surrounding air, resulting in the generation of pressure waves and in turn sound. Arnold and Crandall demonstrated the thermoacoustic effect by passing current through a 700nm thin wire of platinum[94]. They showed that the sound pressure output from the wire was dependent on the surface temperature oscillation frequency. The temperature of the thin platinum wire

oscillated at frequencies below 16Hz, which is below the audible frequency range (20Hz – 20kHz).

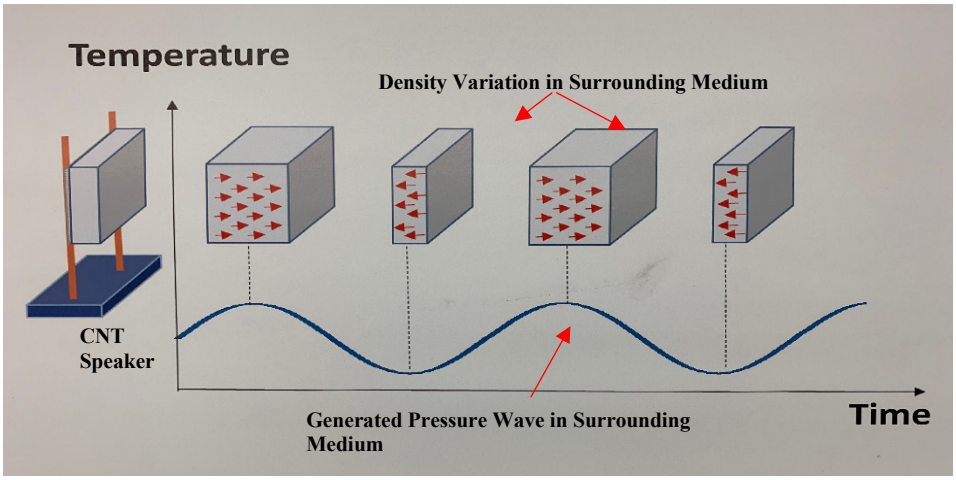

Figure 15: Thermoacoustic working principle of CNT Speaker. The surface temperature oscillation of the CNT film results in density variations in the surrounding medium, setting up pressure waves or sound.

1.2.4.3 CNT Speaker Research

The ability of CNTs to generate sound based on the thermoacoustic effect was first discovered by Yu et.al. when they passed an alternating current (AC) through CNT film[92]. Xiao et.al. first verified the theory put forth by Arnold and Crandall and expanded the theory of thermophone to CNT film planar speakers[93,94]. They put forth a general equation for the calculation of the sound pressure output from both a thin metal wire and CNT thermophones. The formula is mentioned in equation 3.

$$p_{rms} = \frac{\sqrt{\alpha}.\rho_o}{2.\sqrt{\pi}.T_o}.\frac{1}{r}.P_{input}.\frac{\sqrt{f}}{c_s}.\frac{(f/f_2)}{\sqrt{(1+\sqrt{\frac{f}{f_2}})^2+\sqrt{(\frac{f}{f_2}+\sqrt{\frac{f}{f_1}})^2}}} \quad (3)$$

where f is the frequency of sound, P_{input} is the electrical input power to the thermophone, r is the measurement distance between the thermophone and the microphone, C_s is the heat capacity per unit area (HCPUA) of the thermophone material, α, ρ_0, T_0 are the thermal diffusivity, density and temperature of the ambient gas medium, p_{rms} is the root-mean-square sound pressure output from the thermophone, $f1 = (\alpha)/(\pi\kappa)$ and $f2 = (\beta_0)/(\pi C_s)$. The terms $f1$ and $f2$ were added by Xiao et. al. to account for the discrepancy between the experimental results and the theory for dependence of p_{rms} on f and C_s. The formula indicates that the sound pressure output of the CNT speaker is dependent upon the input power as compared to a normal voice coil speaker whose output is dependent upon the input voltage.

Majority of the research has been carried out to understand the properties and response of planar CNT speakers. Kozlov M et.al. studied the thermoacoustic performance of CNT forests and planar thin films[95]. They found that even though both produced audible sounds, the thin films generated sound with higher intensity. Further, the CNT speakers can be operated using infrared lasers that are modulated. Suzuki K. et al. studied the performance of different length speakers made from multi walled CNT webs and normal CNT films[96]. Their results showed that speakers made from CNT webs had higher SPLs compared to normal thin film CNT speakers. However, there was no difference in the SPLs for different speaker lengths in both the cases. Barnard et al. performed non-dimensional analysis of Xiao's equation for speaker output[97]. This analysis helped evaluate the equation for different operating conditions which under direct evaluation would have been extremely complex. Based on the analysis, for a fixed frequency, the parameters that would contribute to increased output SPL from the CNT speaker were determined. The

experiment also studied the effect of film stacking on the output SPL of the speaker. Four layers of CNT films were stacked, and the SPL was measured as well as analytically calculated. The sound from all CNT layers would add up coherently, resulting in a 6dB gain per doubling of sources provided the layers are acoustically transparent and wavelength is longer that the film thickness. Measured results showed that the assumptions made for theoretical calculations were correct.

Aliev A et.al. tested the planar CNT speaker for underwater applications[98]. CNT molecules are nonpolar, have high hydrophobicity and this created a gas cylinders surrounding the film. The results showed that the sound pressure generation efficiency increased by almost 100 times in the selected frequency range of $10Hz<f<60kHz$. Xiao Lin et.al. studied the performance of CNT planar speakers in gaseous medium particularly argon, air and helium[99]. The results indicated lower heat capacity of the medium, higher is the sound pressure level of the speaker. The results agreed with the formula derived by Xiao et.al. with respect to the heat capacity and sound pressure level. Aliev et.al. performed studies to increase the efficiency of carbon nanotube speakers by encapsulating the open speakers in an inert gas environment[100]. At low frequencies, the efficiency of CNT speakers is low as efficiency of open area CNT speakers is related to frequency as $\eta \alpha f^2$. The experiment helped to modify the relation between the efficiency and frequency to $\eta \alpha 1/f^2$ in the low frequency region. Results showed that the measured sound pressure levels for argon filled thermophones were Q times higher than open systems, Q being the resonant quality factor of the enclosure plates. The study also found that modulating the input high frequency carrier current with a low frequency resonant envelope increased the efficiency in the low frequency region.

Barnard et.al. presented the design guidance for building large high-quality CNT speaker assemblies along with their performance with respect to maximum SPL, power efficiency and total harmonic distortion (THD)[101]. Tests were performed on speakers made of 5-layer MWNT films. Results showed that wrapping the film around the electrodes reduced the risk of damage to the CNT films which are very delicate. Even though the THD for the assemblies was higher than conventional speakers, there was not much effect on the speech intelligibility projected by the device which was the authors' opinion. Bouman et.al. studied the performance of planar CNT speakers for different drive signals in order to understand the relation between efficiency and THD[102]. Asgarisabet M. et.al. conducted near field acoustic holography (NAH) measurements for planar CNT speakers[103]. NAH was used to make measurements at the film surface as physical measurements are not possible due to the films being fragile, solid state and have high surface temperature. The results showed that the particle velocity at the film surface was nominally zero. The SPL measurements showed maximum level at the center of the CNT film and varied up-to 10dB over the entire surface. Studies have also been conducted for design, manufacturing and applications of CNT sheets, yarns and fibers[104-123]. These studies suggest new methods for manufacturing various forms of CNTs, their properties, speaker and actuator applications.

Along with planar speakers, some research has been performed for spherical as well as cylindrical CNT speakers. A spherical CNT speaker was design, manufactured and tested for a thesis research undertaken by Micaela Thiery at Michigan Technological University[124]. A telfon sphere was manufactured and the CNT film was wrapped around it with the purpose of creating an omnidirectional source. The results showed that the

speaker was omnidirectional at middle frequency bands while for lowest and highest audible frequency, it displayed significant directivity. The research also considered a planar CNT speaker as a microphone based on the principle of hot-wire anemometry. Results indicated that a CNT microphone was feasible over a large frequency range for pure tones. Xiao et al. built an exterior cylindrical speaker which was capable of emitting sound in all directions[125]. Further experimentation was not done on the speaker to characterize its performance.

Accurate design of mufflers, active control systems and CNT speakers is extremely crucial. Mufflers work on interaction between the reflected sound and target exhaust noise for cancellation/attenuation. In addition, proper positioning of absorptive material along with its dimensions is required for absorption of exhaust noise. In active control systems, the positioning of the side branch, its length and the loudspeaker power have to be selected based on the exhaust noise profile, its dimensions and desired attenuation. In CNT speaker design, the dimensions of the speaker, namely the length of wrap, distance between the electrodes and the number of electrodes present determine the resistance, power density and SPL of the speaker. For the above-mentioned systems and the CNT speaker, the effort needed to do multiple design iterations is reduced by modeling methods.

1.2.5 Modeling

1.2.5.1 Introduction

Design of any new product depends on several parameters such as size, weight, cost and its performance. During the design process, several iterations are needed before the perfect design can be achieved. For every iteration, it is necessary to evaluate the performance of

the system. Manufacturing and testing of every single design iteration are time consuming and tedious. To avoid this, model of the system design is created in a suitable software. Simulation is performed by selecting appropriate technique such as Finite Element Method (FEM), Boundary Element Method (BEM), Multiphysics analysis, etc. The simulation results help to identify the shortcomings in the system performance and allow easy change of system design.

1.2.5.2 Finite Element Method (FEM)

Finite element method is a numerical method used to solve mathematical and engineering models[126]. FEM solves partial differential equations (PDEs) involved in structural analysis, heat transfer, flow, etc. in two- or three-dimensional coordinates. In FEM, the large model is divided into small, simple parts known as finite elements. The model is discretized with the help of a mesh in space dimensions. The solution to the PDEs is obtained on the mesh points which is the numerical domain for the solution. The main result of this process is the conversion of the PDEs into a system of algebraic equations. The solution to these equations is obtained by approximating the associated error function to its minimum value. FEM is very useful for complex geometries such as mufflers and can be used for different materials, operational dynamics, etc.[127]. Mufflers, both reactive and dissipative, have been simulated using FEM for their structural, acoustic and vibrational performance[128-136].

1.2.5.3 Boundary Element Method (BEM)

Boundary element method (BEM) solves the partial differential equations formulated as boundary integral equations[137]. Like the FEM, the model is discretized with the help of a mesh in BEM.

The BEM applies surface elements on the boundary of a three-dimensional model and line elements on the boundary of a two-dimensional model[138]. The major difference in the mesh of BEM compared to FEM is that the mesh is applied only to the boundaries of the model in BEM[139]. BEM results in the numerical solution to the boundary integral equations. The solutions obtained though approximate in nature, are the exact solutions to the differential equations in the domain under consideration. In addition, BEM exert less computational load as compared to FEM as the number of elements in the mesh are less in BEM. Mufflers and active systems have been simulated using various BEM[140-149].

1.2.5.4 CNT Speaker Modeling

CNT speakers operate on thermoacoustic principle. So, the operating principle of CNT speaker is an interaction of three domains or physics – electrical, thermal, and acoustic. Electrical input (AC) is used to generate the surface temperature variation in the CNT film. The heat transfer from the CNT film to the surrounding medium generates density variations. These density variations propagate as sound. So, to model a CNT speaker, a method that incorporates Multiphysics interaction is required. Planar CNT speaker was modeled using COMSOL Multiphysics by Mahsa Asgarisabet[150-152]. The model was simulated using a combination of three modules – AC/DC module, thermoviscous acoustics module and pressure acoustics module. The surface temperature of the CNT film

was simulated using the AC/DC module. Joule heating was applied to the CNT film and the copper electrodes, and the temperature achieved due to the supplied AC current was simulated. The results showed that majority of the high temperature region was in the center of the film and the temperature reduced towards the ends of the speaker, i.e., near and along the copper electrodes. This is expected as the copper electrodes act as heat sinks. Using the obtained surface temperatures and the thermoviscous and pressure acoustic modules, the SPL of the planar CNT speaker was simulated for different frequencies. Good correlation was achieved between the simulated and experimental SPL of the planar speakers.

1.2.6 Motivation for the Research

A small coaxial speaker, when mounted on the tailpipe would act as a point source compared to low frequency sound due to its long wavelength. Such a speaker would prove to be effective in cancelling the exhaust noise. A circular array of loudspeakers can be mounted around the tailpipe to replicate the coaxial speaker. But for each speaker, a side branch would be needed, and this would also increase the complexity of the control system as well as weight added on to the tailpipe. The output of the speakers would also need to be correlated to achieve cancellation of the exhaust sound. In addition to this, the speaker must be capable of handling high exhaust gas temperatures. CNT speakers work on thermoacoustic effect and have high working temperatures. The speakers are extremely lightweight and small in size. All these properties led us to consider CNT speaker for this application. The coaxial CNT speaker was designed as a possible replacement for the loudspeakers used in active noise control, to be used in conjunction with passive mufflers.

The main objective of this research is to develop a method to model an enclosed coaxial CNT speaker for different platforms and conditions with focus on noise cancellation. Modeling is crucial for any new design. With the use of a validated modeling method, design iterations can be simulated to understand their performance. This will save a lot of time and effort that needs to be put into manufacturing and testing every single design iteration. The goal to develop the method to model the enclosed CNT speaker will be achieved by modelling the speaker in COMSOL Multiphysics and experimentally validating the model for the designed prototypes. In addition to this, the research will aim to fill some of the knowledge gaps in CNT speakers. For efficient operation of the CNT speakers, the temperature of the surrounding medium must be cooler than the temperature reached by the film. It is unsure as to how the CNT speaker (planar or coaxial) will behave when operated in a high temperature medium. The effect of continuous heating and cooling of CNT film on its durability for prolonged operation is not yet understood. The cancellation of exhaust sound assumes that plane waves are generated both by the source and the CNT speaker. The generation of cross-modes and the cancellation performance of the coaxial CNT speaker must also be considered for noise cancellation application. CNT films due to their nano thickness are virtually massless and acoustically transparent. There is no established method to model an acoustically transparent CNT film. All these shortcomings will be studied in the proposed research with the help of the demonstrator unit as well as the second-generation prototype.

1.2.7 Explanation of Chapters

Chapter 2 focuses on the pipe acoustics. The transmission of sound through pipes are governed by specific set of equations. The sound also activates modes inside the pipe which are important for the SPL generated by the speakers connected to the pipe. The basic equations for sound transmission in a pipe are described. The equations are then related to one dimensional lumped parameter elements and the equivalent circuit is explained. The limitations of this lumped parameter model are described and then FEM and BEM used in pipe acoustics are illustrated.

Chapter 3 describes the design process of the enclosed coaxial CNT speaker. Three prototypes were designed and manufactured. The first prototype is developed as a proof of concept of the coaxial speaker design. The second and third prototypes are designed with focus on reduced parts for manufacturing, small size and ease of assembly. The design process in selecting the dimensions of any CNT speaker is described. The ideology behind the three coaxial designs, their dimensions and speaker properties (resistance, power density, weight, etc.) are also discussed.

Chapter 4 lays out the methodology of this research. Description is provided for the modeling process of the CNT speaker using COMSOL Multiphysics. It lays out the physics involved in the setup of the model. The setup of the Finite Element model of the operating physics of the CNT speaker is discussed. The axial, cross-sectional and industry standard SPL characterization test setup and simulation has been discussed as well. Flow model simulation set up and parameters are discussed. Optimization of the enclosed, coaxial CNT speaker has been illustrated in this chapter.

Chapter 5 presents the results obtained from the experimental tests as well as the results from the Multiphysics model simulations. Comparison between the Finite Element mode and COMSOL simulation results are presented and discussed. Simulation results from the flow, SPL and optimization models are presented in this chapter.

Chapter 6 discusses the interpretation of the obtained experimental and simulated results. Suitable conclusions are drawn and presented. Some thoughts for future design modification, simulation model setup as well as experimental tests are mentioned in this chapter.

2 Pipe Acoustics and Acoustic Modes

2.1 Introduction

Sound transmission in pipes that are open or closed at ends result in the formulation of standing waves or travelling waves. This behavior of sound in a pipe depends on the properties of the sound transmitted through the pipe, pipe length, relation between the pipe cross-sectional area and the length of the pipe, presence of perforations and boundary conditions at the ends of the pipe[154].

2.1.1 Cutoff Frequencies and Cross Modes in Pipes

Plane waves have a distinct property: they propagate only in one direction. The modes generated due to plane waves traveling in a pipe generate modes that are simple to visualize and evaluate. However, sound transmission in a pipe can happen in more than one direction. The modes generated due to such transmission have complex pressure profiles, exciting different planes across the cross-section of the pipe.

Consider a circular cross-section pipe of radius a and length L (figure 16).

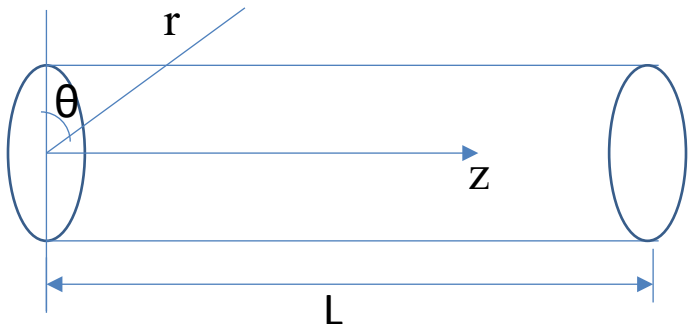

Figure 16: A circular cross-section pipe with r as the radius and L the length of the pipe.

In cylindrical coordinates, the Helmholtz equation (refer appendix A) becomes

$$\frac{\partial^2 p}{\partial r^2} + \frac{1}{r}\frac{\partial p}{\partial r} + \frac{1}{r^2}\frac{\partial^2 p}{\partial \theta^2} + \frac{\partial^2 p}{\partial z^2} + k^2 p = 0 \tag{4}$$

where *r, θ, and z* are the cylindrical coordinates of the pipe. Now, the boundary conditions at the rigid walls are

$$\left(\frac{\partial p}{\partial z}\right)_{z=0} = \left(\frac{\partial p}{\partial z}\right)_{z=L} = \left(\frac{\partial p}{\partial r}\right)_{r=a} = 0 \tag{5}$$

The solution to the Helmholtz equation in cylindrical coordinates includes the terms in *r, θ,* and *z* directions. So, the solution to equation XXI is:

$$p_{ml} = A_{ml} J_m(k_{ml} r) \cos m\theta e^{j(\omega t - k_z z)} \tag{6}$$

$$k_z = [(\omega/c)^2 - {k_{lm}}^2]^{1/2} \tag{7}$$

In the above equation, J_m is the m^{th} order Bessel function which describes the radial variance of pressure, k_z is the wavenumber in the z direction, ω is the angular frequency and c is the speed of sound. The values of k_{lm} are calculated using the boundary condition for the rigid wall as,

$$k_{lm} = j_{lm}'/a \tag{8}$$

where j'_{lm} are the extrema values of $J_m(z)$. The z direction lines up with the length of the cylindrical pipe. Now, equation XXIII provides us with two cases of waves generated in the pipe.

Case 1: $\omega/c > k_{lm}$ ⟶ k_z is real ⟶ wave is a propagating wave and it travels in the +z direction, that is along the length of the pipe. Based on the this property, the cutoff frequency of a *(l,m)* mode generated in the pipe (cross-mode) is determined as:

$$\boxed{\omega_{lm} = ck_{lm}} \tag{9}$$

Up to this value of angular frequency, the value of k_{lm} remains real and we get a cross-mode with a propagating wave.

Case 2: $\omega/c < k_{lm}$ ⟶ k_z is imaginary ⟶ wave is evanescent in nature and its amplitude decreases with distance in the +z direction.

As mentioned previously, any wave has two primary components along the wavefront: the phase speed and the group speed. These two components are important when identifying whether the generated wave is a plane wave mode or a cross-mode wave. The phase speed (c_p) and group speed (c_g) of a mode are defined as,

$$cos\theta = k_z/k = [1 - \left(\frac{\omega_{lm}}{\omega}\right)^2]^{1/2} \quad (10)$$

$$c_p = \omega/k_z = c/[1 - \left(\frac{\omega_{lm}}{\omega}\right)^2]^{1/2} = c/cos\theta \quad (11)$$

$$c_g = ccos\theta = c[1 - \left(\frac{\omega_{lm}}{\omega}\right)^2]^{1/2} \quad (12)$$

The parameter θ is an important property of the wave propagation in the pipe. It defines the angle that the wave propagation vector makes with propagation direction, in this case the +z direction. For plane waves, the wavefront travels parallel to the propagating direction. So, the angle θ is zero and the phase speed is equal to the speed of sound. In cross-modes, the waves travel at an angle different than zero and so, the phase and the group velocities of such waves are lower than the speed of sound.

The values of *l* and *m* determine the type of mode generated inside the pipe. The simplest of all the modes occurs at (0,0) during which a plane wave propagates along the pipe length. This mode has a pressure profile that is uniform along the cross-section of the pipe and has its phase speed equal to the speed of sound for all angular frequencies greater than zero. All other order modes are nonplanar modes, and their profile varies based on the values of *l* and *m.* Some of the modes formed in a pipe are illustrated in figure 17.

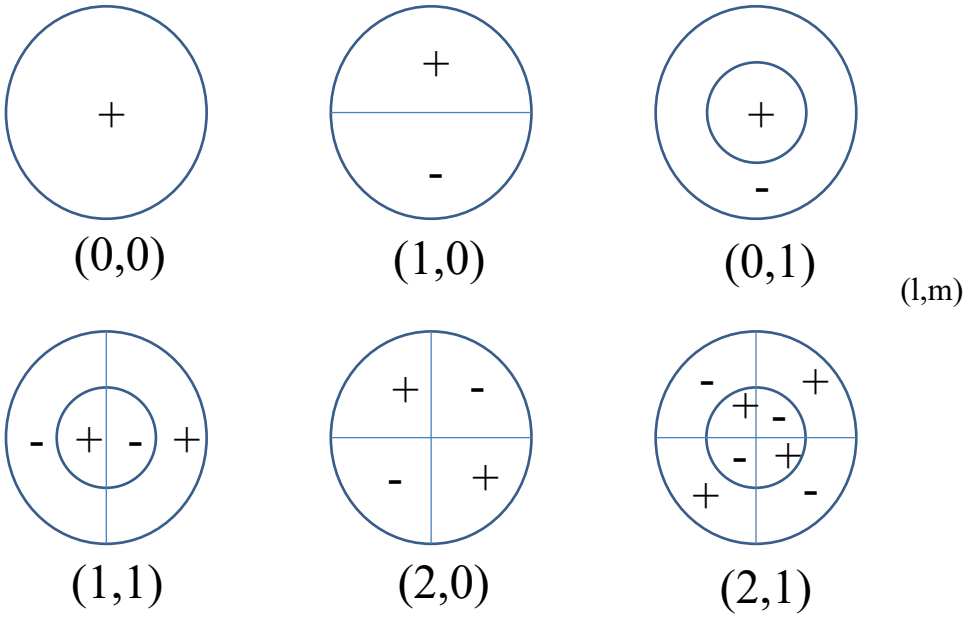

Figure 17: Sound pressure level profile regions for modes in a uniform cross-section circular cylindrical pipe. Different profiles are observed depending on the values of l and m.

As seen from the above figure, for the (0,0) mode, the pressure profile of the mode generated is uniform across the cross-section of the pipe. The behavior of this mode is analogous to the property of a plane wave – constant velocity and phase across the cross-section. For the other modes shown, the pressure profile varies across the cross-section based on the type of mode. More complex the mode profile, difficult it is to cancel it during noise control. Automotive exhaust pipes are generally circular in cross-section. So, if any of the cross-modes are excited during the transmission of exhaust noise, the complex sound field generated will make it difficult to cancel the exhaust noise, either due to passive or

active systems. The entire analysis of determining the cutoff frequencies of the cross-modes and the plane wave frequencies is very important for effective noise cancellation.

All the analytical equations illustrated till now are adept at characterizing the behavior of a pipe transmitting sound, plane wave generation and cross-modes. However, in reality, a uniform cross-section pipe is not always used in exhaust applications. These equations become far more complex when analyzing such pipes. To make matters simple, 1D lumped parameter elements and equivalent acoustical circuits are used to analyze the behavior of these pipes. The following section describes these lumped parameter elements and acoustic circuits.

2.1.2 Finite Element Method (FEM) Modeling for Pipe Acoustics

Finite element method is a modeling method in which a whole continuum is subdivided into several subregions and the relevant physical equations are solved over all the subregions. The results obtained for each of the subregions are then combined to obtain the equivalent behavior of the entire model[156].

The system of interest that is to be modeled using FEM is first divided into several subdomains that are generally called as elements. In these elements, a set of points known as nodes are selected. These nodal points are used to define the geometry of the individual elements that the model has been divided. This discretization process is then completed by defining the properties for each element and the nodes are defined using coordinate locations. Once the discretization process is completed, the model is then ready to solve the governing equations related to the selected physics, which in this case is acoustic wave

equation (equation 14). One main difference between the analytical and FEM solution is that in FEM modeling, the governing equations are converted into a finite element form and then solved for all the elements and their nodes. The solution results in a finite element matrix for every single element, which are then combined to form a single matrix for the entire model. This matrix describes the physical behavior of the entire model, thus determining the necessary parameters required to define the model's response.

There are two types of methods used to convert the governing physics equations into their finite element form: variational method and method of weighted residuals. Both the methods yield the same final form of the finite element equations, which is an integral equation, and they are solved to obtain the unknown parameters at the nodes.

The variational method is also commonly known as the Rayleigh-Ritz method. This method is based on the existence of variational principal equivalent to the governing partial differential equations. Some scalar quantities are defined in an integral form. These scalar quantities can be total energy, strain energy, etc. The variables that are to be determined are approximated using the interpolating function given as,

$$x = \sum b_i \emptyset_i \tag{13}$$

where x is the unknown variable that will be determined, b_i is the unknown interpolation parameter at the i^{th} node and ϕ_i is the shape function defined by the user at the i^{th} node. The solution, i.e., the unknown variable is then determined by minimizing the defined scalar quantity with respect to the selected interpolation parameters.

The method of weighted residuals is also commonly known as the Galerkin method. In this method, the governing partial differential equation is expressed as a residual equation using an interpolating scheme. This residual equation measures the error introduced due to approximation of the unknown variable. The obtained residual is multiplied by the weighting function, which in this case is the shape function (ϕ). The integral of this weighted residual is then equated to zero and the weighted residuals are minimized to obtain the unknown variable. Consider the acoustic wave equation. Expressing this equation using an interpolation function results in an approximate form of this equation. The interpolation function based on the method of weighted residuals is obtained as,

$$\frac{\partial^2 p}{\partial t^2} = \sum \frac{\partial^2 b_i}{\partial t^2} \Phi_i \tag{14}$$

where b is the interpolation parameter that varies only in time and ϕ is the shape function that only varies in space, i.e., in the coordinate system. The residual of the acoustic wave equation is then formulated as,

$$R = \frac{1}{c^2} \sum \frac{\partial^2 b_i}{\partial t^2} \Phi_i - \nabla^2 \sum b_i \emptyset_i \tag{15}$$

where c is the speed of sound and R is the residual of the acoustic wave equation expressed in terms of the method of weighted residuals. This equation is then integrated over the domain of interest, which in this case is the pipe and equated to zero to obtain the matrix form of the acoustic wave equation. The matrix form equation for homogeneous boundary conditions can be written as,

$$[M]\{\ddot{b}\} + [K]\{b\} = 0 \tag{16}$$

where M is the mass matrix, K is the stiffness matrix and $\ddot{b}$ is the second derivative of the interpolation parameter. The mass matrices formed for every element are of the lumped form and depend on the type of nodes the element has. For example, the entire domain may comprise of elements that have two, three, or four node linear elements. Based on the type of nodes the element has, the diagonal of the mass matrix is obtained. In addition, the mass matrix is also dependent on the type of element used to discretize the domain. Some common types of elements used are triangular, tetrahedral, etc. Each of these element types have their own predefined nodes and are selected based on the complexity of the model and the required solution accuracy.

Another important parameter mentioned in both the methods is the shape function (ϕ). It can be observed from both the methods that all calculations of the unknown variables are performed at the nodes of the elements. However, to obtain the behavior of the complete system, it is essential to determine the values of the variables along the region between the nodes. The shape function interpolates the value of the variables between the nodes to complete the FEM solution. The shape function can be a linear function or a higher order function, depending upon the type of system, its governing equations and boundary conditions.

The successful formulation of both the methods mentioned above depend on the boundary conditions that are present and their proper representation in the model. Generally, two main types of boundary conditions are used in a FEM. The first one is known as the Dirichlet boundary condition that have fixed boundary condition values. This boundary condition specifies the fixed values that the solution must follow along the boundary of the

selected domain. The second boundary condition is known as Cauchy boundary condition which is a gradient boundary condition expressed as,

$$\frac{\partial u}{\partial n} = a_1 u + a_2 \tag{17}$$

where $\frac{\partial}{\partial n}$ is the derivative of the selected variable in the normal direction to the boundary and a_1 and a_2 are constants. The general form of the Cauchy boundary condition for acoustic FEM formulations is expressed as,

$$\frac{\partial p}{\partial n} = -\frac{\rho_o}{Z_n}\frac{\partial p}{\partial t} \tag{18}$$

where Z_n is the impedance at the boundary of the selected domain/element. Based on the boundary conditions present, the coordinate system used, pipe geometry, the element type used to discretize the selected geometry and the method utilized to formulate the FEM model, the shape functions and the resulting matrices are formulated and solved to obtain the desired variables such as acoustic modal frequencies. FEM thus offers a unique method to simplify and solve the partial differential equations involved in the acoustic analysis of sound transmission through pipes.

3 CNT Speakers

3.1 Introduction

Carbon nanotubes (CNT) are grown as vertical nano thickness forests on silicon wafers using a process known as chemical vapor deposition (CVD) (figure 18). These forests are either single-walled or multi-walled in nature. When these forests are pulled from one end, they interlock with each other and get drawn in the form of CNT films. These CNT films are the basis of all CNT speakers.

Figure 18: CNT forests grown on silicon wafers. The forests align themselves when pulled and generate CNT films used in CNT speakers.

CNT films are extremely lightweight, flexible, have nano thickness and adhere easily to any substrate. These properties are used to design and manufacture CNT speakers. The working principle of a CNT speaker is the thermoacoustic effect, which is explained in Chapter 1. To summarize the thermoacoustic effect, sound is generated when an alternating

current is passed through a thin conductor due to its surface temperature variation. There are two key requirements of the conductor that can be used successfully to generate sound using thermoacoustic effect. First, the conductor has to be extremely thin. CNT films, due to their nano-thickness satisfy this requirement of the thermoacoustic effect. Second, the conductor should have the ability to transfer the heat generated due to the application of the alternating current extremely quickly. Having a very small heat capacity provides a conductor with this ability. CNT films have extremely low heat capacity, compared to other metal conductors and thus they satisfy the second requirement. CNT films satisfy both the requirements of the conductor required in the thermoacoustic effect and thus they are ideal to be used in the generation of thermoacoustic transducers.

The most basic form of the CNT speaker is known as a planar speaker (figure 19a). In planar speakers, the CNT film is stretched across two copper electrodes. These electrodes are placed parallel to each other, and the CNT film is stretched across the electrodes. The electrodes are housed in an insulating material to prevent shorting the circuit as well as provide stability and support to the speaker. Alternating current is then applied to the two electrodes. The current thus passes through the two electrodes to the low heat capacity CNT film stretched between them. This current causes rapid oscillations in the surface temperature of the CNT film proportional to the frequency of the applied current. These oscillations thus produce density variations in the surrounding medium and sound is generated. The design and construction of planar CNT speakers is extremely simple. In addition, the overall weight of the speaker depends on the weight of the electrodes, the insulating material and the connectors used to provide the alternating current. CNT films are considered massless with respect to the other speaker components.

In addition to the planar speakers, it is possible to manufacture several different types of CNT speakers that are more complex in nature such as cylindrical, spherical, etc. Cylindrical CNT speakers, as the name suggests, have cylindrical geometries (figure 19b). In these speakers, electrodes are arranged in a cylindrical configuration. All the electrodes used in this speaker are parallel to each other. CNT film is then stretched across the electrodes in the form of a continuous wrap. Alternate electrodes are connected to each other, and positive and negative leads are drawn from two electrodes. On application of the electric current, the entire CNT film wrap undergoes surface temperature oscillation as one component and so, the sound field generated is uniform in all directions around the speaker. This arrangement can also be equated to individual planar speakers arranged in cylindrical configuration. For example, if six electrodes are used in the cylindrical speaker, we can have a continuous wrap around the electrodes or three planar speakers with the CNT film stretched between every two electrodes.

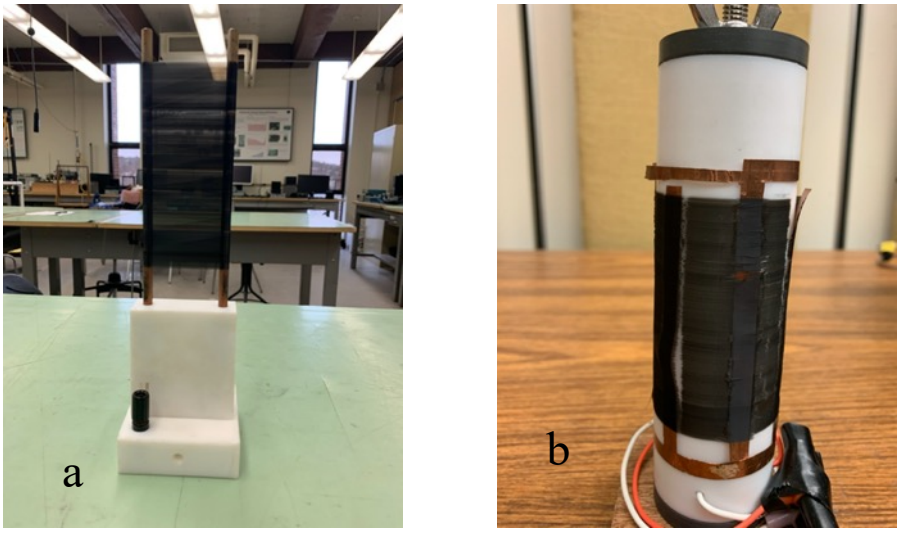

Figure 19: Planar CNT speaker (a). The CNT film is stretched between two parallel electrodes supported by an insulating material. Cylindrical CNT speaker (b). The electrodes are arranged in cylindrical configuration and the CNT film is wrapped continuously around the electrodes.

For any configuration of CNT speaker, it is very important to consider two parameters during its design. The first parameter is resistance, and the second parameter is power density. Both these parameters are essential for the safe operation of the CNT speaker as well as the safe operation of the other components in the circuit such as amplifiers. The next section illustrates the theory behind these parameters and the process to incorporate them in the design of the CNT speaker.

3.2 Design Parameters for CNT Speaker

3.2.1 Resistance

The first parameter to be considered in the design of the CNT speaker is the resistance of the speaker. CNT films are essentially extremely thin conductors and like every other conductor, they have their own resistance. However, CNT films have a unique property with respect to their resistance. Every single film of the CNT film has a resistance of 750Ω/square (figure 20a). To explain this in simple terms, every square area of the single CNT film layer has resistance of 750Ω. This resistance is independent of the area of the square. For example, a square of single CNT film with area of $1cm^2$ will have the same resistance as a square of $0.25cm^2$, that is 750Ω. Based on previous research, it has been observed that the CNT speaker generates sound of superior quality when five layers of CNT film are used to wrap the speaker as compared to any other layers. Five layered CNT film wraps are created by wrapping the CNT film on top of each other five times. This process changes the resistance of the five layered CNT film compared to a single CNT film layer. Each wrap of the CNT film has a resistance of 750Ω. The five layers are connected to each other in parallel which is the equivalent of five 750Ω resistances connected in parallel (figure 20b). So, the net resistance of a five-layered CNT film wrap is 150Ω. For a five-layer CNT film wrap, every square area of CNT film has a resistance of 150Ω, and all the squares are connected in parallel. Due to this, the net resistance of the CNT film is the parallel addition of all the resistances.

For example, if the CNT film is divided into 5 squares, the net resistance of the CNT film is 150Ω/5 or 30Ω.

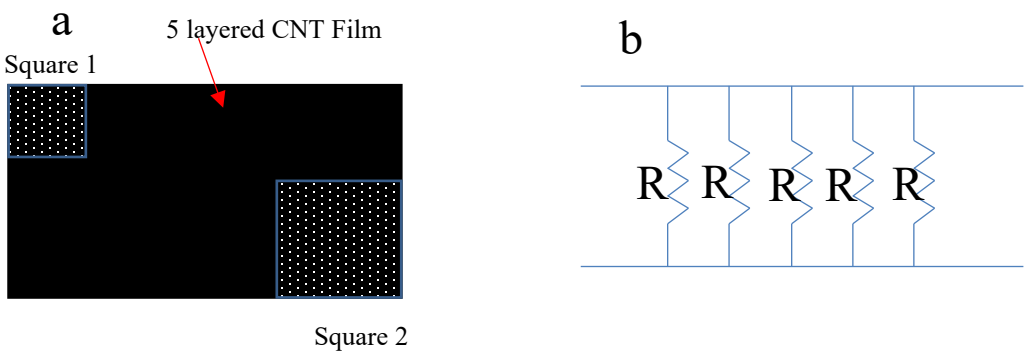

Figure 20: Schematic of five layered CNT film (a). The resistance of the square 1 and 2 is the same irrespective of the area of the square. The parallel arrangement of every single layer in a five-layer CNT film wrap (b). The value of R is the750Ω which is the same for all the layers and the net resistance is 150Ω.

The resistance value mentioned above for a five-layer CNT film and its corresponding squares form the baseline used to calculate the net resistance of any type of CNT speaker. To calculate the net resistance of the speaker, it is essential to determine the number of squares in the CNT film wrap. Any CNT speaker has CNT film stretched between two parallel electrodes. To divide the CNT film wrap into squares, the length of the CNT film is divided by the spacing between the electrodes (figure 21). Based on the number of squares thus obtained, the net resistance of the CNT film or the net resistance of the speaker is calculated. However, it is not always possible to obtain a round number of squares for a given length of the CNT film. In case where a decimal number of squares are obtained, the net resistance is calculated by dividing 150Ω by the obtained number of squares. This does introduce an error in the resistance calculation which is small. For a planar speaker, the process is relatively straightforward as there is only one CNT film wrap between two electrodes. However, for a cylindrical speaker, there are multiple CNT film wraps between

multiple parallel electrodes. In this case, the number of squares of the CNT film in each electrode combination is first calculated. All the square area resistances of these combinations are connected to each other in parallel. So, the net speaker resistance is the parallel addition of these resistances. For example, consider a cylindrical speaker made of six electrodes or three electrode combinations. Let the length of the CNT film wrap between every two electrodes be 10cm and the electrode spacing be 2cm. So, the number of squares in each of the three-electrode combination will be 5 and the total number of square resistances in parallel are 15 (5 squares in 3 electrode combination) These resistances are then added using parallel electric circuit logic and so the net resistance of the CNT speaker would be 150Ω/15 which is equal to 10Ω. The logic mentioned above is used to calculate the speaker resistance for any selected configuration. However, care must be taken as the resistance are not always connected to each other in parallel. Depending on how the electrodes relate to each other and with the external source, it is possible to obtain a series connection as well. This is beneficial when there is a requirement for a high resistance speaker as parallel addition of resistances reduces the net resistance of the CNT speaker.

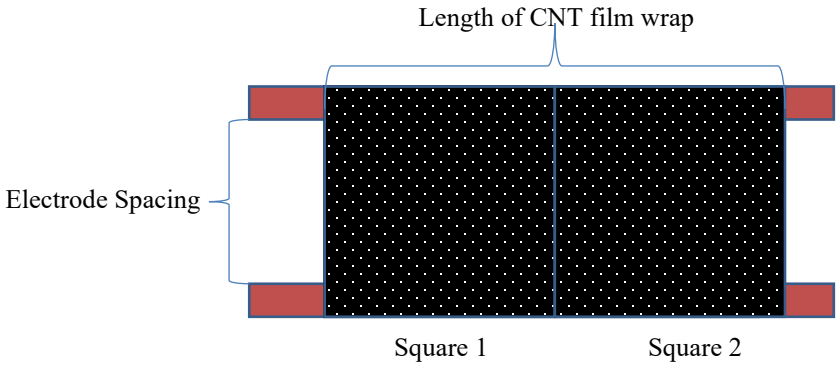

Figure 21: Division of the CNT film wrap into square of 150Ω resistance. The number of squares is determined by dividing the length of the CNT film wrap by the electrode spacing.

From the entire process mentioned above, the number of squares and the net resistance of the CNT speaker depends on the length of the electrodes, the electrode spacing and the number of electrodes. Longer length of the wrap for the same electrode spacing results in a greater number of squares which translates to more resistances in parallel, reducing the net speaker resistance (figure 22b). Alternatively, having a larger electrode spacing for the same CNT film wrap length results in a smaller number of squares and a higher speaker resistance (figure 22a). A similar effect is observed when there are a greater number of electrodes in for example a cylindrical speaker. Increased number of electrodes results in increased electrode combinations and CNT film squares. This reduces the net speaker resistance. In addition, like any other conductor, the resistance of the CNT film reduces with increase in the surface temperature. This reduces the net speaker resistance which might damage the amplifier to which the speaker is connected. So, it is important to properly select the length and the spacing between the electrodes to obtain the desired speaker resistance.

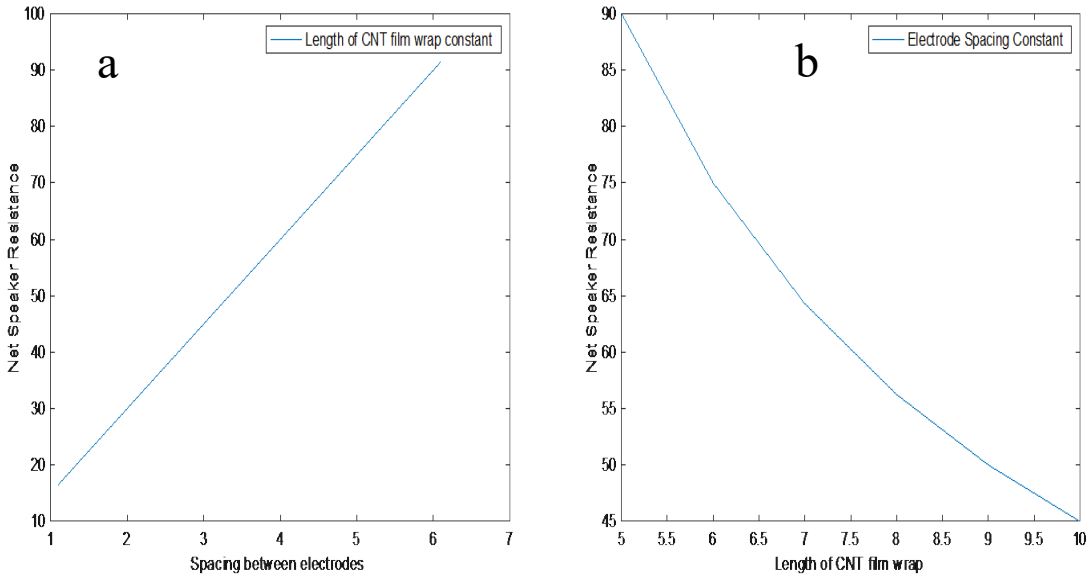

Figure 22: The change in the resistance of the CNT speaker with increasing distance between the electrodes (a). The length of the CNT film wrap is constant. The change in the resistance of the CNT speaker with increasing CNT film wrap length (b). The electrode spacing is constant.

The second design parameter is the power density of the CNT speaker and is illustrated in the next section.

3.2.2 Power Density

CNT speakers generate sound proportional to the applied input power as compared to a standard loudspeaker that generates sound proportional to the applied voltage. Based on this, the safety rating for a standard loudspeaker is given by the voltage that can be applied without burning out the coils. For the CNT speaker, the safety rating is proportional to the input power that can be applied per meter squared of its area. This rating is given as the power density of the CNT speaker.

When alternating current is applied to the CNT speaker electrodes, it passes from one electrode through the CNT film to the second electrode. The input power gets applied across the area of the

CNT film. If this power exceeds the safety value specified by the power density, it results in the cascade failure and burning of the CNT film. The value of power density depends on the total input power applied to the CNT speaker and the total surface area of the CNT film. The formula to calculate the power density of a CNT speaker is given as,

$$Power\ Density\ (P.D.) = \frac{P_{in}}{S}\ (\frac{kW}{m^2}) \tag{19}$$

where P_{in} is the input electrical power and S is the total surface area of the CNT film. The power density for a CNT speaker is expressed in the units of kW/m^2.

For a planar CNT speaker, the total surface area of the CNT film is contained in between the two parallel electrodes. This surface area is calculated by multiplying the length of the CNT film with the spacing between the electrodes. The maximum input power that will be applied to the CNT speaker depends on the application for which the speaker is being designed. The ratio between the electrical power and the total surface area of the planar speaker CNT film gives the power density for the speaker. For cylindrical speakers, the total surface area is the addition of the surface area of the CNT film between all the electrode ring combinations. For example, if there are six electrodes in the cylindrical CNT speaker, there are three electrode combinations consisting of two electrodes each. The surface area of the CNT film in each electrode combination is the product of the length of

the CNT film wrap and the electrode spacing. The total surface area would then be the addition of the three surface areas.

For a single layer of the CNT film, previous research has shown that the power density for safe operation has a value of 50kW/m^2. This value for a five-layer CNT film wrap has been determined to be 20kW/m^2. If the power density at any point during the operation of the speaker exceeds this value, there is a power surge through the CNT film, and it results its burning along the centerline of the wrap. One important point to the noted is that the above-mentioned values are observed when the medium surrounding the CNT speaker is air. Previous experimentation has showed that when the surrounding medium is an inert gas such as argon, xenon, etc., the power density of the CNT speaker increases. This enables the operation of the CNT speaker at a higher power compared to its operation when the medium is air.

Power density, like resistance, is affected by the length of the CNT film wrap and the electrode spacing. Changing either of these parameters changes the surface area of the CNT film and the power density of the CNT speaker. Longer wrap length of the CNT film with constant electrode spacing increases the surface area of the CNT film. This increases the denominator of the power density formula (for a constant input electrical power), thus reducing the power density of the speaker (figure 23a). Alternatively, increasing the electrode spacing while keeping the wrap length constant produces similar effect, that is reduction in the power density for the fixed selected input power (figure 23b). Increasing or decreasing the number of electrodes in a cylindrical CNT speaker does not change the net surface area of the CNT film wrap and so, the power density is not affected by the

number of electrodes. Based on these results, it is important that a suitable length and electrode spacing is selected to obtain the desired value of power density.

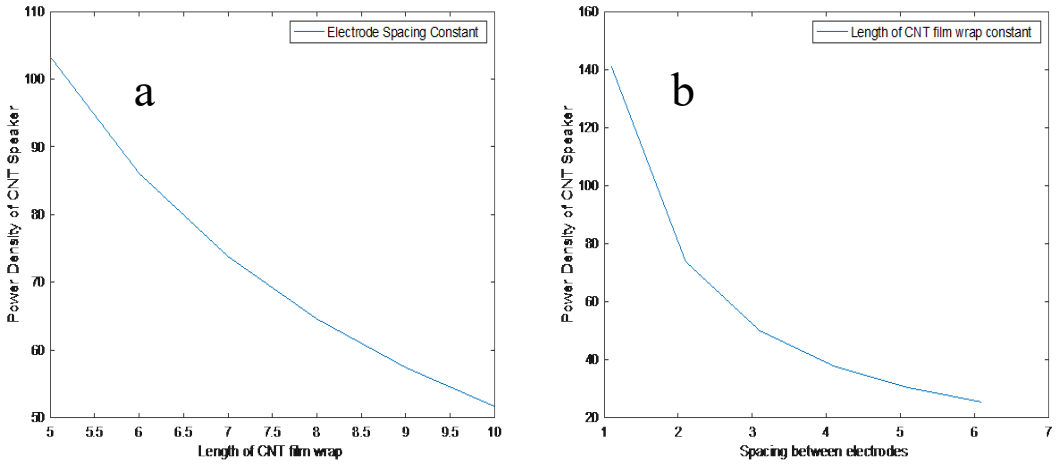

Figure 23: The change in the power density with increasing length of the CNT film wrap (a). The change in the power density with increasing electrode spacing (b). In both the cases, the effect is reduction in the power density of the speaker.

Compared to the resistance where a low resistance presents a problem, having a small value of power density is desired. As mentioned previously, in air, the power density has a limiting value of 20kW/m^2. For the selected input power and the wrap area, if the calculated power density value is significantly lower than the limiting value, it provides a great protection during the operation of the CNT speaker. For example, consider a planar CNT speaker that would be operated with a maximum electrical input power of 1kW and has a CNT film surface area of 0.11m^2. The power density of such a speaker for the selected input power will be 9kW/m^2. This value is significantly lower than the limiting value of 20kW/m^2. Having such a low power density allows the flexibility to operate the speaker at a much higher input power than that selected during the design process. So, in the above

example, even with an input power of 2kW, the power density of the CNT speaker would reach a value of 18kW/m^2, still within the limiting value. This helps to protect speaker from sudden power surges as well as offers more flexibility for its operation. So, during the design process, a factor of safety is always maintained in the calculated value of the power density.

It can be easily seen from the above explanations that the resistance and power density of the CNT speaker are dependent on the length of the CNT film wrap and the electrode spacing, or the area of the CNT film wrap. However, both the parameters are affected equally by the wrap length and the electrode spacing. If the resistance of the CNT speaker has to be higher, it is necessary that there are a smaller number of squares in the CNT film wrap. This can be achieved by reducing the area of the CNT film wrap which can be achieved by reducing the length of the CNT film or the electrode spacing. However, reducing the surface area of the CNT film will result in a higher power density value. If this value is very close to the limiting power density value, it will offer very little room for safe operation of the CNT speaker. So, increasing the value of one design parameter will result in the reduction in the value of the other design parameter (figure 24). For safe and efficient operation of any CNT speaker, it is extremely important that a suitable CNT film wrap length and electrode spacing is used in the design of the speaker to achieve a balance between the desired resistance and power density.

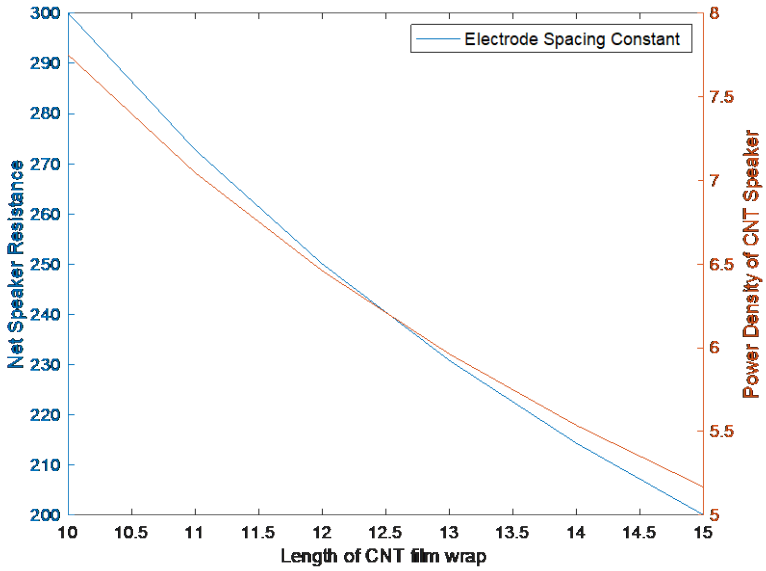

Figure 24: The change in resistance and power density with change in the CNT film wrap. Reducing power density increases the resistance of the CNT speaker.

The design of any configuration of CNT speaker involves calculating the resistance and the power density of the CNT speaker. CNT speakers though are of two main types: open speakers and closed speakers. The difference between the speakers and their operation principles are illustrated in the following section.

3.3 Open v/s Closed CNT Speakers

The main difference between the open and closed CNT speakers is the characteristic of the medium present surrounding the speaker. In open speakers, the CNT film is exposed to the ambient environment and not enclosed in any volume made by a casing. In closed speakers, the CNT film is enclosed in a volume, and it may or may not be exposed to the ambient environment (figure 25).

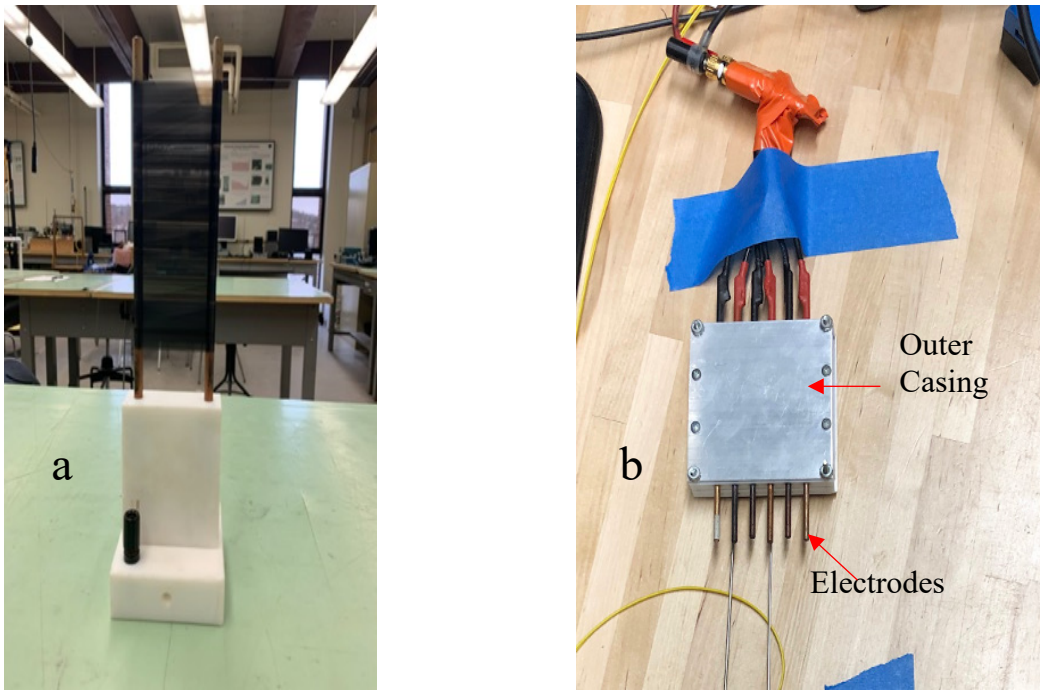

Figure 25: Open CNT speaker(a). The CNT film is exposed directly to the ambient atmosphere without any outer casing. Closed CNT speaker(b). The CNT film wrapped around the electrodes is covered using an outer casing. In this case, the CNT film is in constant contact with the medium present in the casing and not with the ambient atmosphere.

The presence of an open or closed medium has effect on the operating characteristics of the CNT speaker. In an open CNT speaker, the medium in contact with the CNT film is not confined in a fixed volume. So, when the medium next to the CNT film gets heated, it is eventually replaced by the cooler medium due to the setting up of convection in the medium. This helps to maintain the temperature difference between the CNT film and the surrounding medium. In a closed CNT speaker, the medium inside the casing gets heated up and the only way for it cool down is by heat transfer between the medium inside the casing and the ambient atmosphere through the casing. This causes the temperature of the

medium inside the casing to increase continuously, thus reducing the temperature difference between the CNT film and the medium surrounding it. This decreasing temperature difference is expected to have a negative effect on the SPL generated by the closed speaker because the relation between them is proportional.

Extensive research has been done on open CNT speakers to understand their design and characterize their performance. Xiao et. al. first verified the thermophone theory put forth by Arnold and Crandall and expanded this theory to open planar CNT speakers[93,94]. They formulated an equation to determine the SPL generated by the open planar CNT speaker, which is given as,

$$p_{rms} = \frac{\sqrt{\alpha}.\rho_o}{2.\sqrt{\pi}.T_o}.\frac{1}{r}.P_{input}.\frac{\sqrt{f}}{c_s}.\frac{(f/f_2)}{\sqrt{(1+\sqrt{\frac{f}{f_2}})^2+\sqrt{(\frac{f}{f_2}+\sqrt{\frac{f}{f_1}})^2}}} \quad (20)$$

where f is the frequency of sound, P_{input} is the electrical input power to the thermophone, r is the measurement distance between the thermophone and the microphone, C_s is the heat capacity per unit area (HCPUA) of the thermophone material, α, ρ_0, T_0 are the thermal diffusivity, density and temperature of the ambient gas medium, p_{rms} is the root-mean-square sound pressure output from the thermophone, $f1 = (\alpha)/(\pi\kappa)$ and $f2 = (\beta_0)/(\pi C_s)$. From the above formula, the SPL generated by the open CNT speaker is inversely proportional to the temperature of the ambient medium. Higher the temperature of the ambient medium, lower is the SPL generated by the open planar CNT speaker and vice-versa. Aliev A. et.al., in his study of planar CNT speaker for underwater generation has explained the generation of sound in gases with respect to the ideal gas law[98,157]. The ideal gas law is defined as,

$$PV = nRT \tag{21}$$

where *P, V, n and T* are the ambient medium gas pressure, volume, molar mass and temperature respectively and *R* is the ideal gas constant. For an open CNT speaker, the continuous increase and decrease of the surface temperature of the CNT film results in change in the *V, n and R* of the gas. The boundary condition that exists at the interface of the CNT film and the medium is given as,

$$dV/V_o = dT/T_o|_P \tag{22}$$

where Vo and To are the initial volume and temperature of the medium, dV and dT are the change in volume and temperature of the medium respectively[157,93]. This boundary condition exists at constant pressure and the sound pressure wavelength (λP) is much larger compared to the temperature wavelength (λT). This relation and the boundary condition make sense because the ambient medium surrounding the CNT speaker is not enclosed and free to change its volume. This change results in the generation of sound waves or sound energy that propagates in the opposite direction from the source.

In a closed CNT speaker, the dependence of SPL generated on the volume of the medium, its temperature and casing properties is different than that of an open CNT speaker. Aliev A. et.al., in their study has postulated a formula for the SPL generated by a thermoacoustic source that is encapsulated using a rigid enclosure as,

$$p_{rms} = \frac{(\gamma-1)}{\sqrt{2}\pi f V} P_h \tag{23}$$

where p_{rms} is the root-mean-square SPL generated by the speaker, γ is the ratio of specific heats (C_p/C_v), f is the frequency of the sound to be generated, V is the enclosed volume inside the outer casing, P_h is the measure of the input electrical power that is completely transferred to the surrounding medium and is expressed as,

$$P_h = 2S\beta T_a \tag{24}$$

where S is the surface area of the CNT film, β is the heat exchange coefficient of the thermoacoustic source, and T_a is the temperature of the surrounding medium[157].

It has been observed that the variation of the SPL generated by the closed CNT speaker is less dependent on the gas parameters, except the ratio of specific heats (γ). In addition, the volume of the enclosed medium has a significant effect on the generated SPL. It has been observed that smaller the volume of the enclosure, higher is the generated SPL. Further, based on the ideal gas law (equation 77), when the CNT film is placed in a hermetically sealed chamber made of two parallel plates, the medium parameters n, R, and V remain constant during operation and this results in pressure generation in the enclosure[98]. The boundary condition that exists at the interface of the CNT film and the medium in the enclosure is given as,

$$dP/P_o = dT/T_o|_V \tag{25}$$

where, dP is the change in the pressure in the enclosure, P_o is the initial pressure in the enclosure, dT is the change in the temperature of the enclosure and T_o is the initial temperature of the medium in the enclosure. One important point to remember is that there is no change in the volume of the medium inside the enclosure and so, we have $dV = 0$.

One advantage of enclosing the CNT film is the utilization of the resonance property of the plates that form the enclosure. The plates used in the enclosure have their own resonance which can be activated by the sound generated by the CNT film. Using resonantly rigid plates provides magnification of the sound generated by the CNT film that is transmitted external of the enclosure. The general formula expressing this amplification is expressed as,

$$p(r) = \frac{\rho_g(a*b)}{\rho_p 2\pi h_p} . Q . \frac{1}{r} . p_{rms} \tag{26}$$

where, ρ_p and h_p are the density and thickness of the rigid plates respectively, Q is the mechanical quality factor at resonance of the plates. The SPL generated by the CNT film inside the enclosure is amplified by Q times and so, higher SPL can be achieved with lower input electrical power. Another advantage of having an enclosure around the CNT film is the flexibility to use different mediums for the speaker operation. It has been proven that the use of an inert gas such as argon as a medium for the CNT speaker operation increases the operating temperature and power density of the CNT speaker. Also, the enclosure provides necessary protection to the CNT film from oxygen in the atmosphere and other damaging elements.

Despite all the advantages mentioned above for having an enclosure around the CNT film, there is one probable disadvantage. CNT speakers operate based on the temperature difference between the CNT film and the surrounding medium. In the enclosed CNT speaker, the temperature of the volume of gas in the casing will increase faster due to limited heat dissipation from the chamber interior. This will reduce the temperature

difference between the CNT film and the medium and it is expected that the SPL generated will gradually reduce. Increasing the input power will increase the CNT film temperature as well as the temperature of the gas inside the chamber. A point would reach at which any increase in the input power will not result in an equivalent increase in the SPL. This is known as thermal saturation, and it is possible in a closed CNT speaker. One way to avoid this is to use heat sinks or water cooling to increase the heat dissipation from the outer casing.

With all the above information as baseline, three enclosed, coaxial CNT speaker prototypes were designed and manufactured. They are discussed in the following sections.

3.4 Enclosed Coaxial CNT Speaker Design Concept

As mentioned in chapter 1, active control systems for automotive exhaust noise control have the shortcoming of low working temperature of the loudspeakers used in the system. Due to this, the loudspeakers must attached at the end of a side branch connected to the tailpipe. This helps to separate the loudspeaker from the high temperature exhaust gases in the tailpipe. CNT speakers, on the other hand, have a very high operating temperature and can withstand the high temperature exhaust gases without doing any damage to the CNT speaker. So, the CNT speaker can be connected directly to the tailpipe without the need of a side branch.

With this important property of the CNT speaker as a baseline, an enclosed, coaxial CNT speaker was designed. The design idea behind the enclosed, coaxial speaker was modeled along the lines of a spool. A simple spool consists of two discs at the ends and a shaft that

connects the two discs. On the lines of the spool design, the enclosed, coaxial CNT speaker consists of two end discs made of an insulating material(figure 26). Barnard A et.al., in his study, demonstrated that the CNT films are acoustically transparent: sound travels through the CNT films without any change in amplitude and phase[97]. This property is extremely crucial in the design of the enclosed, coaxial CNT speaker. In the previous section, it has been shown that the resistance and power density of the CNT speaker depends on the total area of the CNT film wrap. More the area of the wrap, lower is the resistance and power density. Having a low value of power density is beneficial as it offers more factor of safety for the CNT speaker operation. Secondly, the resistance of the CNT speaker should match the output impedance of the amplifier that is being used. In addition, having more wrap area increases the sound pressure level output of the speaker. The acoustic transparency property of the CNT films allows the stacking of the films so that more wrap area is achieved while keeping the overall length of the speaker small. With this idea, concentric rings of electrodes were housed in the two end plates. The CNT film was wrapped continuously around the electrodes in each of the concentric rings. The two end plates are placed on a pipe which is slotted in the middle to allow the sound generated by the CNT film to travel into the tailpipe. This entire assembly is enclosed in an outer cover making the speaker completely enclosed.

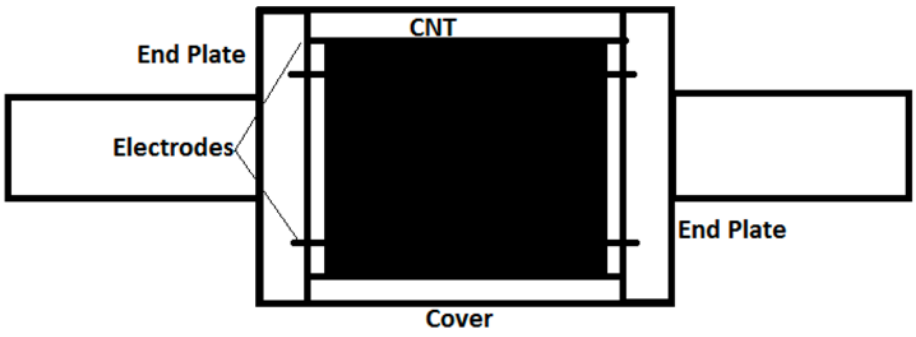

Figure 26: Schematic of an enclosed, coaxial CNT speaker. The electrodes are arranged in concentric rings and alternately connected to positive and negative terminals. The outer cover encloses the CNT film.

The outer cover and acoustic transparency provide another advantage. The sound generated by the CNT film is reflected by the inner surface of the outer cover back into the speaker. The CNT films allow this reflected sound to travel through them without any change in amplitude and phase. The reflected sound and the generated sound add with each other and the net sound traveling into the tailpipe is 6dB higher than the generated SPL of the CNT speaker. This happens because the reflected and generated sounds add coherently.

With this basic idea of the enclosed, coaxial CNT speaker, three prototypes were designed and manufactured. The following sections describe each of the prototype in detail.

3.4.1 Prototype 1

The first prototype had two endplates with electrodes between them. The overall length of the speaker was 7.6”. The inner diameter of the end plates was matched to the tailpipe dimensions, in this case 2”. The outer diameter of the end plates was 3.76”. The end plates

were made of Teflon which acted as an electrical insulator. Copper electrodes of diameter 1/8” were selected based on the amount of input current to the speaker. The prototype had three concentric rings of diameter 2.34”, 2.94” and 3.54” with each ring consisting of 6 electrodes. The resistance of the speaker was designed to be approximately 1.98Ω with a power density of 9.79Kw/m2 for an input of 1kW. The end plates were machined from Teflon blocks into circular discs with three concentric rings for the electrodes. In each ring, every alternate electrode was positive, and the remaining electrodes were negative (figure 27).

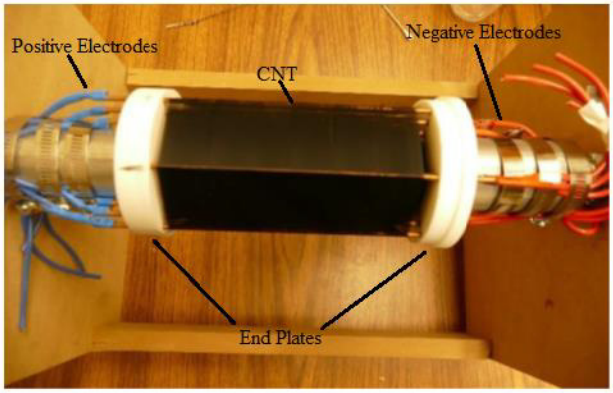

Figure 27: The fully wrapped first prototype of the enclosed coaxial CNT speaker. Three electrode rings were used in this prototype. The electrodes on one side were connected to positive terminal (red wires) and the electrodes on the other side were connected to the negative terminal (blue wires) of the power supply.

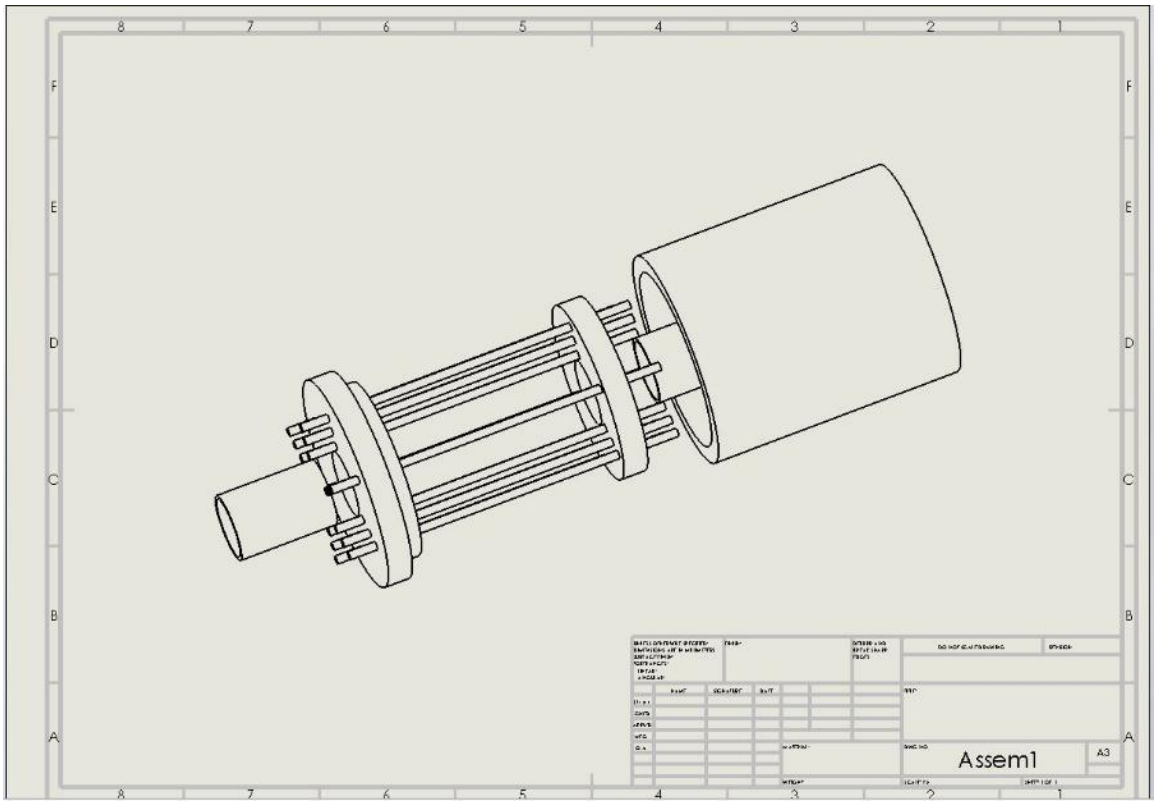

Figure 28: 3D assembly drawing of first coaxial CNT speaker prototype.

The speaker was mounted between two brackets and a crank was used to turn the speaker. The pawl was used to prevent the speaker from turning in the opposite direction. Prevention of backward motion is important as any loss of tension in the CNT film would break the film. Despite preventing the backward motion of the speaker, there was some backlash which reduced the tension in the wrapped CNT film. It was found that wrapping the film manually by rotating the speaker was easier than using the wrapping assembly. Electrodes were inserted one ring at a time and CNT was wrapped. An aluminum cover was used to protect the CNT from the atmosphere. The inner diameter of the cover was matched to the outer diameter of the end plates.

There were certain shortcomings in the design of the first prototype. Firstly, Teflon is a very smooth material. On insertion of the electrodes in the two end discs, it was found that the electrodes had a tendency to rotate in their holes. This rotation was damaging to the CNT film wrapped around the electrodes. The rotation of the electrodes resulted in the twisting of the wrapped CNT film, destroying it completely. Secondly, the clearance between the electrode rings was too small. The design of the speaker made it necessary that each electrode ring be inserted after wrapping of the inner electrode ring. Care had to be taken that the while inserting the electrodes, there was no contact between the electrode and the wrapped CNT film. This process was extremely time consuming. In addition, the end pipes did not extend all the way through the speaker. They were just inserted into the end discs and so, the speaker did not have the desired stability. All these shortcomings were overcome by the design of the second speaker prototype.

3.4.2 Prototype 2

The main design requirement of the second prototype was to reduce the overall dimensions and weight compared to the first prototype and make the speaker more robust. Hot exhaust gases pass through the tailpipe and in turn, through the speaker. It is crucial that the speaker is completely sealed and does not allow the exhaust gases to contact the CNT films. In the first prototype, there was not sufficient sealing between the cover and end plates. The end plates were manufactured to have a sliding fit between the circular electrodes and their respective holes. The second prototype had two concentric electrode rings with the electrode diameter of 1/8”. Each electrode ring had 6 electrodes. The rings had a diameter of 2.52” and 3.07”. To prevent the sliding and rotation of the electrodes, one end of the

electrodes was fixed by brazing to a bracket which was attached to the end plate using screws. Figure 30 shows the 3D model of the electrodes brazed to the bracket. The other end of the electrodes was fixed using circlips and nuts. The length of the CNT wrap was 4.84” and the outer diameter of the end plates was 3.35”. The resistance of the speaker was designed to be approximately 1.8Ω and power density of 8.4Kw/m2 for an input of 500W (figure 29).

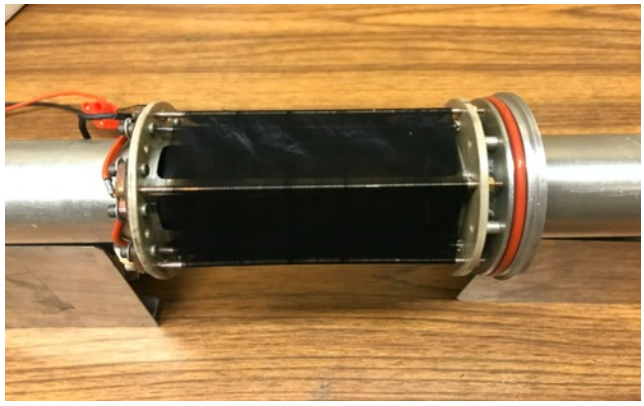

Figure 29: The fully wrapped second prototype of the enclosed coaxial CNT speaker. Two electrode rings were used in this prototype. O-ring was used to provide better seal between the outer cover and end discs.

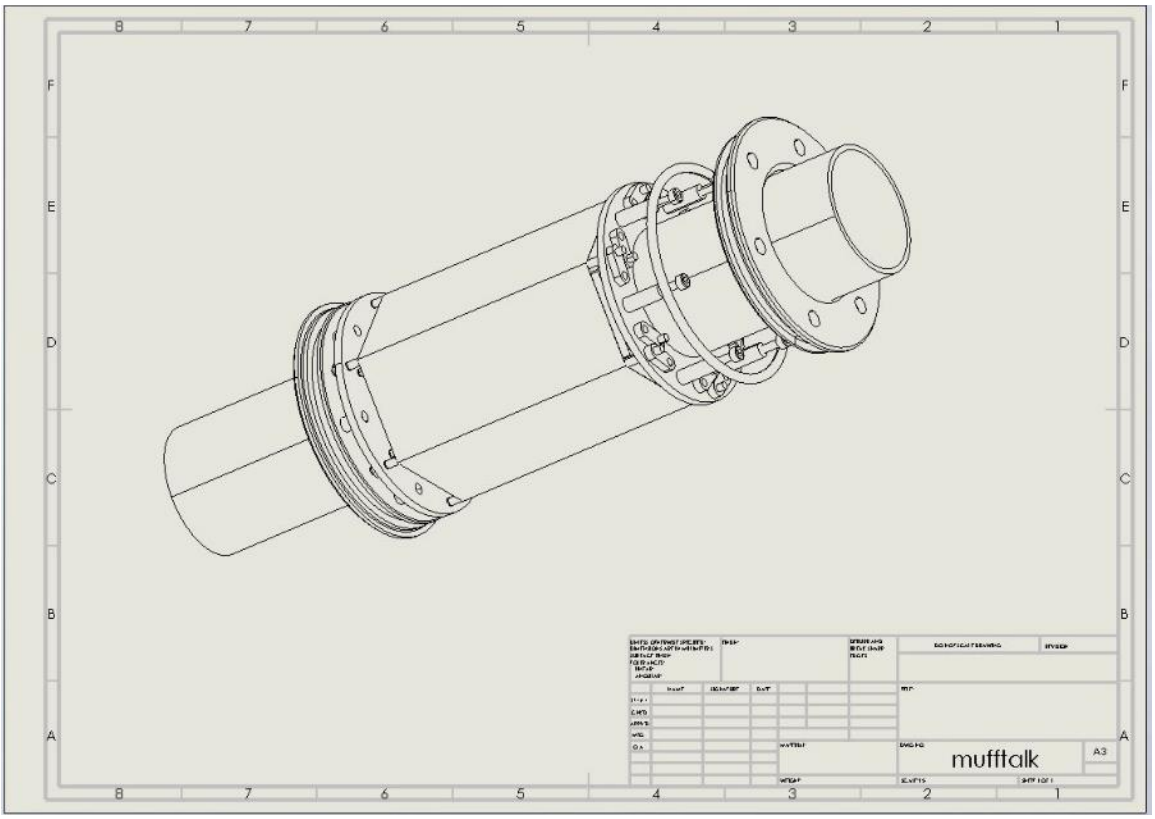

Figure 30: 3D assembly drawing of second coaxial CNT speaker prototype

Teflon has a heat deflection temperature of 65ºC which is very low compared to the exhaust gas temperatures. So, to increase the heat bearing capacity of the end plates, PEEK plastic was used which has heat deflection temperature of 315ºC. To provide a seal in the speaker for preventing leakage of exhaust gases, o-ring was used on one end plate which was welded to the pipe. CNT film was wrapped manually by rotating the speaker for five layers in each ring. When the speaker is mounted on the exhaust, the CNT film must be protected from the exhaust gases as a lateral flow over the CNT film would destroy it. The CNT film must be separated from the exhaust gases using a film which is acoustically transparent and has a very low value of thickness. Kapton film manufactured by DuPont was used which had a thickness of 1mil. The film was wrapped on a slotted pipe which extended

through the speaker. The Kapton film was wrapped around the slots in the pipe which also provided stability and support to the speaker.

One major shortcoming of this design was the replicability of the CNT film. If the CNT film wrapped in the inner electrode ring was damaged, it became necessary to destroy the CNT film in the outer ring and then rewrap the entire speaker. This process is too time consuming and not cost effective. To overcome this shortcoming, the third enclosed, coaxial CNT speaker prototype was designed and manufactured.

3.4.3 Prototype 3

The third prototype was made in the form of a modular design. Instead of having a continuous wrap of the CNT film, six planar CNT speakers were arranged in a concentric configuration around a slotted pipe (figure 31). The six planar speakers were housed in the end plates that had slots corresponding to the insulating block that supported the electrodes.

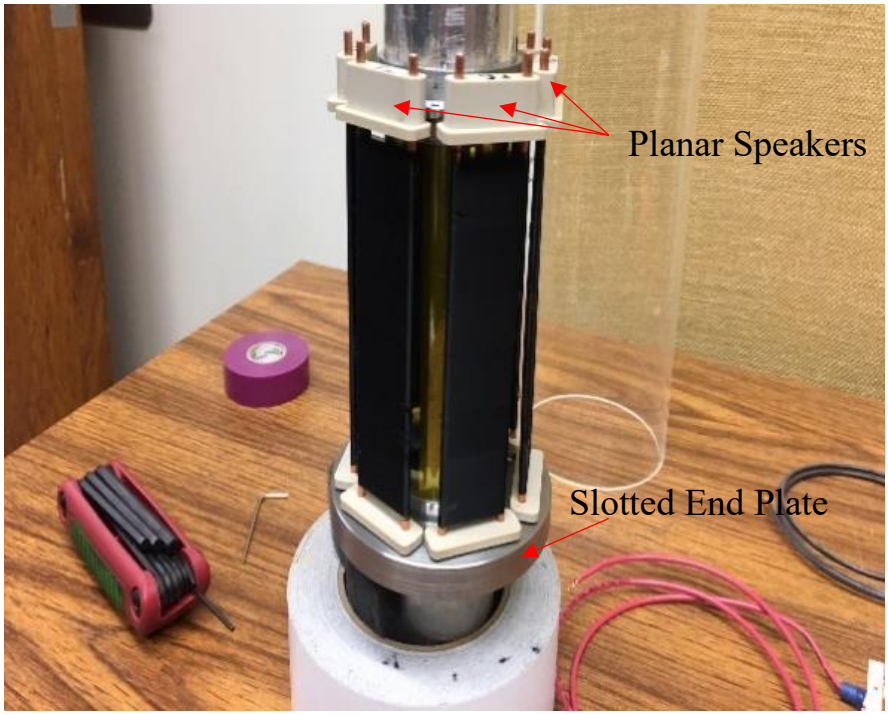

Figure 31: Fully wrapped third CNT speaker prototype. The six planar speakers arranged in concentric configuration around the slotted pipe allowed flexibility in replacement of the CNT film.

Some of the design parameters of the CNT speaker such as resistance, power density, maximum operational power, and number of wraps of the CNT film used were redesigned compared to the first two prototypes. One of the main observations from the characterization tests of the first two prototypes was the resistance change with input power. It was observed that the resistance of the CNT speaker reduced as the input power was increased. This is a problem during the operation of the speaker as it may cause the amplifier to overload if the resistance of the speaker drops below the impedance limit of the amplifier. So, the resistance of the third prototype was kept high (8.64Ω) compared to the first two prototypes. Also, the designed power density was below the nominal value of 20kW/m^2, at a value of 9.94kW/m^2. The third prototype was designed to operate at a

maximum input power of 1kW. In the earlier versions, the end rings were made of Teflon and PEEK materials that are insulators. However, it was found that due to the generation of heat inside the outer cover during the speaker operation, the plastics tend to deform. So, to avoid this problem, the end rings were made of steel in this prototype. Insulation between the end rings and the copper electrodes was achieved by mounting the electrodes in PEEK isolators as shown in figure 31. To cover the slots in the pipe that extended through the speaker, Kapton film was used and wrapped in tension over the slots.

All the three prototypes had the same baseline idea: enclosed design with coaxial CNT film around a slotted pipe. All of them were designed for in-line connection with the tailpipe for active noise cancellation. Out of the three prototypes, it was found that the second prototype showed the most promise and so, it was selected to be used a baseline to develop the modeling method in COMSOL.

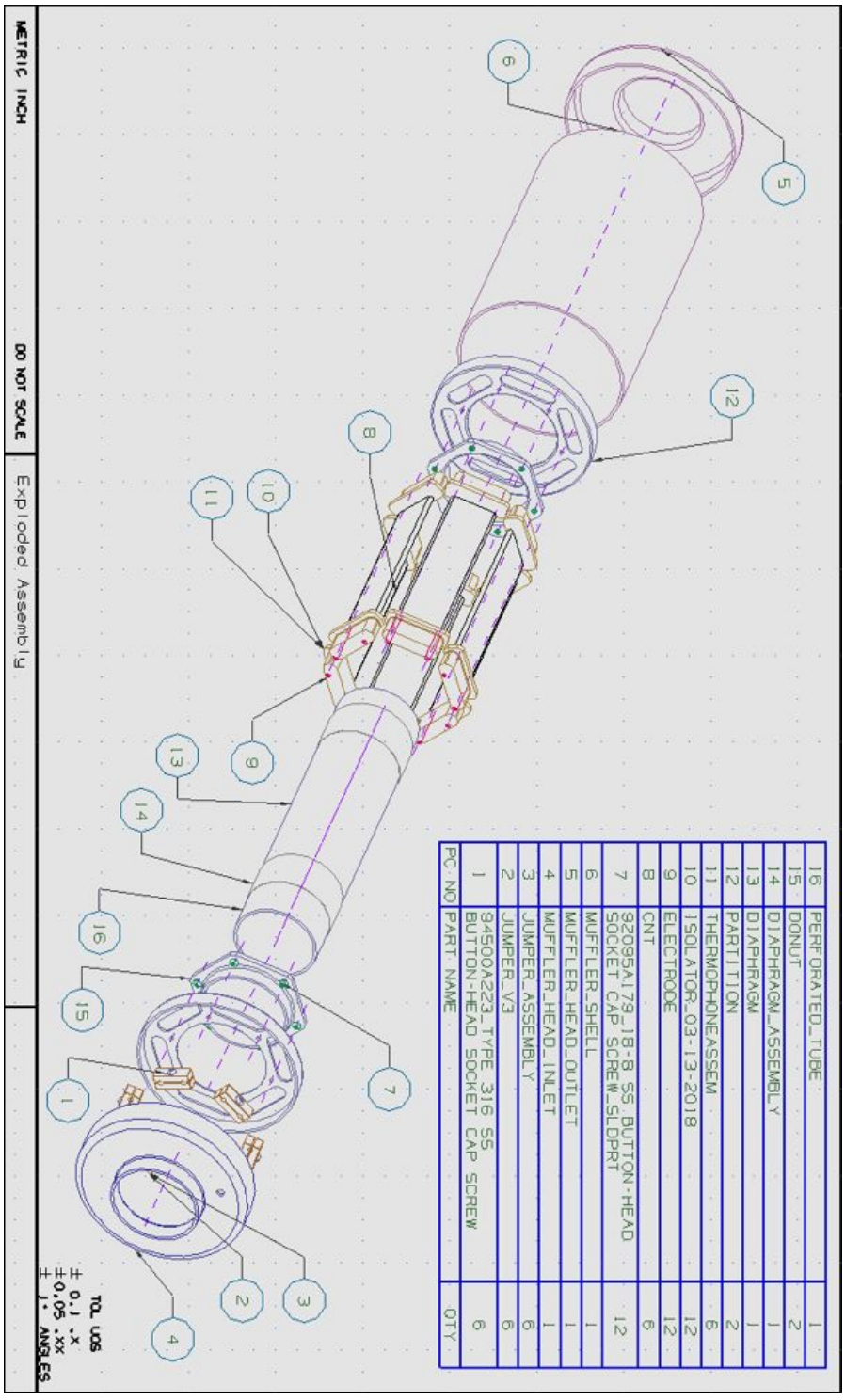

Figure 32: 3D assembly drawing of third coaxial CNT speaker prototype.

4 Methodology

4.1 Introduction

The primary focus of this research is to develop a method to model an enclosed, coaxial CNT speaker for different applications. In the start of the research, three enclosed, coaxial CNT speaker prototypes were designed and manufacture, particularly for automotive exhaust noise cancellation applications. Characterization tests were performed on these prototypes to understand their SPL performance, electrical resistance, efficiency, and manual noise cancellation performance. The design principle and components used in these prototypes are described in previous chapter.

The focus of the next step of this research shifted to modeling the CNT speakers using COMSOL Multiphysics. CNT speakers, as illustrated in Chapter 2, operate on the thermoacoustic principle. The sound generated by these speakers depends on the temperature oscillation of the CNT film due to the application of alternating current to the electrodes across which the CNT film is stretched. Based on the temperature achieved by the CNT film, the surrounding air experiences density changes and this generates sound. So, it is evident that the operation principle of CNT speakers involves Joule heating principle, thermoviscous acoustics and pressure acoustics. COMSOL Multiphysics is a tool that can model the CNT speaker while incorporating these different physics. COMSOL Multiphysics model also provides the capability to simulate the performance of the CNT speaker in the presence of flow as well as different ambient temperatures. For CNT speakers, optimization is a major factor in the success of the design and project. It is very

difficult to manufacture every single design iteration of the CNT speaker and perform characteristic testing on it. The COMSOL Multiphysics model provides the ability to simulate various design iterations and quantify their performance. Based on the optimization module, the best possible design can be selected for manufacturing and testing, reducing costs and effort.

This chapter illustrates the MATLAB model of a planar CNT speaker, particularly the setup of the model, boundary conditions used and the CNT film temperature and SPL results. A detailed description of the COMSOL Multiphysics model of the planar CNT speaker is provided in this chapter. The main goal of this is to compare the MATLAB and COMSOL results to demonstrate the understanding of the FEM of the CNT speaker.

Next, the methodology used to simulate the effect of flow on the SPL performance of the coaxial CNT speaker is discussed. It is important to understand the effect of flow on the sound field generated inside the coaxial speaker as plane waves are extremely important for noise cancellation. In addition, the model to simulate the effect of temperature of the medium inside the coaxial speaker is described.

For the enclosed design, acoustic modes are important as they can contribute positively to the SPL generated by the speaker at the modal frequencies. The experimental and simulation procedure to determine the acoustic modes are described in this chapter.

4.2 COMSOL Multiphysics Model of CNT Speaker

The COMSOL Multiphysics model is divided into two main parts: the Joule heating model that determines the temperature achieved by the CNT film and the Thermoviscous Acoustics model that simulates the SPL generated by the CNT speaker based on the temperature determined by the Joule heating model.

4.2.1 Joule Heating Model

The two physics involved in Joule heating are the electric current and the heat transfer in solids. COMSOL Multiphysics model allows the user to set the two physics involved in Joule heating to simulate the temperature oscillation of the CNT film.

The first step in COMSOL is to select the appropriate dimension in which to solve the model. Once the appropriate dimension is chosen (3D in this case), joule heating module and a time dependent study are selected. This step populates the COMSOL model with the necessary physics and then the next step is geometry creation.

In this step, geometry is created based on the dimensions of the electrodes and the CNT film area. This is done using the geometry feature in COMSOL. The geometry can be created using work plane to sketch the CNT speaker and then extruding it to the required thickness.

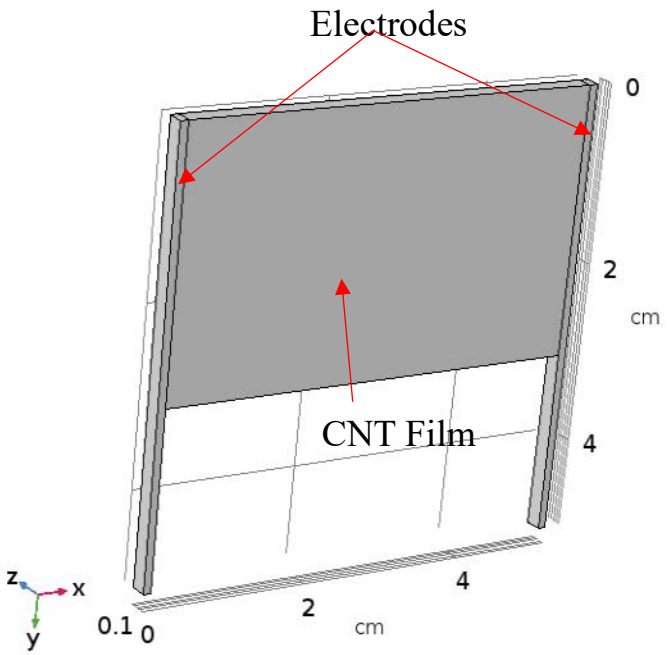

Figure 33: Planar CNT film model in COMSOL Multiphysics. The electrodes are modeled as domains and the CNT film is defined as a boundary in the model.

As shown in the above model, the electrodes are defined as solid domains on either side of the CNT film. The CNT film is defined as a boundary that is stretched between the two electrodes. In this model, the CNT film is on either side of the electrodes, i.e., the CNT speaker has a double-sided film wrap. The domain in between the CNT film is defined as air which is present in the physical double-sided planar CNT speaker. One important thing to remember when defining the model in COMSOL is that all domains must be solid to get the simulation result in that domain.

The next step is to define the materials used in the speaker. The materials are assigned under the Materials tab in the COMSOL model. For the electrodes, the obvious choice of the material is copper. COMSOL provides the flexibility to create a new material in which

one can define the material properties based on the physics that is chosen for that domain. In this case, CNT is a new material and so, using the Blank material feature, a new material was created. The material properties that are required for the new material depend on the physics which is assigned to the domain or boundary to which the new material is assigned. For the CNT film material, both the physics – electrical current and heat transfer are applied. So, the material properties for the CNT film material focuses on those properties that are essential for these two physics. The material properties and their values used in the COMSOL simulation are given in table 1.

Table 1: CNT material properties used in the COMSOL model. The material properties include all the important values necessary for the physics that are selected for the boundaries.

Property	**Variable**	**Value**	**Unit**
Density	rho	2430	kg/m^3
Heat Capacity at Constant Pressure	C_p	3168	J/(kg*K)
Thermal Conductivity	k_iso	134.45	W/(m*K)
Relative Permittivity	epsilon_iso	12	1
Electrical Conductivity	sigma_iso	10^8	S/m

CNT film has two important properties that play a major role in the surface temperature value. These properties are heat transfer due to conduction, convection, and radiation (β_o) and heat capacity per unit area (c_s), that influence the surface temperature of the CNT film. In the COMSOL model, variables are created and the above mentioned two properties are defined. These variables are assigned to the CNT film boundary defined in the model. So, during the simulation, all calculations that are performed use these variables only for the CNT film boundary and not the entire geometry.

Once all the appropriate materials are assigned in the model, the next step is to assign the correct physics and the boundary conditions to the model. The first physics in this model is the Electric Currents (EC). This physics allows the application of alternating current across the two copper electrodes and the CNT film. There are various sub-sections under the Electric Currents physics. One of them is the terminal which is the positive connection to the model. This is a boundary condition that can be applied to either the entire domain or boundary and defines the input value of the alternating current to the model. CNT speakers' operation and their surface temperature depends on the value of the input electrical power (I^2R). A sinusoidal input is defined in the terminal boundary condition for the model. An important point to note here is that the input can be defined in terms of voltage, current, or power. The second boundary condition applied is the Ground, which can be applied only to a boundary in the model. The Electric Current physics calculates the electric field and potential distributions in the model in the selected domain.

The next step of the model is to define the heat transfer from the CNT film to the ambient atmosphere. This is done by setting up the Heat Transfer in Solids (ht) module. The

definition of the boundary conditions in this physics is very important as the oscillating behavior of the CNT film surface temperature is set under this physics. CNT film acts as a thin conductor and when alternating current is passed through the film, the heat flux from the film surface is sinusoidal in nature. This was shown by Xiao et.al.[158] in their supporting material for their paper. The sinusoidal heat transfer from the CNT film to the ambient surrounding medium is given as,

$$Qo = -\kappa * k * \widehat{T_f} * [\sin(2\omega t + \varphi) - \cos(2\omega t + \varphi)] \tag{27}$$

$$k = \sqrt{\omega/\alpha} \tag{28}$$

$$\widehat{T_f} = -\frac{I^2 R}{4a} * \left[\frac{1}{\sqrt{(\beta_o + \kappa k)^2 + (\omega c_s + \kappa k)^2}}\right] \tag{29}$$

where Q_o is the instantaneous heat from per unit area from the CNT film to the surrounding, κ is the thermal conductivity of the ambient gas (W/m*K), $\widehat{T_f}$ is the amplitude of the oscillating temperature of the CNT film (K), ω is the frequency of the electrical signal (rad/s), β_o is the heat loss from the CNT film due to conduction, convection and radiation (W/m^2*K), c_s is the heat capacity of the CNT film per unit area (J/m^2*K), a is the surface area of the CNT film wrap (m^2), I is the electrical current (A), R is the resistance of the CNT speaker (Ω).

The heat transfer equation must be used a heat flux condition in the model to get the correct oscillating surface temperature. This is done by using the heat flux boundary condition under the Heat Transfer in Solids (ht) physics. It is important to note that this boundary condition is applied to only those geometry boundaries that are defined using CNT film as

material. Another important point is the amplitude of the temperature oscillation, $\widehat{T_f}$. This amplitude must be defined as a variable applied over the CNT film boundary as defined in the geometry. So, along with the variables β_o and c_s, this term is calculated and then used in the heat flux equation. In addition to the heat flux from the CNT film, the copper electrodes also lose heat to the surrounding. So, a separate heat flux boundary condition must be applied to the copper electrodes to account for their heat loss. Normal heat transfer conditions are assumed from the copper electrodes, and it is not sinusoidal in nature.

In addition to all these steps, there is one more step that must be completed before the model can be run. This step is to define the parameters important for the study. Some of these parameters are input electrical frequency (f), sampling frequency (Fs), thermal diffusivity of ambient gas (α), thermal conductivity of ambient gas (k), heat capacity of ambient gas at constant pressure (cp), and density of ambient gas (ρ). These parameters are defined in the model using the Parameters option under Global Definitions. Defining any parameter or variable under the Global Definitions applies it to the entire model and not just a particular boundary or domain.

Once all these steps are completed, the model is ready to be meshed and then run. The meshing of the model can be done using either tetrahedral or quad elements. It is important to make sure that there are enough elements in the model to have a proper resolution of the temperature oscillation of the CNT film. The size of the mesh elements can be chosen by the software based on the physics that are used in the model or the size can be defined manually by the user.

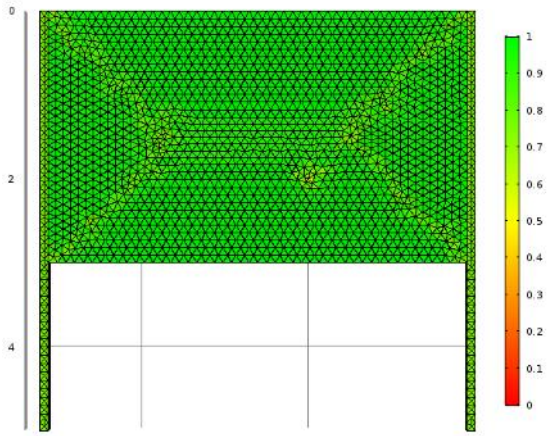

Figure 34: The mesh element quality plot based on the skewness of the mesh elements. In the legend, a value of 0 is extremely bad mesh element while a value of 1 indicates good mesh element.

Once the meshing is done, the last step is to setup the study to run the model to get the necessary results, in this case, the surface temperature of the CNT film. Based on whether time dependent or frequency domain study is selected, the necessary evaluation parameter (time or frequency) is used as input to complete the study. Once the run has been completed, the results are presented under the Results section of the model. The completed model builder for the Joule heating model looks like that shown in figure 35.

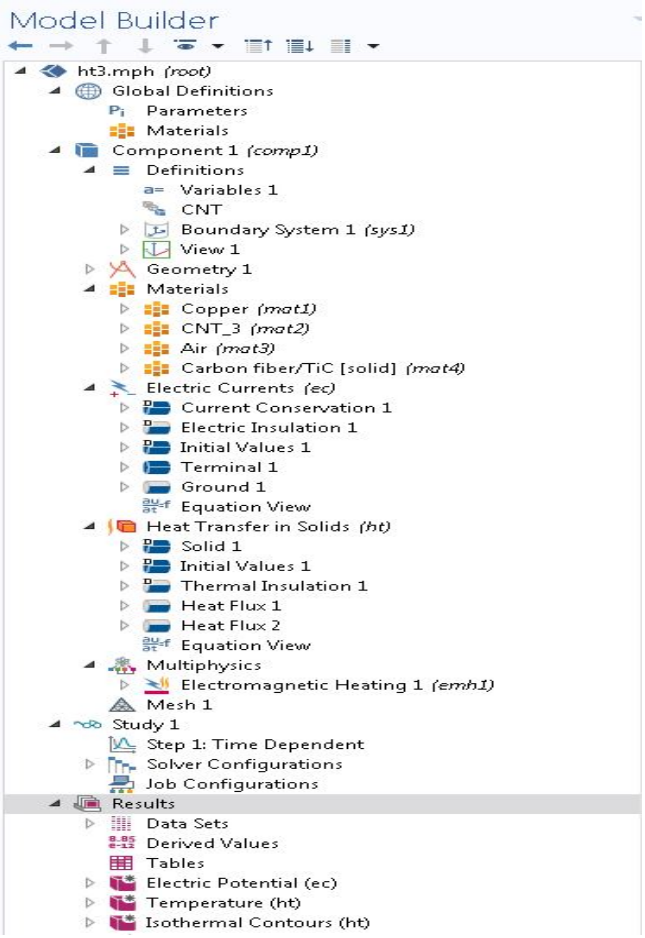

Figure 35: The fully setup model builder for the Joule heating model of the CNT speaker. All the parameters, variables, physics, mesh, and study are completely defined as seen in the model builder.

4.2.2 Thermoacoustics Model

Once the temperature results are obtained from the Joule heating model, the next step is to use the temperature result as an input to the Thermoviscous Acoustics-Pressure Acoustics model to simulate the SPL performance of the CNT speaker. An important point to note is that both the models – Joule heating and Thermoviscous Acoustics-Pressure Acoustics models cannot be used simultaneously. The Joule heating model must be run first and then

the Thermoviscous Acoustics-Pressure Acoustics model to get the SPL simulation result of the CNT speaker.

The base geometry used in this model is the same as the one used in Joule heating model. So, there are two copper electrodes, and the CNT film is stretched between them and defined as boundaries. In addition to this, there are two things included in the model. The first one is two thin air domains next to the CNT film boundaries, one on each side for a double-sided wrapped CNT speaker. In the operation of thermoviscous acoustics, there is a generation of thermal and viscous boundary layers in the thermoviscous domain. These layers are generated close to the boundary of the material that operates on the thermoviscous acoustic principle, in this case, the CNT film. So, these boundary layers must be accounted for in the model when it is simulated for the generation of the sound. The thermal and viscous boundary layer thicknesses are calculated as,

$$\delta_{visc} = \sqrt{\frac{2\mu}{\omega\rho_0}} \tag{30}$$

$$\delta_{therm} = \sqrt{\frac{2k}{\omega\rho_0 c_p}} \tag{31}$$

where δ_{visc} is the viscous boundary layer thickness (m), δ_{therm} is the thermal boundary layer thickness (m), μ is the dynamic viscosity of the surrounding medium (Pa-s), ω is the angular frequency of the sound (rad/s), ρ_0, k and c_p are the density, thermal conductivity, and specific heat at constant pressure of the surrounding medium.

From the above equations, the thicknesses of both the boundary layers depends on the frequency of the sound. So, for a study with multiple frequencies, these values will change

with frequency. In addition, if the surrounding medium changes, it will change these values for the same frequencies. When creating the geometry with the air domain (in this case as surrounding medium) around the CNT film boundary, care must be taken to make sure that this changing thickness is accounted for during simulation. One way to do this is to calculate the thicknesses with respect to the frequencies that are going to be simulated and then assign the maximum thickness value to the air domain around the CNT film. Another way to account for this is to create a parameter under Global Definitions that will calculate the thickness of the boundary layer and update the geometry for every single frequency value used in the simulation. The second method model will take considerably longer time to run but it will be more accurate in its representation of the thermoviscous acoustic domain and SPL generated. In the model that is explained in this study, a constant thickness of the thermal boundary layer is selected to create the air domain surrounding the CNT film boundary.

Another addition to the geometry in this model is the air domain surrounding the entire CNT speaker. The sound generated by the CNT speaker is propagated out into the surrounding medium. So, unlike the Joule heating module where the surrounding medium was set as air by default, in this model, it is necessary to define the surrounding domain. One of the reasons for this is the principle of sound propagation from a source into the surrounding. It is known that there are different fields created in the surrounding medium when sound is generated by a source. These fields are near field, far field, direct field, and reverberation field. The SPL reduces by 6db per doubling of distance in the direct field. In the reverberation field, this change is insignificant with respect to distance. In addition to the effect of distance on the SPL, the directivity of the speaker is also important and must

be modeled in COMSOL. To perform all these tasks, an additional air domain is modeled around the CNT speaker. The model with air domain surrounding the CNT film and the sphere surrounding the entire CNT speaker is shown in figure 36 and figure 37.

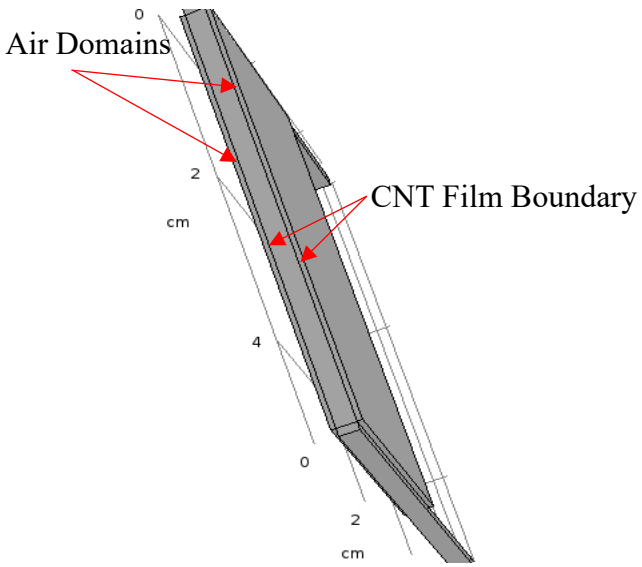

Figure 36: The CNT speaker geometry with the air domain surrounding the CNT film. This air domain is used to define the thermoviscous acoustic physics for SPL generation via temperature oscillations.

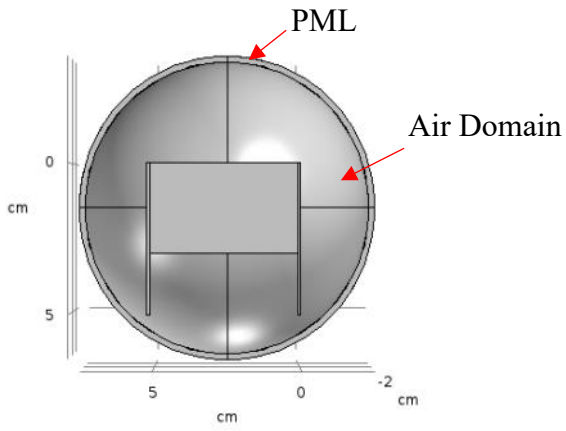

Figure 37: The surrounding medium modeled as a sphere around the CNT speaker. The air domain is shown as hollow because it is a cut section of the geometry. It is a solid spherical domain.

In the above figure 37, there is a layer around the sphere labeled as PML. PML means a Perfectly Matched Layer, an absorbing type of boundary. During the physical operation of the CNT speaker, the surrounding medium is infinite for an open speaker. So, the sound waves will travel till their amplitude is reduced to a negligible value. If this were to be replicated in simulation, it would make the model and the mesh elements insanely large in number and impossible to solve completely. So, to make the model manageable and reduce the simulation time, the surrounding air domain is truncated using the PML. PML terminates the sound waves at the boundary, providing a reasonable approximation of free space and provides a set of boundary conditions. The diameter of the air domain sphere and the thickness of the PML is selected based on the distance from the CNT film at which the SPL is to be determined.

Once the geometry is completed along with the surrounding domain, the next step is to assign the appropriate materials to the correct domains and boundaries. The CNT material is assigned to the interior boundaries shown in figure 36. Copper is assigned to the two electrodes and the remaining domains are assigned as air. This completes the material assignment to the model.

The next step is setting up the physics – thermoviscous acoustics, frequency domain (ta) and pressure acoustics, frequency domain (acpr) to simulate the SPL generated by the CNT speaker. The ta domain is setup in the air domains that are defined next to the CNT film boundary. All the thermoviscous acoustics calculations are performed in this selected air domain. CNT speakers, as mentioned earlier, generate sound through heat based on the temperature oscillation of the CNT film. The temperature oscillation of the CNT film is obtained from the previous Joule heating model. This temperature value is used as input to the interior temperature variation boundary condition in the ta module. This boundary condition is applied only to the CNT film boundaries defined in the model. Now, the temperature variation of the CNT film is sinusoidal in nature. It has been observed that the average value of the surface temperature oscillation of the CNT film depends on the input power value and not the input electrical frequency. Higher the input power, higher is the average value of the CNT film surface temperature. So, either the average value or the maximum value of the surface temperature of the CNT film is used as input to simulate the SPL generation by the CNT speaker.

Once the ta physics has been completely defined, the next step is to define the pressure acoustics physics in the model. All the remaining domains – copper electrodes, surrounding

spherical air and PML are to be included in the pressure acoustics physics. The coupling between the ta and acpr domains calculates the SPL generation by the CNT speaker. Care must be taken when assigning the domains to this physics that the ta domains are not selected. If they are selected, then the model will not run as COMSOL will not be able to distinguish between the two physics for same boundaries and domains. The sound wave will be propagated from the end of the ta domain into the spherical acpr domain. In addition to the SPL generated by CNT speaker, the spherical air and PML domains can be used to simulate the far field response of the speaker and its directivity. This can be done using the far field calculation option in the pressure acoustics physics. The far field calculation radiates the sound in the pressure acoustics domain and determines the directivity of the sound from the CNT speaker.

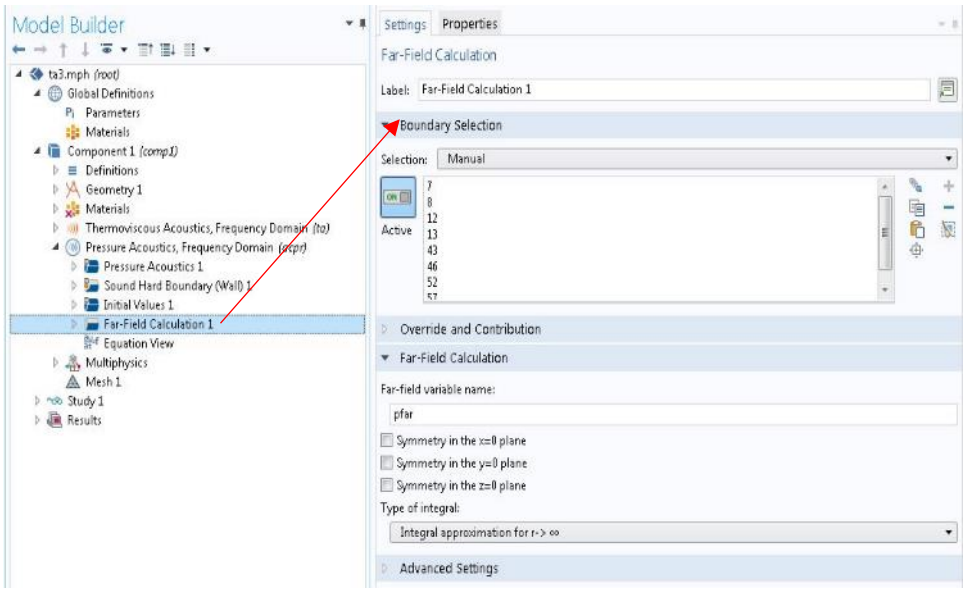

Figure 38: The setup of the pressure acoustics physics in the COMSOL model. The far-field calculation can be added and used to calculate the directivity of the CNT speaker. The boundaries selected are the end boundaries of the surrounding medium domain.

All these steps complete the physics setup of the CNT speaker model. Once this is done, the next step is to mesh the model. The steps involved in the meshing of the SPL model are like that of the Joule heating model. There are two major differences in the meshing of the SPL model compared to that of the Joule heating model. First, the boundary layers must be included in the mesh with the help of boundary layers' mesh. The boundary layer mesh incorporates the thermal boundary layers that are created next to the CNT film due to the thermoacoustic effect. There are two parts to setup the mesh (figure 39). In the first part, the domain in which the boundary layer mesh elements must be created is selected. For this model, the air domain defined for the ta physics that is next to the CNT film is selected. The next step is to define the boundary layer properties which is done by selecting the CNT film boundaries. The boundary layer properties that must be defined are the number of boundary layers, and the thickness of the first layer. The thickness of the first layer can be estimated from the thermal boundary layer value calculated by the equation 31. The rest of the model can be meshed using the tetrahedral or triangular elements. The quality of the mesh can be estimated using similar procedure described in the Joule heating model.

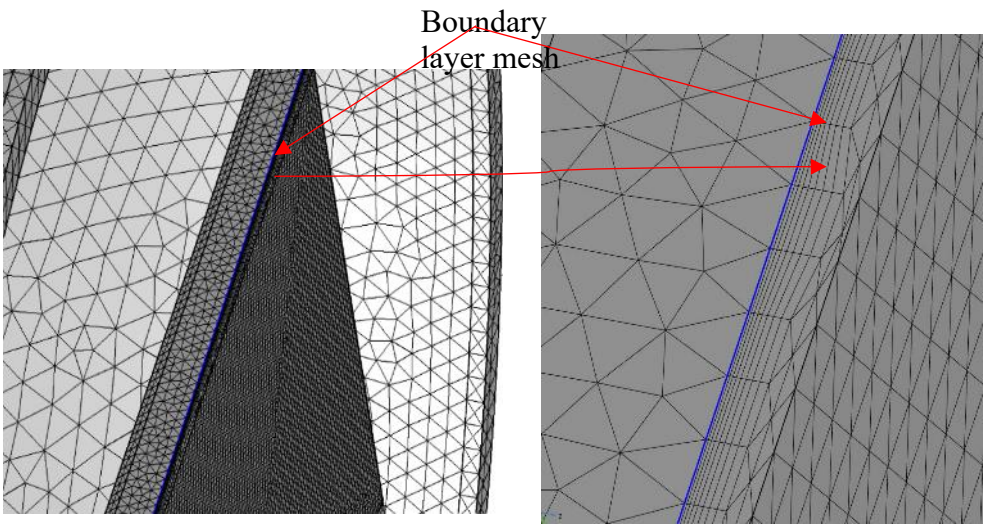

Figure 39: Boundary layer mesh in the SPL model of the CNT speaker. The boundary layer mesh is created in the domain defined by the thermoviscous acoustics physics next to the CNT film boundary.

The last step of the model is to set up the study and then run the model. In the study step, the frequency at which the model must be run is defined. The results that are calculated after the model has been run are the acoustic pressure, sound pressure level (with respect to the reference pressure defined) from the pressure acoustics physics and the acoustic pressure, velocity, and temperature from the thermoviscous acoustics physics.

This modeling procedure described above can be used for any design of the CNT speaker with any medium surrounding the CNT speaker. So, the enclosed, coaxial CNT speaker was also modeled using this procedure.

4.3 Finite Element Modeling

The main objective of this modeling is to understand the process that goes behind the COMSOL Multiphysics software, particularly the processes involved in finite element analysis of the enclosed, coaxial CNT speaker model. The two parts modeled are: Joule Heating and Themoviscous Acoustics.

4.3.1 Joule Heating Model

There are two physical domains involved in the Joule heating physics: electrostatics and heat transfer. The electrostatics physics calculates the electric potential across the CNT film due to the applied electric current across the copper electrodes between which the CNT film is wrapped. The electric potential generates heat in the CNT film due to its resistance to the flow of electric current. This heat generated is then radiated out to the ambient medium (air in this case) by conduction, convection, and radiation from the CNT film surface. This transfer of heat is modeled using the heat transfer physics. So, the coupling between the two physics is one-way: temperature of the CNT film depends on the electric potential and not reverse.

For simplicity, a 2D CNT speaker model was used for this process. The governing equations for the electrostatics and heat transfer physics in 2D are given as,

$$-\frac{\partial}{\partial x}\left(G_x \frac{\partial V}{\partial x}\right) - \frac{\partial}{\partial y}\left(G_y \frac{\partial V}{\partial y}\right) = 0 \tag{32}$$

$$-\frac{\partial}{\partial x}\left(k_x \frac{\partial T}{\partial x}\right) - \frac{\partial}{\partial y}\left(k_y \frac{\partial T}{\partial y}\right) = Q(x,y) + F(x,y) \tag{33}$$

where G is the electrical conductivity, V is the electric potential, k is the thermal conductivity, T is the temperature of the CNT film, Q is the heat generated due to the application of the electric potential and F is the heat flux. In the electrostatics equation, the variable to be calculated is the electric potential V and in the heat transfer equation, the variable to be calculated is the temperature T.

To model the Joule heating physics, the standard procedure is followed. First, the above equations are converted into their weak forms using the Galerkin method. In this method, the residuals of the PDEs (all the terms on the left-hand side with the right side as zero) are multiplied by a weight function (w_i) and integrated over the area. The integration equations are then simplified using integration by parts and an approximate solution is defined for the variables V and T. The solutions defined are of the form

$$V = \sum_{i=1}^{n} V_i * \varphi_i \tag{34}$$

$$T = \sum_{i=1}^{n} T_i * \varphi_i \tag{35}$$

where n is the number of nodes of the mesh elements, φ_i is the shape function used to interpolate the data between the nodes. In the Galerkin method, the shape function and the weight function are the same. So, substituting the assumed solutions in the weak form, the stiffness, temperature, and source matrices are determined based on the mesh elements. For

isotropic material, the value of k in the x and y directions are the same. The final equation that is solved for determining the electric potential and temperature is

$$[G]_e * \{V_i\}^e = \{p^e\} \tag{36}$$

$$[k]_e * \{T_i\}^e = \{F^e\} + \{Q^e\} \tag{37}$$

The next step is to define the boundary conditions for each physics. For the electrostatics physics, sinusoidal voltage is applied at one end boundary while for the heat transfer physics, the vertical end boundaries are at ambient temperature and the CNT film boundaries have a heat flux defined by equations (38-40). Once the boundary conditions are applied, the matrix equations are solved to obtain the electric potential across the CNT film and the surface temperature of the CNT film.

4.3.2 Thermoviscous Acoustics Model

The modeling of thermoviscous and pressure acoustics involve the generation of acoustic wave due to thermal effects, particularly the temperature of the CNT film. The modeling process is divided into three parts: thermoviscous acoustics, acoustic-structure interaction, pressure acoustics.

The thermoviscous acoustics results in the generation of the thermoacoustic wave with pressure, velocity, and temperature as the main parameters. The thermoviscous acoustics physics exists in a very narrow region of the medium surrounding the thermoviscous element. In the case of the CNT speaker, the thermoviscous element is the CNT film and the thickness of the surrounding medium is proportional to the thermal boundary layer. The

root mean square value temperature of the CNT film obtained from the Joule heating simulation is used as the temperature boundary condition for the thermoviscous acoustic physics. There are a couple of assumptions made when sound propagation is considered in a thermally conductive fluid:

1. Linearity and time harmonic wave behavior
2. Medium is considered uniform and without flow
3. The medium is considered as ideal fluid and and it follows the Fourier's law of heat conduction

Based on these assumptions, the governing equations for the thermoviscous acoustics are the time harmonic linearized Navier Stokes equations of mass, energy and momentum equations given as,

$$i\omega\rho + \rho_0 \nabla . v = 0 \tag{38}$$

$$i\omega\rho_0 C_p T - \lambda \Delta T - i\omega p = 0 \tag{39}$$

$$i\omega\rho_0 v = -\nabla p + \left(\mu_B + \frac{4}{3}\mu\right)\nabla(\nabla . v) - \mu \nabla x \nabla x v + f \tag{40}$$

where medium properties are density ρ_0, specific heat at constant pressure C_p, thermal conductivity λ, shear viscosity μ, and bulk viscosity μ_B.

These NS equations are converted into their weak form using the Galerkin method: multiplication with a weight function and integrated over the surface. The domain is discretized and shape functions for the thermoviscous acoustic variables pressure p, velocity v, and temperature T are defined. The shape functions are Lagrangian shape

functions. The FE matrix formulation is evaluated and the thermoviscous acoustic pressure, velocity and temperature are obtained.

The second step is the coupling between the thermoviscous acoustic and the pressure acoustic domain via the CNT film boundary. This is done using the BEM for acoustic structure interaction. The structure boundary must be flexible and thin enough for this process to work successfully.

The pressure acoustic domain is defined extending outward from the structure. Separating the thermoviscous and pressure acoustic domains using the structure boundary reduces the computation time as well as provides a good approximation of the acoustic wave generated by the thermoviscous acoustics physics and the structure, which in this case is the CNT film. The governing equations for the pressure acoustics physics are given as,

$$\nabla.\left(-\frac{1}{\rho_c}(\nabla p_t - q_d)\right) - \frac{k^2{}_{eq} p_t}{\rho_c} = Q \tag{41}$$

$$k^2{}_{eq} = \left(\frac{\omega}{c}\right)^2 \tag{42}$$

4.4 Acoustic Modal Analysis of the Enclosed, Coaxial CNT Speaker

When sound travels through any enclosed structure, there is resonance due to the geometry and dimensions of the structure. The same is true when sound is generated inside an enclosed geometry. This phenomenon, in acoustic terms is known as acoustic resonance. The resonance has a dual effect on the sound generated in the enclosed geometry. If there is constructive interference at the acoustic resonant frequency between the sound inside the speaker and sound generated due to acoustic resonance, the net result is increase in the SPL. If there is destructive interference between the above-mentioned sounds, it will result in decrease in the SPL. So, if the acoustic resonant frequencies are properly defined, they can be used to increase the SPL of the enclosed acoustic structure.

The coaxial CNT speaker designed, tested, and simulated is a closed type of CNT speaker. From previous research, it has been observed that the SPL of a closed CNT speaker decreases with increase in the frequency. However, for the enclosed, coaxial speaker, experimental results show that there is increase in SPL at certain frequencies while a reduction in SPL at other frequencies. This was observed for a frequency range of 50Hz-500Hz in $1/3^{rd}$ octave bands. One of the reasons for this was assumed to be the acoustic resonance due to the geometry of the CNT speaker. Also, the coaxial CNT speaker is not completely enclosed. The pipe that runs through the speaker has slots that are covered using a heat resistant diaphragm. Due to this, the volume between the outer cover and the heat resistance diaphragm is changing by a very small amount. So, to understand if the SPL behavior of the enclosed, coaxial CNT speaker was influenced by the acoustic resonance,

an acoustic modal analysis was performed experimentally and the COMSOL model was used to simulate the SPL at the resonant frequencies found in the experiment.

For the experiment, two condenser microphones were placed at either ends of the coaxial CNT speaker. These microphones measured the SPL at the two ends of the CNT speaker. To determine the acoustic modes of the enclosed, coaxial speaker, first a broadband signal was used as input to the speaker in the frequency range of 20Hz-10kHz. The sound generated by the speaker was measured and a FRF was constructed between the SPL and the input signal in terms of power. Coherence was calculated between the SPL and the input signal, and it was observed that there was very poor coherence across the frequency range. So, a sine chirp was used as input to the CNT speaker to determine its acoustic modes and frequencies. The frequency range of the sine chirp signal was from 20Hz-20kHz. Sound pressure level measurements were made for the speaker output. Three power levels were used for this experiment. The main goal of testing at three different power levels was to ensure that the speaker had good repeatability at different power levels, especially in terms of the sound pressure profile and acoustic modal behavior. The experimental setup is shown in figure 40.

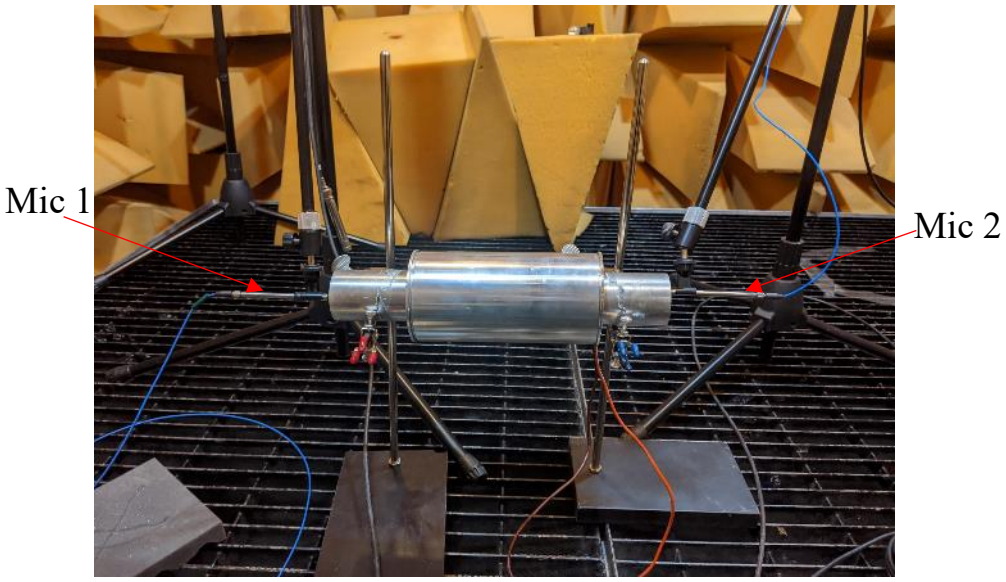

Figure 40: Experimental setup for acoustic modal test. Two microphones are placed at the two ends of the speaker. A sine chirp signal was used as input to the CNT speaker.

Once the FRF was plotted for the experimental test performed, a simulation was performed of the coaxial CNT speaker in COMSOL. For one input power value selected from the experimental test, SPL generated by the CNT speaker was simulated for several frequencies selected from the FRF. A comparison was made between the FRF values and the simulated values for the selected frequencies. The main reason to perform this comparison was to validate the CNT speaker COMSOL model and to make sure that the acoustic modal behavior of the actual CNT speaker was accurately replicated in the COMSOL model. One point to note here is that the simulation was performed at individual selected frequencies and not using a sine chirp. It is extremely difficult to set up a sine chirp signal in COMSOL and so, to save time and reduce complexity, individual frequencies were simulated.

4.5 Axial, Cross-sectional and Industry Standard Measurement

The enclosed, coaxial CNT speaker generates sound radially that is then propagated along the length of the speaker. This sound is then radiated from the two ends of the speaker out into the surroundings. One of the main purposes of the coaxial speaker was to cancel the automotive exhaust noise inside the coaxial speaker. So, the axial SPL generated by the CNT speaker is very important. Also, the cavity created due to the outer cover adds acoustic resonance to the CNT speaker. Along with this, there is a slotted pipe that extends through the length of the coaxial speaker. So, it is crucial to consider the frequencies where cross modes are generated. Cross modes are difficult to cancel and so, it is important to understand the cross-section SPL generated by the coaxial speaker. In the automotive industry, sound generation ability of a loudspeaker or the sound through the exhaust tailpipe is measured at a specific distance and angle from the radiating surface. This distance is 500mm and the angle is 45^{o}. A measurement made at this location is as per the automotive industry standard. This measurement is very useful for comparison with a loudspeaker that is generating sound at the same input power level.

For the measurement of the axial, cross-sectional and industry standard SPLs, the enclosed, coaxial CNT speaker was placed in the anechoic chamber. For the axial SPL measurement, a PCB probe microphone (377B26) was used for the SPL measurement. The probe of the microphone was positioned at three locations along the longitudinal axis of the CNT speaker. Care was taken to ensure that the probe was not touching the CNT film at any location. For the cross-sectional SPL measurement, the face of the end pipe of the speaker

was divided into 17 points – 1 point in the center of the end pipe and 8 points in two concentric circles (figure 41). The probe microphone was positioned at every single point and SPL measurement was made. For the industry standard measurement, a PCB condenser microphone was positioned at 45° and 500mm from the face of the end pipe. AC input power of 100W was used as input to the CNT speaker. The frequency ranges for the three SPL measurements were from 100Hz-500Hz in 1/3rd octave bands. For the cross-sectional SPL measurement, two additional frequencies were tested: 4000Hz and 6300Hz.

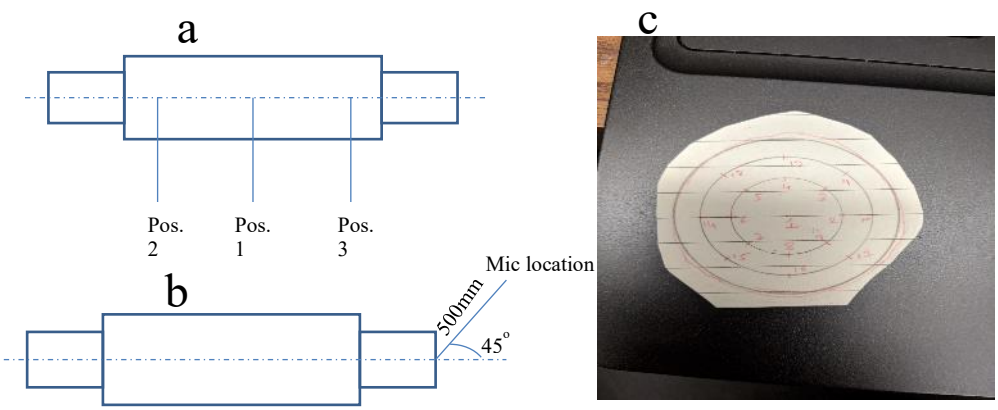

Figure 41: Axial SPL measurement locations (a), industry standard SPL measurement locations (b), points used to measure the cross-sectional SPL across the face of the end pipe of the CNT speaker (c).

4.6 Effect of flow on the acoustic of the coaxial CNT speaker

The main aim of the enclosed, coaxial CNT speaker was to cancel and/or attenuate the automotive exhaust noise. The coaxial design allowed the exhaust gases to travel through the speaker without any change in the flow direction or obstruction, thus eliminating the generation of backpressure. So, in actual operating conditions, there is flow of exhaust gases through the coaxial CNT speaker. All simulations and experimental measurements were made in the anechoic chamber in the absence of flow. It was observed that a plane acoustic wave field was generated inside the speaker along its length in the absence of flow. It is expected that when the sound is generated in the presence of flow, there will be a change in the plane wave field as well as change in the SPL observed inside the speaker. This will affect the sound that is radiated out from the two ends of the coaxial speaker. To understand this phenomenon and its effect, COMSOL simulation was performed on the coaxial speaker model in the presence of flow.

The setup of the flow model is significantly different from the Joule heating and Thermoviscous Acoustics models. The flow model is split into two parts. The first part simulates the flow field inside the speaker along its length. The Turbulent flow physics is used to simulate the background flow through the coaxial speaker. The flow simulation is performed for varying Mach numbers. The results of this model are the mean flow velocity, pressure and turbulent viscosity. Once these variables are obtained, the next step is to setup the acoustics model to get the sound pressure level and sound field profile in the presence of flow. This is performed using the Linearized Navier-Stokes physics. The result of this

simulation can then be used to understand the effect of varying Mach number flows on the sound pressure level and acoustic field inside the CNT speaker.

The variables – mean flow velocity, pressure and turbulent viscosity obtained from the turbulent flow model must relate to the Linearized Navier Stokes model. This is done by a process called mesh mapping. Mesh mapping is used to map the solution from one physics to another physics and is a remeshing analysis technique. Generally, mesh mapping is used when the original mesh elements are severely distorted and thus cannot discretize the model to the desired degree of accuracy. In the case of the CNT speaker model, mesh mapping helps to reduce the overall time required to simulate the combined model as well as provides the flexibility to run the two physics individually. This helps to change any elements of the model that can show errors as well as help to improve the accuracy of the CNT speaker model. In addition, the turbulent flow module requires a finer mesh to account for the boundary layers created along the walls of the pipe as well as to accurately resolve the flow parameters. For the acoustic simulation, there is no need for an extremely fine mesh as compared to the turbulent flow model. So, mesh mapping helps to separate out the two meshes required to discretize the model, thus reducing the overall simulation time.

Mesh mapping must be done very carefully as the two physics are not solved on the same computational mesh. So, if the variables are not correctly mapped from the CFD mesh to the acoustic mesh, it will result in errors due to non-physical noise being introduced in the acoustic solution. In COMSOL, to map the solution from the CFD physics to the acoustics physics, a separate study known as the mapping study is used. This study makes use of an

additional equation that maps and smooths the flow variables. The mapping equations for the CFD computed variables are set up using the Weak Form PDE interface found in the mathematics branch of the COMSOL software. The mapping equations used for this are,

$$p_{0,aco} - p_0 = \delta h^2 \nabla\left(\nabla p_{0,aco}\right) \tag{43}$$

$$u_{i,0,aco} - u_{i,0} = \delta h^2 \nabla\left(\nabla u_{i,0,aco}\right) \tag{44}$$

$$\mu_{T,aco} - \mu_T = \delta h^2 \nabla\left(\nabla \mu_{T,aco}\right) \tag{45}$$

where p_0, u_0 and μ_0 are the flow pressure, velocity and turbulent viscosity variables, $p_{0,aco}$, $u_{0,aco}$ and $\mu_{T,aco}$ are the acoustic pressure, velocity and turbulent viscosity variables, δ is a control parameter and h^2 is the mesh element size squared. The smoothing of the CFD variables is achieved by the terms on the right-hand side of the above equations using isotropic diffusion. The amount by which the smoothing is achieved is controlled by the control parameter δ and the mesh size squared term h^2. The control parameter can be tuned based on the smoothing required for the CFD physics calculated variables. These three equations are implemented in COMSOL using a special operator known as withsol() operator. This operator retrieves the values of the CFD variables from the CFD mesh and interpolates it correctly to the integration points on the acoustic mesh. This step is very important because the number and size of mesh elements are different for the CFD and acoustics mesh.

There is an easy method to check how good is the mapping of the CFD variables on the acoustic mesh. This is done by observing the 1D mapping comparison plot that compares the CFD variables and the acoustic mesh variables mapped from them. If both the variables follow each other closely in terms of profile and values, then it can be safely inferred that the mesh mapping has been successful. This can be observed in the plots shown in figure 42.

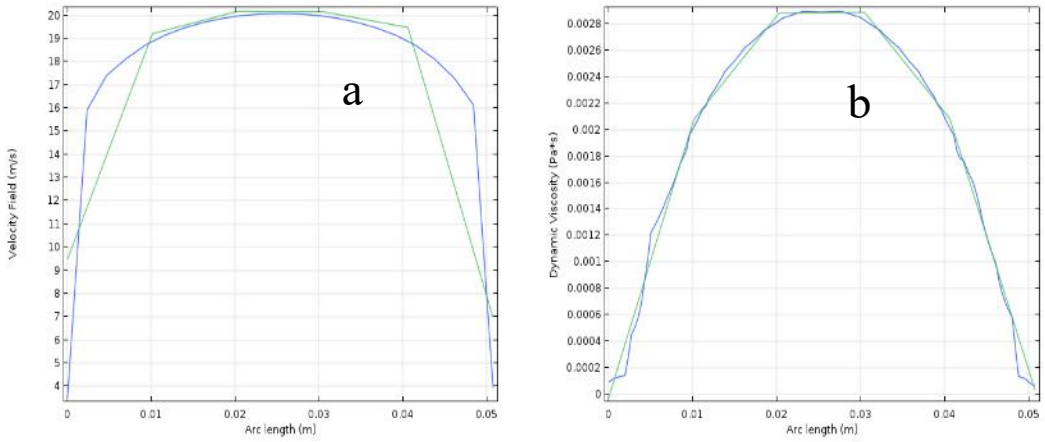

Figure 42: Mapping comparison between the flow velocity (a) and dynamic viscosity (b) for the CNT speaker flow model. There is good correlation between the variables, both in terms of value and profile.

For the Linearized Navier Stokes physics, the sound that is produced by the CNT speaker must be submitted as an input to simulate the flow effect on the sound field thus generated. For this, the thermoviscous acoustics simulation results are used. The SPL and the plane wave that is obtained from the simulation in the absence of flow is defined as an input in the Linearized Navier Stokes physics. This sound profile is applied in the domain in which the CNT film is defined as a boundary (figure 43). Defining this sound source will make

sure that SPL results obtained in the presence of flow will mirror the expected performance of the speaker when it is physically operated in the presence of flow.

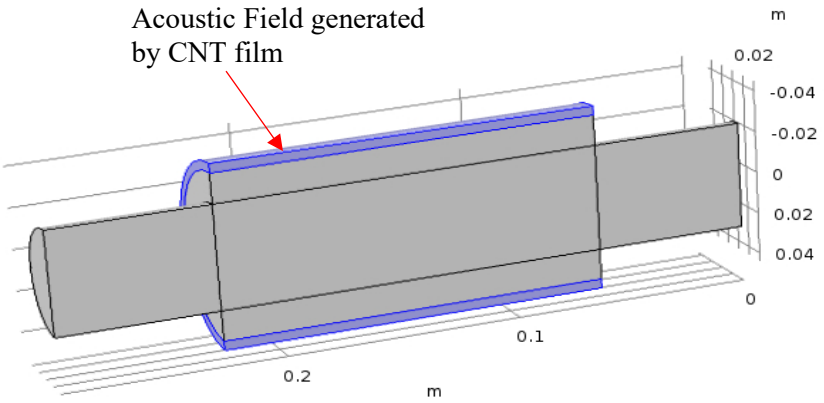

Figure 43: Background acoustic field (blue region) based on the simulation result of the Thermoviscous Acoustics model. This field acts as the sound source in the flow model.

4.7 Optimization of the CNT speaker model using COMSOL

One of the main goals of a design process is to optimize the design of a product to satisfy one or more design requirements. Optimizing a design provides with the best possible solution to a design problem, whether be it dimensions, performance, input requirements, etc. In addition, it also helps save considerable amount of time required to model and simulate every single design iteration of the desired product.

Control variables are values that can be changed to find an optimal solution to the design problem. These variables can be dimensions, input parameters such as power, voltage, force, etc. and output parameters such as SPL, efficiency, etc. The solution of the optimization problem is the set of values assigned to the control variables. The objective function is based on the control variables. When the control variables are changed during the optimization process, a single valued solution for the objective function is obtained. The optimizer module then works on maximizing or minimizing this value based on the end goal of the optimization process. At the desired value of the optimizer function (maximum or minimum), the corresponding values of the control variables are the ideal values for obtaining the desired performance.

Now during the optimization process, the control variables have values that are changed. However, if there is no restriction to the change in their values, the optimization process would continue forever. Also, it might result in values that are not feasible. To prevent this and to get feasible values, constraints are set on the control variables. These constraints are

generally upper and lower bounding values (ranges) within which the control variables are defined. This provides a feasible set of values for the control variables which can then be used to optimize the design problem.

The optimization module in COMSOL is a very useful tool as it can link the simulation result to the optimization problem. In this module, any input of the COMSOL model such as dimensions, material properties, or material distribution can be assigned as control variables. The objective function in the optimization module can be any model output such as SPL, current, velocity, etc.

There are two main types of optimization algorithms available in COMSOL – gradient free and gradient based. The primary difference between these algorithms is the way in which optimization is performed and the type of problem present for optimization. Gradient based algorithms use gradient or slope during every single iteration to determine if that control variable value is the best compared to the previous value. If there is a local minima or maxima in the function, it will result in a gradient of zero and the algorithm might get stuck. In addition, if there is a discontinuity in the objective function, it will result in an error in the optimization. In these situations, a gradient free algorithm is the best to obtain the optimum design parameters. Another important parameter in the selection of the correct optimization algorithm is the presence of a range for the control variable values. Gradient based algorithms cannot handle optimization problems that have a defined lower and upped bound to the control variable values.

COMSOL has three gradient based algorithms – SNOPT, MMA and Levenberg-Marquardt. The three gradient free algorithms are – Nedler-Mead, BOBYQA and

COBYLA. Ideally, if your optimization problem is correctly defined, all the algorithms should result in solution that is nearly identical.

For this study, two optimizations were performed. First, a simple expansion chamber was optimized to achieve the length and diameter of the central chamber that would result in the highest transmission loss. The control variables used were the length and diameter of the central chamber. Once the optimized dimensions were obtained, the transmission loss was recalculated and compared with the original as well as the optimized result. The main purpose of this was to validate the optimization process. Based on this, optimization was performed to determine the best possible dimension combination for the coaxial CNT speaker.

5 Results and Discussion

5.1 Joule Heating Model

The main result of the Joule heating model is the surface temperature oscillation of the CNT speaker. This temperature oscillation is very important as it is responsible for the generation of the sound from the CNT speaker. An enclosed, coaxial CNT speaker with a resistance of approximately 3Ω was simulated at an input power of 200W. The surface temperature oscillation result for the Joule heating model is shown in figure 44.

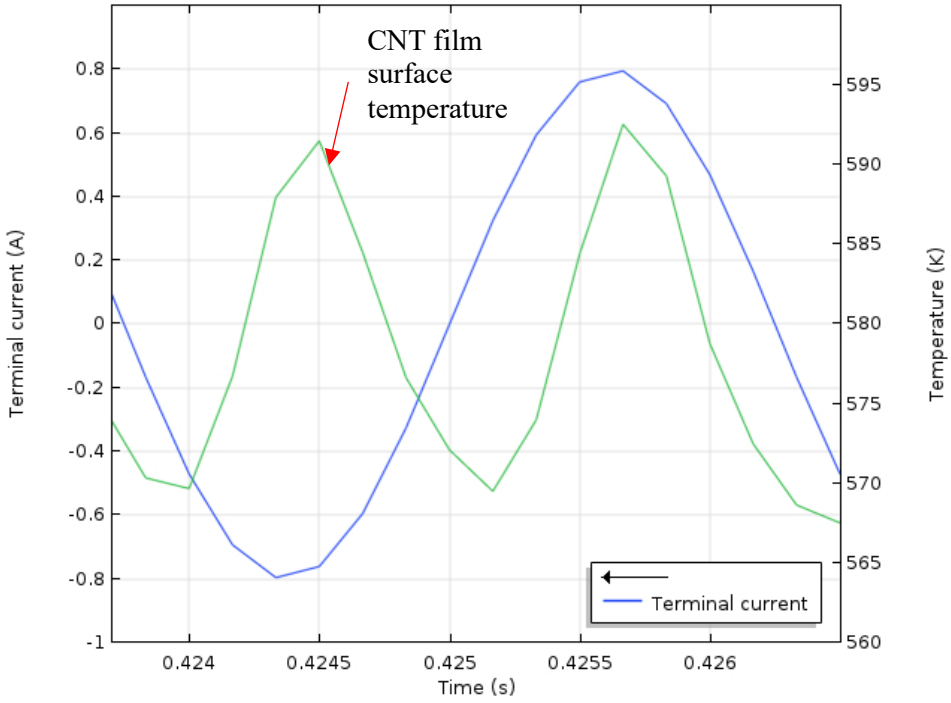

Figure 44: CNT film surface temperature from the Joule heating COMSOL model. The terminal current is the input alternating current to the CNT speaker.

It can be clearly seen that the frequency of the temperature oscillation is twice the frequency of the input electrical current. This is a point of validation for the model as CNT

speakers operate on input power and so, they double the frequency on the output side. In addition, it was also observed that the sinusoidal temperature oscillation profile of the CNT film surface temperature was replicated successfully using the COMSOL model. Another observation with regards to the Joule heating module was the definition of the input electrical signal to the model. As mentioned before, there are four ways in which the electrical input can be defined: voltage, current, power, and electrical circuit. It was observed that all the four input methods generated temperature results that were sinusoidal in nature with very little variation in amplitude (<+/-5K). Either of the four methods could thus be used as input to the model. However, care must be taken to make sure the amplitude used in the input should agree with the basic electrical circuit laws.

Another important observation with respect to the surface temperature of the CNT film is its behavior with respect to frequency. It is observed that for different frequencies, the mean value of the surface temperature remains the same. The only change observed is the maximum and minimum amplitudes (both same in value) of the sinusoidal surface temperature. With change in frequency, this value undergoes change (increases), but the average temperature of the sinusoidal excitation remains the same. One reason for can be deduced from the temperature equation of the CNT film. The constant term in the equation is dependent on the input power, area of the CNT film and the heat capacity per unit area. In the situation that the input power remains the same, this value will remain the same. This value can be considered as a DC offset added to the sinusoidal surface temperature. The second part of the temperature equation involves the sinusoidal component. The amplitude of the sinusoidal component depends on the frequency of the electric signal applied to the CNT film. Due to this, the amplitude (maximum and minimum) of the CNT

film surface temperature changes but not its average value. So, during the thermoviscous acoustic simulation of the CNT speaker, one can use the constant average surface temperature to simulate the generated SPL. The generated SPL depends on the frequency of the applied electrical signal in the case that the applied input power remains the same.

5.2 Thermoacoustic Model

The SPL simulated by the thermoviscous acoustic model showed that the SPL was uniform along the longitudinal axis of the CNT speaker (figure 45). In other words, the sound field generated inside the speaker is planar in nature. This was one of the main aims of the design process as having a plane wave generation inside the speaker is crucial for active noise cancellation. In addition, the CNT film is wrapped around the copper electrodes in the physical prototype. So, the sound generated by the CNT film is radial in nature and propagates radially into the speaker. For the model, the CNT film is modeled by wrapping it on the inside surface of the outer cover. The simulation result shows that in this configuration, the sound pressure level around the circumference of the outer cover is uniform, like the actual prototype (figure 46). The sound pressure levels generated by the COMSOL model were compared with the experimental measurements. It was observed that there was good correlation between the experimental and simulation results (figure 47). This is also a point for validation of the CNT speaker COMSOL model.

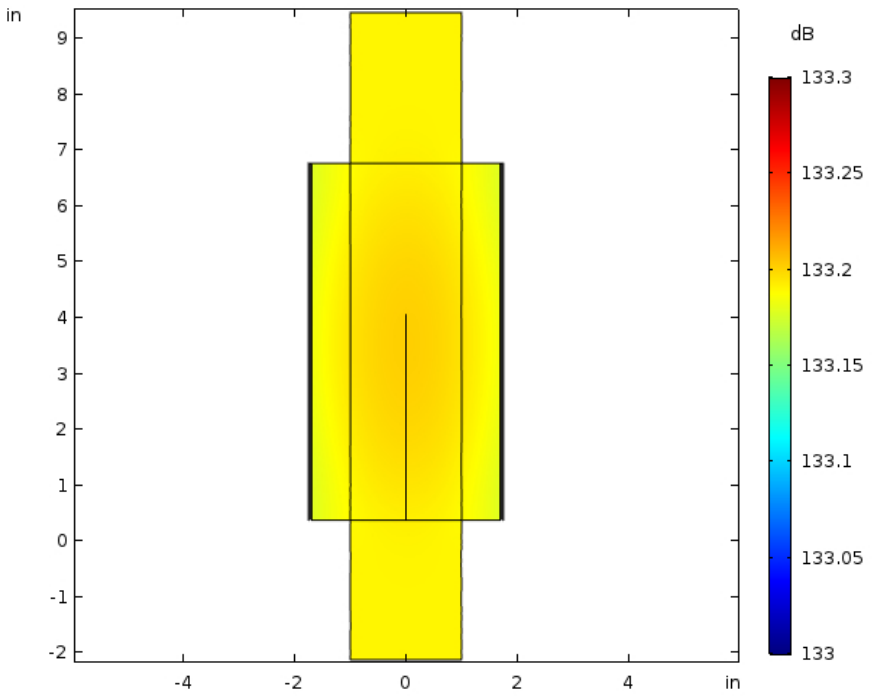

Figure 45: SPL inside the coaxial speaker mode obtained by the COMSOL model. The SPL level is uniform along the length of the speaker and planar in nature.

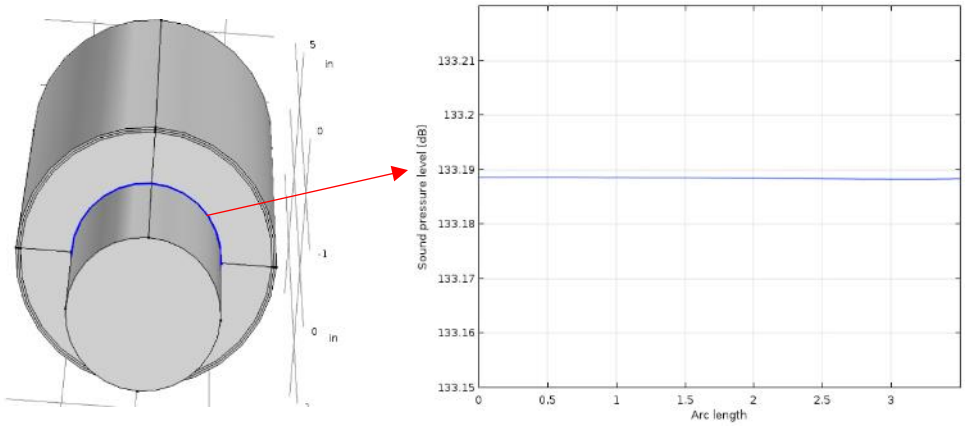

Figure 46: SPL generated along the arc of the CNT speaker model in COMSOL. The SPL value is uniform along the arc length, indicating that the sound generated along the circumference of the speaker is uniform.

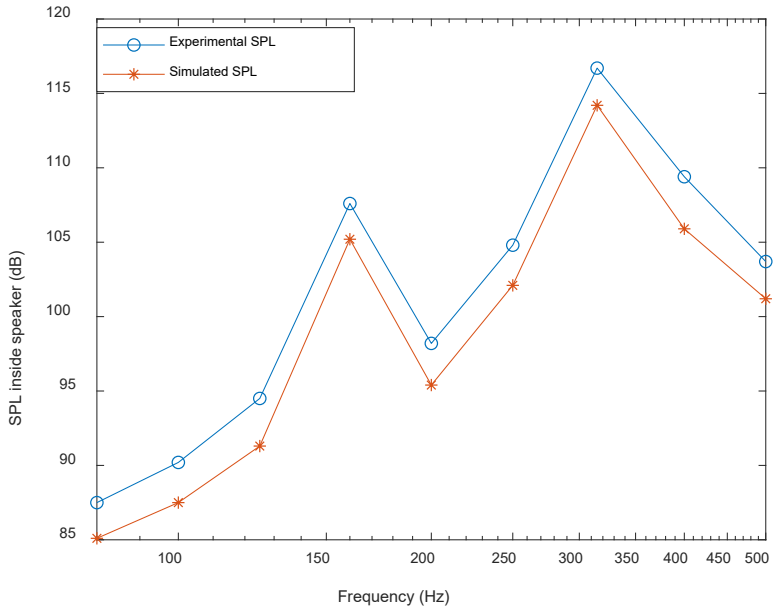

Figure 47: Comparison of SPL between the experimental results and simulation results. The difference between the two SPLs is less than 3dB.

The models for the Joule Heating and Thermoviscous acoustics are validated using experimental results. However, both the models have certain limitations.

Firstly, the CNT material defined in both the models require material properties based on the physics that is being simulated. Even if the accurate material properties such as heat capacity per unit area (c_s) and heat loss due to conduction, convection, and radiation (βo) are defined, they are not used if the physics cannot incorporate it. This is because the governing equations used for the physics in COMSOL are predefined with variables. This is a limitation in setting up the model as the two properties mentioned above are extremely important in the operation of the CNT speaker. A more accurate method of defining these material properties and incorporating them in the built-in physics is required.

In the Joule Heating model, the definition of the electric current is using the Terminal domain condition. This is okay when the electrode used is defined as domain the geometry of the CNT speaker in the model. However, when there is a need to define the electrode as a boundary or edge, this condition is not correct. In COMSOL, the Terminal condition cannot be applied to the boundary. It can be applied only to the domain. There is a work around, but it increases the steps in the modeling, and it can produce errors if not set up correctly.

Ideally, for an enclosed, planar CNT speaker, the SPL decreases with increase in frequency. The main reason for this decrease is the presence of the frequency term in the denominator of the SPL equation for an enclosed CNT speaker (equation 24). From the result shown in figure 47, it is seen that the SPL of the enclosed, coaxial CNT speaker consists of peaks (increasing SPL) and valleys (decreasing SPL). This behavior is in line with the expectation that the acoustic modes of the outer enclosing chamber affect the SPL generated by the CNT speaker. Depending on the chamber modes, its dimensions and shape, the SPL profile generated by the enclosed, coaxial CNT speaker would vary from ideal. The effect of the acoustic modes and their contribution to the SPL profile are illustrated in the next section.

5.3 Finite Element Model Formulation and Result

5.3.1 Joule Heating

5.3.1.1 Electrostatics Physics

The residual form of the PDE for electrostatic physics is given as[167],

$$-\frac{\partial}{\partial x}\left(G_x \frac{\partial V}{\partial x}\right) - \frac{\partial}{\partial y}\left(G_y \frac{\partial V}{\partial y}\right) \tag{46}$$

The above equation is then integrated over the area after multiplication with a weight function w_i. The main purpose of doing this step is to reduce the order of the PDE, in this case is from 2nd order to 1st order. The integration expression is simplified using the integration by parts rule. The final expression obtained after this step is given as,

$$\int_\Omega \left[\frac{\partial w_i}{\partial x} * G_x * \frac{\partial V}{\partial x} + \frac{\partial w_i}{\partial y} * G_y * \frac{\partial V}{\partial y}\right] dxdy = 0 \tag{47}$$

Now, an approximate solution for the electric potential V is assumed as,

$$V = \sum_{i=1}^{n} V_i * \varphi_i \tag{48}$$

Calculating the partial derivatives of V with respect to x and y and plugging them in equation, we get the final matrix equation as,

$$[G_e] * \{V_i^{\,e}\} = 0 \tag{49}$$

where G_e is the element stiffness matrix of electrical conductivity whose values are known, V_i^e is the electric potential matrix whose values are to be determined. The G_e matrix is expressed as,

$$G_{ij} = \int_\Omega \left[G_x \frac{\partial \varphi_i}{\partial x}\frac{\partial \varphi_j}{\partial x} + G_y \frac{\partial \varphi_i}{\partial y}\frac{\partial \varphi_j}{\partial y}\right] dxdy \tag{50}$$

where φ_i and φ_j are the shape function defined to interpolate the date between the nodes of the elements.

The electrical conductivity and electric potential matrices are defined based on the number of elements and the type of elements used in the discretization of the model. For this modeling, the CNT film was discretized using four triangular elements as shown in the figure below.

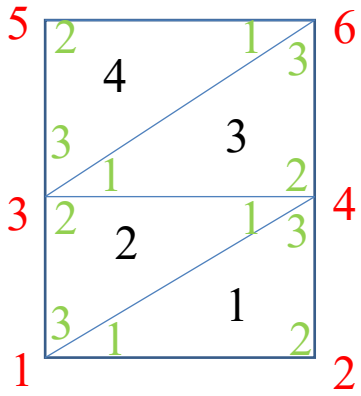

Figure 48: Discretization of the CNT film model to estimate the electric potential and the surface temperature due to the applied electric potential.

In the above figure, the numbers in black denote the element number of the discretized model. The numbers in red are global nodes of the elements while the numbers in green are the local nodes of the discretized model elements. The local nodes are selected in such a way that the element stiffness matrix $[G_e]$ of all the elements will be the same. The connection between the local and the global nodes for the four elements are shown in table below.

Table 2: Connection of Local and Global nodes for the discretized elements

Element	1 (Local Node)	2 (Local Node)	3 (Local Node)
1	1	2	4

2	4	3	1
3	3	4	6
4	6	5	3

From the above table, for element 1, the 1st local node represents the 1st global node, 2nd local node represents the 2nd global node, and the 3rd local node represents the 4th global node. Similar connections are made between the local and global nodes for the remaining elements.

The next step is to calculate the element stiffness matrix of the individual elements. Consider that the coordinate system has its origin at the 1st global node for element 1 as shown in the figure below.

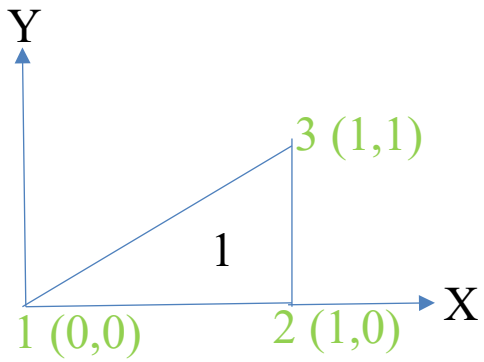

Figure 49: Element 1 with local nodes defined according to the coordinate system at local node 1.

The element represents a right-angled triangle, and its area must be determined. So, for the right-angled triangle, the area is ½ * length * height. For the element 1 and all other elements, the area of the element is ½.

The next step is to generate the shape function for the triangular elements. For triangular elements, the shape function is defined as,

$$\varphi_i = (\alpha_i + \beta_i * x + \gamma_i * y) * \frac{1}{2A} \tag{51}$$

where α_i, β_i and γ_i are the constants defined using the x and y coordinates of the nodes of the element for which the shape function is being determined and A is the area of the element. The general formulation of these constants is given as,

$$\alpha_1 = x_2 * y_3 - x_3 * y_2 \tag{52}$$

$$\alpha_2 = x_3 * y_1 - x_1 * y_2 \tag{53}$$

$$\alpha_3 = x_1 * y_2 - x_2 * y_1 \tag{54}$$

$$\beta_1 = y_2 - y_3 \tag{55}$$

$$\beta_2 = y_3 - y_1 \tag{56}$$

$$\beta_3 = y_1 - y_2 \tag{57}$$

$$\gamma_1 = x_3 - x_2 \tag{58}$$

$$\gamma_2 = x_1 - x_3 \tag{59}$$

$$\gamma_3 = x_2 - x_1 \tag{60}$$

Based on the x and y coordinates of the local nodes for each element, using the above equations, the values for α_i, β_i and γ_i can be calculated. For the triangular element represented in figure, the values of α_i, β_i and γ_i are as follows:

Table 3: Values of shape function constants for the selected triangular element

α_1	1
α_2	0
α_3	0
β_1	-1
β_2	1
β_3	0
γ_1	0
γ_2	-1
γ_3	1

Using the above calculated values, the partial derivate of the shape function are calculated with respect to x and y. These derivates are then plugged back into the integral equation of the element stiffness matrix for electrical conductivity and on simplification, the matrix

form of the element stiffness matrix is obtained. So, for element 1, the elemental stiffness matrix can be expressed as,

$$[G]_1 = \frac{G}{2} * \begin{bmatrix} 1 & -1 & 0 \\ -1 & 2 & -1 \\ 0 & -1 & 1 \end{bmatrix} \tag{61}$$

In the matrix for element 1, row 1 represents the global node 1, row 2 represents the global node 2 and row 3 represents the global node 4. As the local nodes for all the elements are selected in such a way that the stiffness matrix is the same, the values of $[G]_2$, $[G]_3$, $[G]_4$, $[G]_5$ and $[G]_6$ are the same as $[G]_1$. The rows for each of the element stiffness matrix will represent the global node for that element.

So, for element 1, the final matrix equation will be of the form

$$\frac{G}{2} * \begin{bmatrix} 1 & -1 & 0 \\ -1 & 2 & -1 \\ 0 & -1 & 1 \end{bmatrix} * \begin{Bmatrix} V1 \\ V2 \\ V4 \end{Bmatrix} = \begin{Bmatrix} {p_1}^1 \\ {p_2}^1 \\ {p_3}^1 \end{Bmatrix} \tag{62}$$

where V1, V2 and V4 are the scalar electric potentials at global nodes 1, 2 and 4 and p_1, p_2 and p_3 are the charge densities for the nodes 1, 2, and 3. On calculating the element stiffness matrix for all the remaining elements and assembling them, the global stiffness matrix is expressed as

$$\frac{G}{2} * \begin{bmatrix} 2 & -1 & -1 & 0 & 0 & 0 \\ -1 & 2 & 0 & -1 & 0 & 0 \\ -1 & 0 & 4 & -2 & -1 & 0 \\ 0 & -1 & -2 & 4 & 0 & -1 \\ 0 & 0 & -1 & 0 & 2 & -1 \\ 0 & 0 & 0 & -1 & -1 & 2 \end{bmatrix} * \begin{Bmatrix} V1 \\ V2 \\ V3 \\ V4 \\ V5 \\ V6 \end{Bmatrix} = \begin{Bmatrix} P1 \\ P2 \\ P3 \\ P4 \\ P5 \\ P6 \end{Bmatrix} \tag{63}$$

where P1, P2, P3, P4, P5, and P6 are the charge densities (source term) and expressed as,

$$P_1 = {p_1}^1 + {p_3}^2 \tag{64}$$

$$P_2 = {p_2}^1 \tag{65}$$

$$P_3 = {p_2}^2 + {p_1}^3 + {p_3}^4 \tag{66}$$

$$P_4 = {p_3}^1 + {p_1}^2 + {p_2}^3 \tag{67}$$

$$P_5 = {p_2}^4 \tag{68}$$

$$P_6 = {p_3}^3 + {p_1}^4 \tag{69}$$

The above-mentioned equations are obtained from the matrix equation formulation for all the elements. The charge density values for the individual global nodes are added from all the elements and the resultant charge density vector is obtained.

The next step is to apply the boundary conditions to define the model. In the case of CNT speakers, an alternating current is applied across the electrodes. So, for the model defined in this section, the boundary condition at nodes 1, 3, and 5 is sinusoidal and is given as

$$\sigma * \sin(2 * pi * f * t) \tag{70}$$

where σ is the amplitude of the charge applied, f is the frequency of the input signal and t is the time. For the nodes on the opposite side, i.e., 2,4, and 6, the initial charge is zero and that is used as the second boundary condition. After substituting the boundary conditions

and solving the global element stiffness matrix, the result is the stationary electric potential across the CNT film.

For this model, the amplitude of the sinusoidal signal was 10V. The modeling result compared with COMSOL result is shown in figure 50.

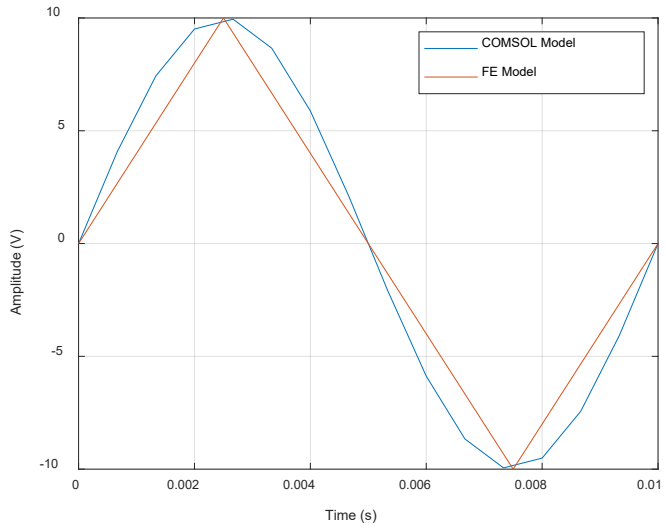

Figure 50: Comparison between the MATLAB model and COMSOL model electric potential for the CNT speaker.

The COMSOL model yields a smoother curve as compared to the MALTAB model. The primary reason for this is the selection of the number of elements and the type of element (rectangular instead of triangular) to discretize the domain that is modeled. Higher number of elements provide more nodal points at which the data is calculated. So, the unknown variable that is calculated is defined more uniformly over the domain, yielding better resolution of the results. However, the comparison between the two simulation results shows that even though there is difference in the profile, the maximum and minimum

values of the electric potential are very close to each other, validating the model. One point to remember is that increasing the number of elements increases the computation time for the model. In this model, for a 6-element discretization, the global element stiffness matrix is of the order 6x6. So, for n elements, the global stiffness matrix will be of the order nxn. Higher the number of elements, larger will be the matrix and more time will be required for the simulation to complete. However, higher number of elements does not always mean better results compared to lower number of elements. It depends on the model dimensions, type of physics involved and the convergence of the solution to the expected value that decides how many number of elements are sufficient to achieve good resolution of the unknown variable.

Another point of improvement is the use of the shape function. The shape function used in this model is linear triangular as triangular elements are used to discretize the model. Use of higher order (quadratic, etc.) shape functions will provide a better interpolation of the data between the node points. It will make the model results align more closely with the COSMOL simulation result.

5.3.1.2 Heat Transfer Physics

The second physics that determines the surface temperature of the CNT film is the heat transfer. This physics takes the heat generated by the electric potential as the input source and determines the surface temperature based on the heat loss from the domain, in this case CNT film. The temperature of the domain depends on the electric potential and not vice-versa, making it one way coupling.

When heat transfer mechanism involves convection along with conduction, modification is required for the heat transfer equation. The general equation for heat transfer in the presence of conduction and convection is given as[167],

$$k_x \frac{\partial T}{\partial x} n_x + k_y \frac{\partial T}{\partial y} n_y + \beta(T - T_\infty) = \widehat{q_n} + f \tag{71}$$

where β is the convective conductance, T_∞ is the ambient temperature of the medium and $\widehat{q_n}$ is the specified heat flow. The heat transfer by conduction is calculated by the first two terms, the heat transfer by convection is calculated by the third term and the heat flux from the CNT film is accounted by the term on the right.

Using the process described in the Joule heating section to formulate the weak form of the PDE using Galerkin method, we get the following equation

$$0 = \int_\Omega \left(k_x \frac{\partial w_i}{\partial x} \frac{\partial T}{\partial x} + k_y \frac{\partial w_i}{\partial y} \frac{\partial T}{\partial y} - w_i f \right) dxdy - \oint_\Gamma w_i * [q_n - \beta(T - T_\infty)] ds \tag{72}$$

Defining the shape function as φ_i and the temperature solution approximation as

$$T = \sum_{i=1}^{n} T_i \varphi_i \tag{73}$$

and substituting them in the above equation, we get the final matrix formulation of the heat transfer PDE as

$$\sum_{j=1}^{n}\left({K_{ij}}^{e}+{H_{ij}}^{e}\right){T_j}^{e}={F_i}^{e}+{P_i}^{e} \tag{74}$$

where

$${K_{ij}}^{e}=\int_{\Omega}\left(k_x\frac{\partial w_i}{\partial x}\frac{\partial \varphi_j}{\partial x}+k_y\frac{\partial w_i}{\partial y}\frac{\partial \varphi_j}{\partial y}\right)dxdy \tag{75}$$

$${F_i}^{e}=\int_{\Omega} f\varphi_i dxdy+\oint_{\Gamma} {q_n}^{e}\varphi_i ds\equiv {f_i}^{e}+{Q_i}^{e} \tag{76}$$

$${H_{ij}}^{e}=\beta^{e}\oint_{\Gamma}\varphi_i\varphi_j ds \tag{77}$$

$${P_i}^{e}=\beta^{e}\oint_{\Gamma}\varphi_i T_{\infty} ds \tag{78}$$

In the above equation, β is the heat transfer coefficient for convection. The coefficients H_{ij}^{e} and P_i^{e} are the terms due to the convective boundary conditions evaluated using boundary integrals. Depending on the mesh element chosen (triangular or rectangular), these coefficients are defined. For this simulation, there is heat loss due to conduction and convection from the CNT film and the copper electrodes. So, to model the heat loss more accurately, rectangular elements are used to discretize the model. For a linear rectangular element, the coefficients H_{ij}^{e} and P_i^{e} are defined as,

$$H_{ij}{}^{e} = \beta^{e}{}_{12}\int_0^{h^{e}{}_{12}} \varphi_i{}^{e}\varphi_j{}^{e}ds + \beta^{e}{}_{23}\int_0^{h^{e}{}_{23}} \varphi_i{}^{e}\varphi_j{}^{e}ds + \beta^{e}{}_{34}\int_0^{h^{e}{}_{34}} \varphi_i{}^{e}\varphi_j{}^{e}ds + \beta^{e}{}_{41}\int_0^{h^{e}{}_{41}} \varphi_i{}^{e}\varphi_j{}^{e}ds \quad (79)$$

$$P_i{}^{e} = \beta^{e}{}_{12}T_\infty\int_0^{h^{e}{}_{12}} \varphi^{e}{}_{i}ds + \beta^{e}{}_{23}T_\infty\int_0^{h^{e}{}_{23}} \varphi^{e}{}_{i}ds + \beta^{e}{}_{34}T_\infty\int_0^{h^{e}{}_{34}} \varphi^{e}{}_{i}ds + \beta^{e}{}_{41}T_\infty\int_0^{h^{e}{}_{41}} \varphi^{e}{}_{i}ds \quad (80)$$

where $\beta^{e}{}_{ij}$ is the heat transfer coefficient by convection, $h^{e}{}_{ij}$ is the length of the side and $T^{ij}{}_{\infty}$ is the ambient temperature. The above-mentioned coefficients are essentially line integrals and are evaluated using interpolation functions. The local coordinate is along the side where these coefficients are evaluated with the origin at the first node of the element. So, using 1D interpolation function for each side of the element, the coefficients for linear rectangular element in matrix for are

$$[H^e] = \frac{\beta^{e}{}_{12}h^{e}{}_{12}}{6}\begin{bmatrix}2&1&0&0\\1&2&0&0\\0&0&0&0\\0&0&0&0\end{bmatrix} + \frac{\beta^{e}{}_{23}h^{e}{}_{23}}{6}\begin{bmatrix}0&0&0&0\\0&2&1&0\\0&1&2&0\\0&0&0&0\end{bmatrix} + \frac{\beta^{e}{}_{34}h^{e}{}_{34}}{6}\begin{bmatrix}0&0&0&0\\0&0&0&0\\0&0&2&1\\0&0&1&2\end{bmatrix} + \frac{\beta^{e}{}_{41}h^{e}{}_{41}}{6}\begin{bmatrix}2&0&0&1\\0&0&0&0\\0&0&0&0\\1&0&0&2\end{bmatrix} \quad (81)$$

$$\{P^e\} = \frac{\beta^{e}{}_{12}T^{12}{}_{\infty}h^{e}{}_{12}}{2}\begin{Bmatrix}1\\1\\0\\0\end{Bmatrix} + \frac{\beta^{e}{}_{23}T^{23}{}_{\infty}h^{e}{}_{23}}{2}\begin{Bmatrix}0\\1\\1\\0\end{Bmatrix} + \frac{\beta^{e}{}_{34}T^{34}{}_{\infty}h^{e}{}_{34}}{2}\begin{Bmatrix}0\\0\\1\\1\end{Bmatrix}$$

$$+ \frac{\beta^{e}{}_{41}T^{41}{}_{\infty}h^{e}{}_{41}}{2}\begin{Bmatrix}1\\0\\0\\1\end{Bmatrix} \quad (82)$$

The discretized model consisting of rectangular elements is as shown in the figure below.

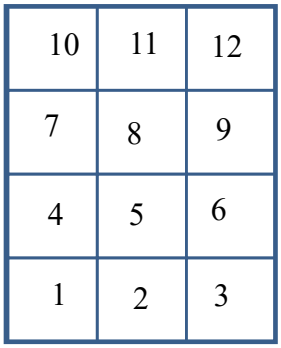

Figure 51: Discretized model of the CNT speaker consisting of rectangular elements. Twelve elements are used to discretize the CNT film domain.

From the above figure, elements 5 and 8 lie completely in the CNT film domain. For all other elements, there is a combination of the CNT film domain and the copper electrode domain (left side of elements 1, 4, 7, 10 and right side of elements 3, 6, 9, 12). So, when determining the coefficients H_{ij}^{e} and P_i^{e}, the value of β will be for CNT film and the copper electrodes based on the side of the element. For the copper electrodes, the heat transfer coefficient is a single value. For the CNT film, the heat transfer coefficient value is defined as β_o and is a combination of the heat transfer coefficient due to conduction, convection, and radiation.

The boundary conditions are applied at the local nodes of the elements 1,4,7,10,36,9, and 12. These boundaries are the assigned copper material, and they are at ambient temperature T_∞. The heat flux (q_n) from the CNT film is defined using equations 82, 83 and 84 (page 92). This considers the sinusoidal behavior of the CNT film surface temperature and the impact of the electric current applied to the CNT film through the copper electrodes. It is

important to make sure that this heat flux is applied only to the nodes that are in the CNT film domain and not the copper electrode boundary. The internal heat generation is defined from the electric potential calculated using the electrostatics physics. This is applied over the entire domain for all the elements in the CNT film. The equation for the internal heat generation is given as,

$$f^{e}_{i} = G * \nabla V \tag{83}$$

where G is the electrical conductivity of the CNT film and V is the electric potential. The CNT film heats up and cools down much faster than the copper electrodes and so for this reason, the internal heat generation in the CNT film is more prominent than that in the copper electrodes. So, using this relation, the source matrix consisting of the internal heat generation and heat flux matrices are formulated. The final step is then to solve the net matrix equation to calculate the temperature at the nodes of the CNT film domain elements using equation. The comparison between the modeled surface temperature and the COMSOL model simulated temperature is shown in figure below.

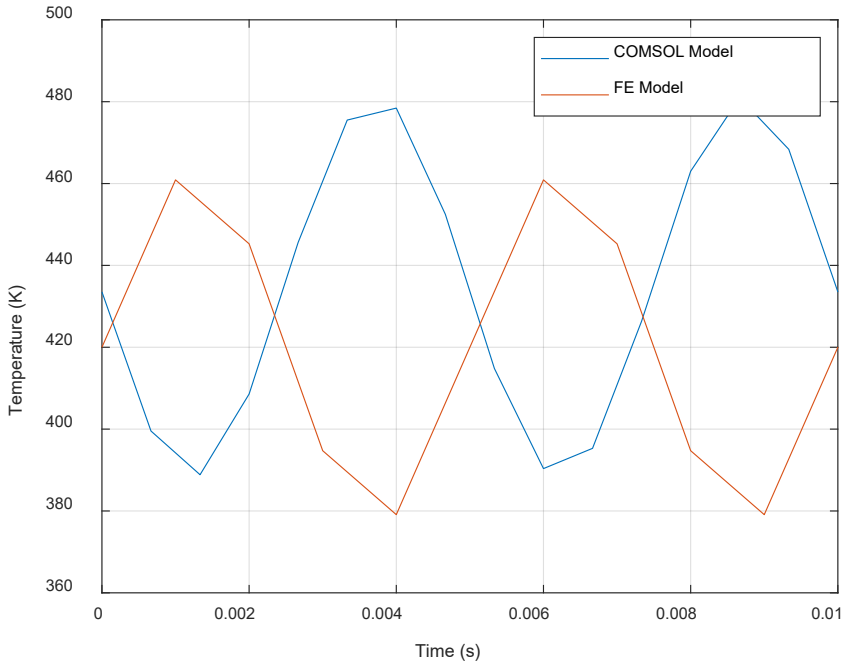

Figure 52: CNT film surface temperature comparison between the COMSOL and MATLAB model. The doubling effect of the CNT film is evident in both the results.

From the above figure, the doubling effect of the CNT film is modeled in both the COMSOL as well as the MATLAB model. There is some difference in the amplitude as well as phase of between the two models. One reason for this difference is the number of elements used for discretizing the model. Increasing the number of elements provides a better approximation of the surface temperature of the CNT film. Also, the heat transfer coefficient for the CNT film is a combination of the heat loss due to conduction, convection, and radiation. The MATLAB model requires separate values for these heat transfer modes. But the same value is used in the MATLAB model for all three heat transfer modes. This could be a reason for the difference in the amplitude of the surface temperature oscillation. In addition, there is a phase difference between the two temperature results.

The MATLAB model does not consider the phase term in the heat flux from the CNT film. Identifying a method to include this phase term provide a better correlation between the two results with respect to the phase.

Based on the electrostatics and heat transfer results, it can be concluded that the FE equation formulations and the discretization is good on comparison with the COMSOL model results.

5.3.2 Thermoviscous Acoustics[168]

For simplicity, a 2D axisymmetric model of the enclosed, coaxial CNT speaker is considered. The net area of the revolved CNT film is the same as the area of the CNT film used for the Joule heating model. This ensures that the surface temperature oscillation obtained from the Joule heating model can be used as input for the thermoviscous acoustics model.

The thermoviscous acoustics governing equations (33-35) can be combined so that acoustical a, thermal h, and velocity v components are defined for the total domain where the simulation is performed. These components can be expressed as,

$$p = p_a + p_h \tag{84}$$

$$T = T_a + T_h \tag{85}$$

$$v = v_a + v_n \tag{86}$$

These variables each satisfy one of the three LNS equations (33-35) and the thermal terms are generally restricted to the thermal boundary layer that forms near the rigid walls of the CNT speaker. These solutions can be used for a single equation that has higher order and is in its strong form. However, when it is converted to its weak form for discretization, it requires boundary conditions for the derivatives present in the surface integral. This is problematic as the conditions at the boundary for the acoustic and thermal component may be unknown for the whole domain. Even in the situation where the net pressure and temperature variables are considered, the boundary conditions may be defined for a perfect fluid, but they might be inconsistent for a thermoviscous fluid that is the consideration here.

It has been observed that for the thermoviscous acoustic model, the pressure variation can be expressed in terms of the other two variables – v and T. When the thermal and viscous boundary layers are accurately modeled, the particle velocity (v) and temperature (T) are considered as the basic variables for the formulation of the finite element matrices. This process considerably simplifies the matrix formulation, helps define the boundary conditions more easily, and avoids lengthy computation times. Another variable in the LNS equations is the density of the thermoviscous fluid, ρ. As the acoustic wave is generated due to the temperature variation along the thermoviscous and pressure acoustic boundary, the heat generated is transmitted to the surrounding medium. This heat causes temperature change in the medium, thus changing its density. So, both the density and the acoustic pressure can be expressed in terms of v and T as,

$$\rho = -\frac{\rho_0}{i\omega}\nabla . v \tag{87}$$

$$p = \hat{\beta}_T - \frac{\rho_0 c^2}{i\omega\gamma} \nabla . v \tag{88}$$

where ∇. is the divergence of the total velocity, and β_T is the isothermal compressibility of the surrounding medium. Substituting the values of density and acoustic pressure in the momentum and energy conservation equation yields the particle velocity and temperature variation formulation for the thermoviscous acoustics physics. The equations thus obtained are as follows,

$$\omega^2 v + B(\nabla(\nabla . v) + C(\nabla x \nabla x v) - D(\nabla T) = 0 \tag{89}$$

$$i\omega T + Q(\nabla . (\nabla T) - R(\nabla . v) = 0 \tag{90}$$

where

$$B = c^2/\gamma + i\omega c l_v \tag{91}$$

$$C = -i\omega c l'_v \tag{92}$$

$$D = i\omega\hat{\beta}/\rho_0 \tag{93}$$

$$Q = -\gamma l_h c \tag{94}$$

$$\mathrm{R} = -(\gamma - 1)/(\gamma\hat{\beta}) p_0 c^2 \tag{95}$$

In the equations (91-95), the length terms are the characteristic lengths for the shear viscosity (l'_v), bulk viscosity (l_v) and thermal diffusion (l_h). These lengths are expressed as,

$$l'_v = \mu/\rho_0 c \tag{96}$$

$$l_v = (\eta + \frac{4\mu}{3}) \tag{97}$$

$$l_h = \frac{\xi}{c} \tag{98}$$

Defining the variables velocity and temperature are crucial not only to simplify the model but also for the application of the boundary conditions on the thermoviscous and pressure acoustic common boundary, CNT film in this case. The boundary conditions applied are the Dirichlet and Neumann boundary conditions for temperature variation and particle velocity variables.

For the CNT film, the temperature variation Dirichlet condition can be applied in two ways. First, the sinusoidal variation can be considered as the temperature variation and applied to CNT film boundary. The other condition is a constant temperature whose value is the average temperature of the oscillating surface temperature of the CNT film. Both conditions yield good results, but the use of the average temperature value remains the same irrespective of the simulation frequency. The mechanical Dirichlet condition pertains to the particle velocity. CNT films do not vibrate to generate the sound wave. They use the thermal perturbation to cause density variations in the surrounding medium to generate the acoustic wave. So, for the purpose of this model, the mechanical Dirichlet condition is the particle velocity with a value of zero, making the CNT film behave as a rigid wall.

For the axisymmetric model considered in this modeling process, the Neumann condition and the Dirichlet conditions are combined for the temperature variation and the particle velocity. For the CNT film, the temperature variation Neumann condition is $\partial T/\partial r = 0$ and the particle velocity Neumann condition is $v_r = 0$ and $\partial v_z/\partial z = 0$. The derivative of the

temperature variation with respect to r is zero as stationary temperature is assumed for the CNT film surface for this model. For the particle velocity, it is assumed that the acoustic particle velocity along the CNT film is zero (rigid) and the particle velocity in the propagation direction (z) is linear in nature.

Equations 88 and 89 can then be discretized and expressed in the finite element matrix form as

$$\begin{bmatrix} \omega^2[M_v] + [K_v] & -D[Grad] \\ -R[Div] & i\omega[Ms] + Q[K_s] \end{bmatrix} \begin{Bmatrix} v \\ T \end{Bmatrix} = \begin{Bmatrix} Tvar \\ 0 \end{Bmatrix} \tag{99}$$

This Finite Element formulation mentioned above is obtained using the Galerkin finite element for axisymmetric models. For axisymmetric models, the mesh used is planar in the one half of the fluid domain, where one element is the representation of the volume obtained after revolving the surface around the symmetry axis. In cylindrical coordinates, the gradient and divergent operators are expressed as,

$$Grad(v) = \begin{bmatrix} {\partial v_r}/{\partial r} & 0 & {\partial v_r}/{\partial z} \\ 0 & {v_r}/{r} & 0 \\ {\partial v_z}/{\partial r} & 0 & {\partial v_z}/{\partial z} \end{bmatrix} \tag{100}$$

$$div(T) = \begin{Bmatrix} \frac{\partial T_{rr}}{\partial r} + \frac{\partial T_{rz}}{\partial z} + \frac{T_{rr}}{r} \\ 0 \\ \frac{\partial T_{zr}}{\partial r} + \frac{\partial T_{zz}}{\partial z} + \frac{T_{zr}}{r} \end{Bmatrix} \tag{101}$$

The shape function used for interpolation of the finite elements is a function of the parameters ξ and η. There are n nodes for the elements in the mesh and each node is resolved in the normal fashion of the FEM.

On solving the equation 99, the acoustic pressure in the surrounding medium can be back calculated using the relation between the acoustic pressure and the particle velocity and the temperature variation set in the medium. For this model, the temperature value (Tvar) on the CNT film surface was assigned a value of 420K. The model was solved for frequency range of 50Hz – 250Hz in 1/3rd octave band. The comparison between the COMSOL and FE model result is shown in the figure below.

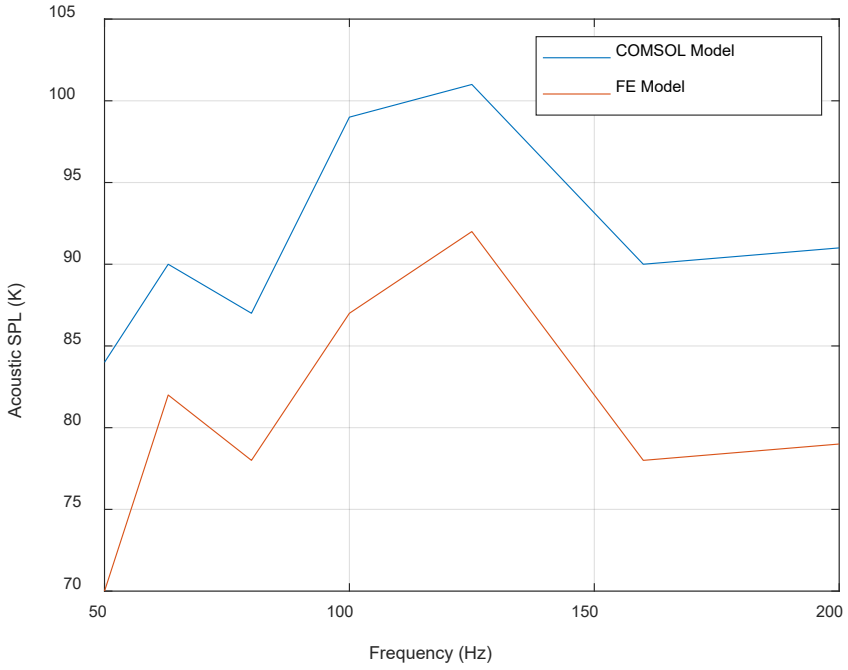

Figure 53: Comparison between COMSOL model and the FE model SPL generated by the CNT speaker.

It is seen from the above comparison that the FE model follows the profile of the COMSOL model simulated SPL. There is a difference in the amplitude between the two results. The main reason for this difference is the FE model assumes uniform shape function for all the variables – v and T. This causes the matrix formulation to become unstable sometimes during the solving of the FE matrix equation. Also, using the same shape function for all the variables has a lower degree of convergence as compared to using different order shape functions for individual variable. In addition, the simplification of the LNS equations in this model was done for ease of understanding the process behind the thermoviscous acoustics. A more robust weak formulation of the LNS equations can be derived using the Newton Fourier ideal gas model for the air medium used in this model. The FE matrix equation obtained from this weak formulation provides a more detailed relation between the dependent and control variables and the source terms. Overall, this model helped to understand the finite element process involved in the Thermoviscous acoustic physics.

5.4 Acoustic Modal Analysis of Coaxial CNT Speaker

5.4.1 Modes of Propagation in the Pipe through the CNT speaker

The pipe that runs through the coaxial CNT speaker is cylindrical in nature. So, when the exhaust noise travels through this pipe, there is chance that along with longitudinal modes, transverse modes are excited. Longitudinal modes have wave motion along the principal axis and in planes orthogonal to the principal axis of the pipe. The transverse modes, or cross-modes have pressure profile that is not uniform across the cross-section of the pipe (figure 24). Based on the type of transverse mode activated, the pressure profile across the

cross-section of the pipe will vary and it is difficult to cancel the sound with transverse modal behavior.

The main application of the coaxial CNT speaker was active cancellation of the automotive exhaust noise. It is very important that the sound pressure profile be uniform along the length of the speaker as well as across the cross-section of the pipe. For this reason, during the design of the coaxial speaker, the diameter of the pipe must be chosen in such a way that the cutoff frequencies of the higher order modes (modes other than (0,0)) are large in value. For the coaxial speaker, the pipe that extends through the speaker has a diameter of 2”. Assuming the speed of sound in air traveling through the pipe is 343m/s, the cutoff frequencies of the modes of propagation in the pipe are given in table 4 calculated from equations 8 and 9.

Table 4: Cutoff frequencies of the modes of propagation in the pipe of the coaxial CNT speaker

Mode Number	**Cutoff Frequency (kHz)**
ω_{00}	0
ω_{10}	24.84
ω_{20}	41.18
ω_{01}	51.72
ω_{11}	71.97
ω_{21}	90.61

The cutoff frequency is the minimum value above which the mode exists and can propagate along the pipe. Below the cutoff frequency, the mode is evanescent and decays exponentially with distance. From the values in the above table, it is evident that all the higher modes (other than mode (0,0)) have a frequency that is higher than the exhaust sound frequencies. So, these modes, if generated, will be evanescent in nature and will not have a major effect on the sound transmission through the exhaust tailpipe as well as the coaxial CNT speaker. The mode (0,0) is the one-dimensional plane wave that propagates through the pipe. Its cutoff frequency is 0Hz and in this mode, there is no transverse wave motion. It is this mode that is the most desired for active noise cancellation.

One important point to note here is the effect of the presence of the diaphragm on the slots in the coaxial CNT speaker pipe. Now, the diaphragm is fixed as rigidly as possible over the slots. The diaphragm material was chosen such that it has minimum insertion and transmission loss to allow maximum sound generated by the CNT film into the pipe for noise cancellation. The equations used to determine the cutoff frequencies in table 4 are for a cylindrical pipe that has rigid boundaries along the length of the pipe and do not transmit sound through them. So, for the slotted pipe with the diaphragm, the cutoff frequencies will most likely be different from those mentioned in table 4 but high enough to not affect the exhaust noise cancellation by the coaxial CNT speaker.

Based on the above results, checking for modal propagation frequencies is an important step in the design of the enclosed, coaxial CNT speaker. As mentioned previously, higher order modes have non-uniform patterns of acoustic wave transmission. Based on the intended application of the CNT speaker, generation of higher order modes can be problematic. The calculation of the acoustic modal frequencies is related to dimensions of the CNT speaker. Performing this calculation is like an optimization process for selecting the dimensions of the speaker, within the required limits. Once the appropriate dimension range is determined based on the acoustic mode calculation, COMSOL model of those speaker designs can be simulated, and optimization can be performed to further tune the speaker performance. This will save a lot of effort in case the speaker does not produce the desired acoustic profile for the selected dimension due to higher order mode generation.

5.4.2 Acoustic Modes of the Enclosed, Coaxial CNT Speaker

To determine the acoustic modal response of the enclosed, coaxial CNT speaker, the speaker was operated using sine chirp signal at three power levels: 14W, 50W and 100W. The FRF of the three power levels is shown in figure 54.

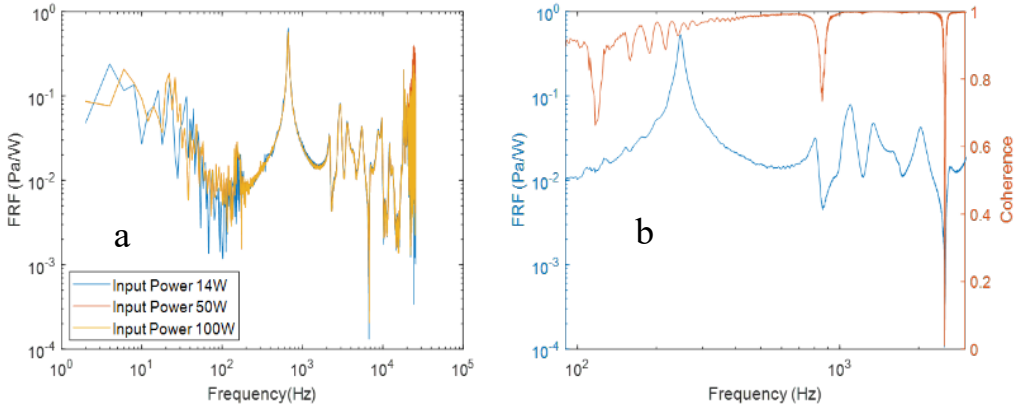

Figure 54: FRF of SPL and input power for the sine chirp input to the enclosed coaxial CNT speaker (a). All the three FRFs line up with each other, indicating the repeatability of the experiment. FRF and coherence of 100W sine chirp input to the coaxial speaker (b).

From the above graphs, it is clear that the FRF of the enclosed, coaxial CNT speaker remains the same irrespective of the input electrical power. This provides a validation that the acosutic modes of the CNT speaker remain the same and are independent of the input signal. Also, for the sine chirp input, the coherence obtained is high (>0.95) for the majority of the frequency range. So, the acoustic repsonse of the CNT speaker is entirely due to the input electrical signal and the acoustic modes of the speaker.

Using the COMSOL model for the enclosed, coaxial CNT speaker, the SPL at the peaks and valleys found in the FRF of the sine chirp test was determined. The input power used

to simulate the model was selected to be 100W. Because the three FRFs line up with each other, it did not matter which input power was selected. The SPL that was obtained from simulation were normalized using the input power used in the simulation, that is 100W. By doing this, the units on the final value of the simulated SPL obtained were Pa/W. A comparison was made between the two results (figure 55).

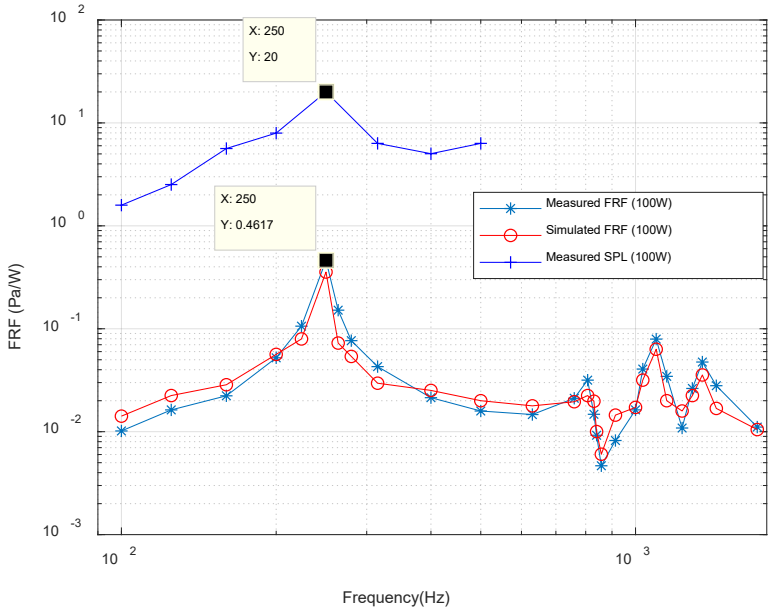

Figure 55: Comparison between the experimental and simulated FRFs and measured SPL for the coaxial CNT speaker. Not all points from the experimental FRF are simulated. Only the prominent peaks and valleys are included.

The first observation from figure 55 is that the simulation results align at all the selected points of the experimental results in the FRF. In the FRF, there is a prominent peak at approximately 250Hz, indicating the presence of an acoustic mode. It is believed that this mode would have a major contribution in the SPL generated by the coaxial CNT speaker.

To verify this, the SPL measurements made inside the coaxial speaker have also been plotted in the graph. From the SPL results, the maximum value of SPL generated by the coaxial speaker is observed at 250Hz. It is evident from this comparison that the acoustic mode present at 250Hz does assist the SPL generated by the coaxial CNT speaker. From previous research studies, it has been found that for an enclosed CNT speaker, the SPL is linear and decreases with increase in frequency. However, this behavior was not observed for this coaxial speaker design. The presence of an outer cover and the presence of acoustic modes of this arrangement are the main contributors to the observed SPL profile of the enclosed, coaxial CNT speaker.

The main advantage of performing acoustic modal analysis is to fine tune the design of the CNT speaker to make sure that the acoustic modes contribute constructively to the SPL generated by the speaker. This will help to achieve higher SPLs at target frequencies without having a high input power. CNT speakers, compared to standard loudspeaker, require higher input power to generate equivalent SPL. So, having the assistance of acoustic modes will help the reduce the input power and bring the CNT speakers closer to the conventional loudspeakers in performance and input requirements.

5.5 Axial, Cross-sectional and Industry Standard Measurement

5.5.1 Axial SPL Results

The axial SPL comparison between the measured and simulated values show a good correlation with the difference between the values less than 3dB (figure 56). This indicates that the COMSOL model can predict the SPL generated inside the coaxial speaker at a close approximation to the physical performance. One of the reasons for the difference in the values is the geometry of the slotted pipe and the presence of the diaphragm over the slots. The impedance of the slots used in the model approximates the actual slotted pipe region. Also, the impedance is used as a boundary condition and the slots are not actually modeled in COMSOL. So, some of the effects of the slots on the acoustic profile have not been accurately reproduced in the model. Another reason for the difference in the value is that a single CNT film wrap is used in the COMSOL model. In the actual prototype, there are two concentric rings of CNT film. The COMSOL model has one CNT film ring attached to the inner surface of the outer cover. To account for the reflections from the outer cover, double input power is used in the simulation. This change in the CNT film is expected to have some effect on the axial SPL observed in simulation.

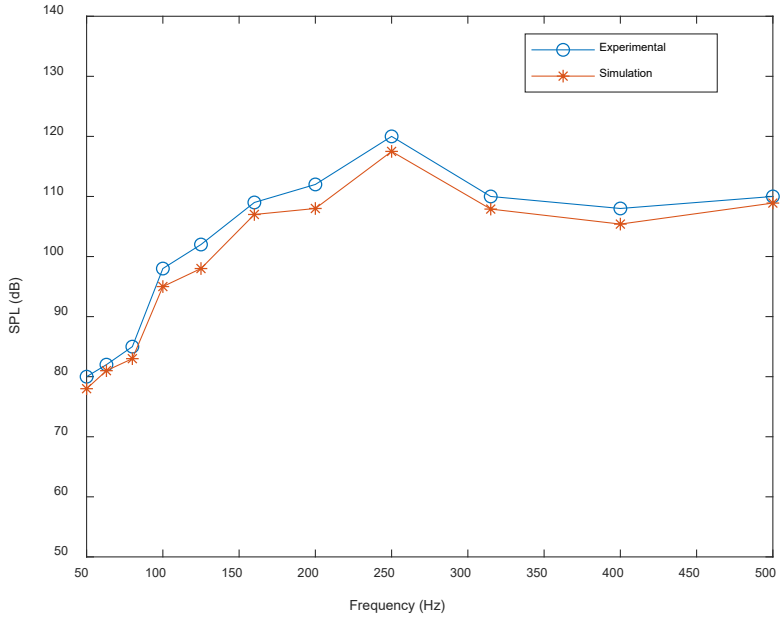

Figure 56: Comparison between measured and simulated axial SPL for the coaxial CNT speaker.

Axial SPL is important if the application of the CNT speaker involves the use of the sound generated inside the speaker, also called as in-pipe SPL. The generated sound propagates along the speaker and is then radiated out from the speaker ends. Depending on the geometry and dimensions of the speaker ends, they can be either good or bad radiators of acoustic energy. In the application where the radiated sound is of primary importance, it is always beneficial to have the in-pipe SPL several dB higher than the target SPL value. Due to this, even if there are losses present during the sound radiation form the speaker ends, the resultant radiated SPL will be close to the target SPL value. Simulating the axial SPL will help tune the design as well as select appropriate CNT film wrap area to increase the in-pipe SPL for conditions where there is no flow in the medium as well as flow present in the medium.

5.5.2 Cross Sectional SPL Results

The cross-sectional SPL is important in understanding the modes generated in the speaker as well as the plane wave cutoff frequency. Comparison between the experimental and simulated results showed that they were in good correlation with the each other (figure 57, 58). The sound pressure level was higher at the center of the end pipes. For low frequencies, the SPL variation across the face of the end pipe was around 8dB while for higher frequencies, the SPL variation was around 25dB. The reason for this is that as the frequency of sound increases beyond the cutoff frequency, the acoustic field becomes less planar and cross-modes are observed in the pipe.

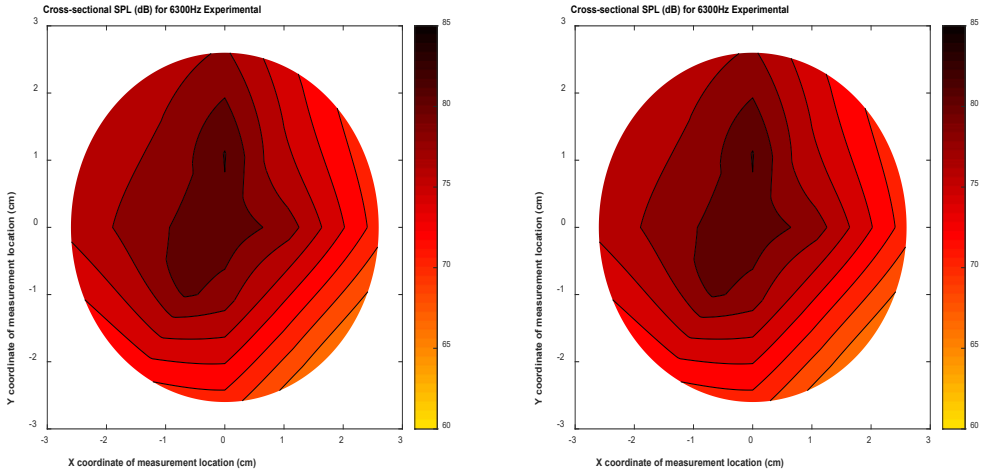

Figure 57: Cross-sectional SPL across the face of the end pipe. For a frequency of 6300Hz, there is a 25dB difference in the SPL.

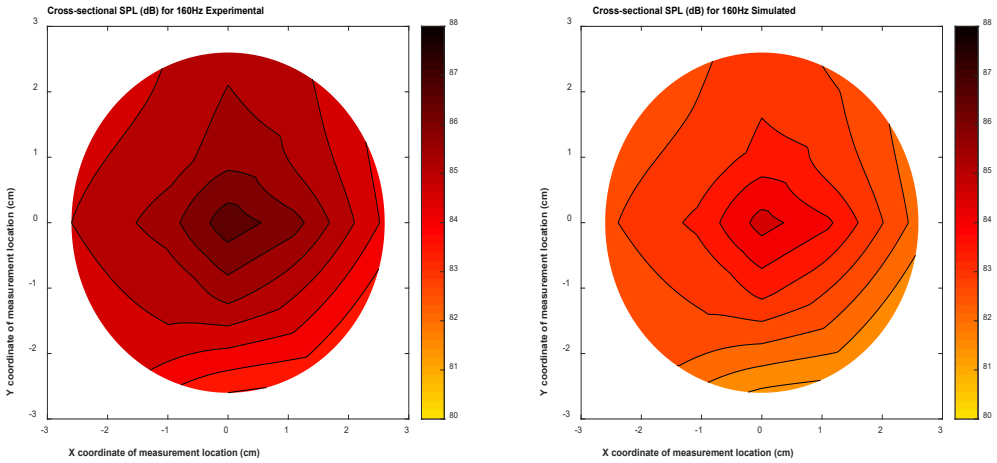

Figure 58: Cross-sectional SPL across the face of the end pipe. For a frequency of 160Hz, there is an 8dB difference in the SPL.

Ideally, if the CNT film was mounted at one end of the coaxial speaker, it would behave as a piston vibrating back and forth. However, in this case, the CNT film is wrapped along the circumference of the center pipe and the sound field generated is radial. In addition, the pipe walls are not completely solid due to the presence of slots to allow sound to travel into the pipe. These factors affect the sound pressure profile across the cross-section of the CNT speaker center pipe. It is important to quantify and characterize this profile for all the frequencies of interest. This will help to improve the understanding of the radiation of the sound from the ends of the coaxial CNT speaker and provide a baseline to improve the radiation characteristic of the speaker.

5.5.3 Industry Standard SPL Results

A comparison was made between the SPL measured in-pipe at the center of the coaxial speaker and the industry standard measured SPL (figure 59). The difference between the two SPLs was found to be more than 30dB, the industry standard SPL being lower. One of the reasons for this relates to the radiation impedance of the pipe end face of the coaxial speaker. The coaxial CNT speaker generates sound that in radial in nature due to the circular arrangement of the CNT film. This sound propagates along the length of the speaker and is radiated out by the end face of the coaxial speaker pipe. This radiation mechanism can be equated to a circular piston that is radiating sound through motion. In this case, the circular piston can be considered as the air that is present as ambient surrounding and inside the CNT speaker.

Radiation impedance provides the phase relation between the surface pressure and object velocity[167]. At low frequencies, as considered in the case of the coaxial CNT speaker, the phase difference between the two quantities is 90^{o} i.e., the velocity lags the pressure by 90^{o}. In this situation, there is non-efficient transfer of energy from the vibrating air column to the surrounding medium, resulting in low sound radiation from the coaxial CNT speaker. So, to increase the sound radiation, it is necessary to increase the in-pipe sound pressure level generated by the coaxial CNT speaker.

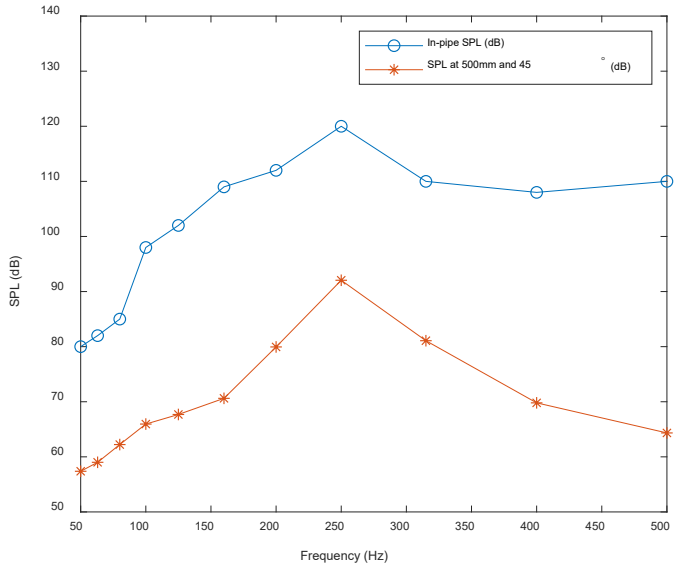

Figure 59: Comparison between the in-pipe SPL and SPL measured at 500mm and 45° from the pipe end face of the coaxial CNT speaker. The radiated SPL is lower by more than 30dB compared to the in-pipe SPL.

As mentioned in Chapter 4, industry standard SPL is measured at 500mm and 45° from the vibrating face of a conventional loudspeaker. In the case of the coaxial CNT speaker, this measurement is made from the cross-sectional face of the end of the slotted pipe that runs through the speaker. So, to obtain the SPL radiating out from the CNT speaker, an air domain must be modeled around the CNT speaker. The radiation of sound from the CNT speaker pipe is spherical in nature. So, the air domain is modeled as a sphere surrounding the coaxial CNT speaker like that described in the planar CNT speaker model.

A validation was performed for the air domain modeled around the CNT speaker. A single piston oscillating in air was used for this validation. The directivity of a vibrating piston can be easily determined using the analytical formulae. In COMSOL, the piston was

modeled as a line that was vibrating the Y direction. The air domain surrounding the piston was modeled in COMSOL in the shape of a quarter of a circle (figure 60). The properties of the air domain were set based on the temperature. The piston was given a velocity at which it underwent oscillations. To determine the directivity, far-field condition was used at the boundary of the air domain. This condition calculates the directivity based on the Rayleigh distance and the sound that is propagating into the air domain from the source.

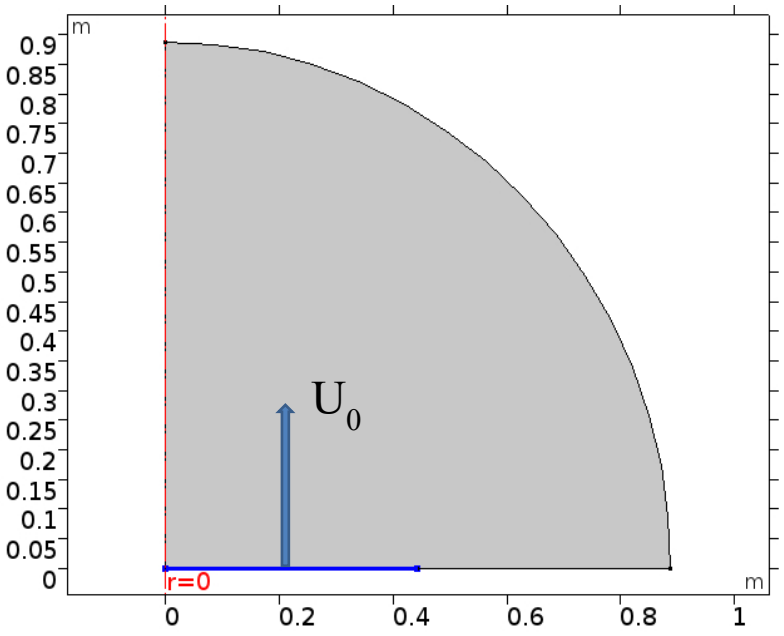

Figure 60: Vibrating piston model in COMSOL with the air domain surrounding the piston. The blue line represents the piston with its length equal to the radius of the circular piston.

On comparison between the experimental and simulation result, it was found that the directivity of the vibrating piston aligned perfectly for both low as well as high frequencies (figure 61). This demonstrated that the method and the properties used to define the air

domain are correct and so, the industry standard SPL was determined by simulation and compared with experimental results.

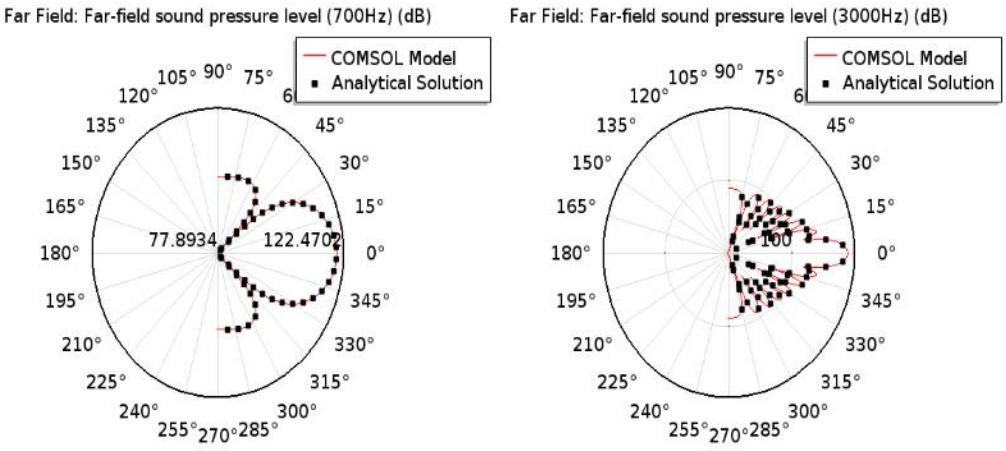

Figure 61: Directivity comparison between the COMSOL simulation result and the analytical solution for a single vibrating piston. The directivities aligned perfectly providing validation for the air domain model.

The comparison between the simulated and experimental industry standard results of the SPL of the coaxial CNT speaker is shown in figure 62. The difference between the two results in around 4dB with a maximum value of 6dB. The simulated in-pipe SPL of the coaxial CNT speaker is around 2dB. So, it is expected that the simulated industry standard results will be less than the experimental results. Another reason for the difference in the values is the modeling of the end face of the coaxial speaker pipe as a radiator. The radiation from the pipe, as mentioned earlier is like a vibrating circular piston. The air domain around the CNT speaker is modeled using standard material properties and radiation conditions. However, based on the actual medium properties and the pipe end face geometry and pipe material properties, the radiation from the end face might not

always be perfectly spherical. So, this will cause a difference between the experimental and simulated SPL results. The main advantage of this model is the ability to predict the expected approximate SPL from the CNT speaker in the presence of any medium other than air, such as inert gases.

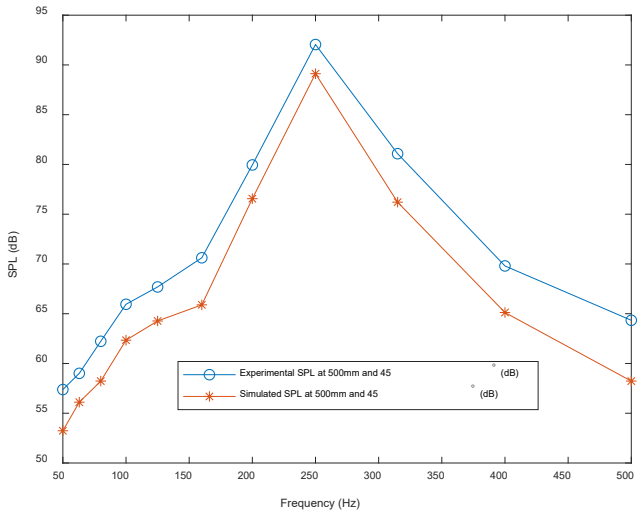

Figure 62: Comparison between the experimental and simulated industry standard SPL results of the coaxial CNT speaker. Both the results show similar profiles with a difference of approximately 4dB between the values.

The industry standard measurement result shown in figure 59 reiterates the point mentioned in the previous two sections. For any two SPLs, a difference of 30dB is significantly huge. For example, if the desired radiated SPL is 110dB, then the in-pipe SPL must be atleast 140dB to achieve that target. Such a high SPL, even in-pipe could be difficult to obtain while keeping the input power small, say for example 100W. This would make the coaxial CNT speaker high power consuming when compared to conventional loudspeakers. So, the simulations performed to estimate the axial, cross-sectional and industry standard SPLs

will help to tune the design of the coaxial CNT speaker to improve its SPL generation withing the specified input power and dimension requirements.

5.6 Effect of flow on the acoustic field generated by the coaxial CNT speaker

5.6.1 COMSOL Flow Model Validation

Before setting up the flow model for the coaxial CNT speaker, it was important to validate the procedure used in setting up the model. The effect of turbulent flow on the acoustic wave travelling through the pipe is analyzed by observing the attenuation of the SPL. So, analytical equations to determine the attenuation of sound by the turbulent flow was used and compared with the attenuation obtained from the COMSOL flow model.

Howe et.al. studied the damping of the sound in a pipe with turbulent flow. Four mechanisms contribute to the attenuation of sound transmitting through a pipe with fully developed turbulent flow. These mechanisms are:

1. Viscous (shear) effects in bulk fluids
2. Thermal conduction in bulk fluids
3. Molecular absorption in bulk fluids
4. Thermoviscous boundary layer losses

The model described by Howe et.al. considers the effect of eddy viscosity-controlled momentum and thermal wall boundary layers that are generated when acoustic wave interacts with a low Mach number turbulent boundary layer. The equation derived by Howe

is effective only when the turbulent boundary layer thickness is much smaller than the wavelength of sound travelling through the pipe. The main objective behind the coaxial CNT speaker design was to cancel low frequency sounds and their harmonics (mainly in the range of 50Hz-500Hz). So, the sound that was to be generated by the coaxial CNT speaker had large wavelengths compared to the turbulent boundary layer thickness. This makes the use of this model appropriate to validate the COMSOL flow model.

In the analytical model, the pipe through which sound is propagating is smooth pipe with a uniform cross-section A and perimeter l. The turbulent flow is fully developed, with a low Mach number and high Reynolds number. The acoustic frequency is small enough with a wavelength much larger than the diameter of the pipe, resulting in a one-dimensional propagation of the acoustic wave, in other words, a plane wave. The limiting condition for the frequency of sound in a pipe of radius R is

$$\omega < 1.84 * c_o/R \tag{80}$$

where, ω is the angular frequency (rad/s), c_o is the speed of sound in the medium (m/s) and R is the radius of the pipe(m)[165,166]. With high Reynolds number flows, the mean velocity variation is slow along the cross-section of the pipe except near the walls of the pipe. In such a case, the mean flow velocity U is constant in the center of the pipe. In addition, all dissipative mechanisms are neglected compared to the damping caused by the acoustic-turbulence interactions at the pipe wall[164].

With these assumptions, the attenuation of sound both upstream and downstream of the pipe is determined as

$$\alpha_+ = \frac{\sqrt{2\omega}}{c_0 D_p(1+/-M)} * Re(\sqrt{2}e^{-\frac{i\pi}{4}}[\frac{1}{\left(1+\overline{-M}\right)^2}\sqrt{\upsilon} * F_A\left(\sqrt{\frac{i\omega\upsilon}{\kappa^2 {v_*}^2}}, \delta_v\sqrt{\frac{i\omega}{\upsilon}}\right) +$$

$$\frac{\beta {c_0}^2}{c_p}\sqrt{\chi}F_A\left(\sqrt{\frac{i\omega\chi {P_t}^2}{\kappa^2 {v_*}^2}}, \delta_v\sqrt{\frac{i\omega}{\chi}}\right)) \quad (81)$$

where, α_+ is the attenuation downstream (dB), ω is the angular frequency of sound (rad/s), c_0 is the speed of sound in the medium, D_p is the hydraulic diameter of the pipe (4*A/L), M is the mach number, υ is the kinematic viscosity of the medium, κ is the Von Karmann constant, v_* is the friction velocity, δ_v is the frequency dependent length, β is the inverse of the absolute temperature in K, χ is the thermometric conductivity of the fluid, c_p is the specific heat of the medium at constant pressure.

In the above equation, Fa is defined as

$$F_A(a,b) = \frac{i(H_1^{(1)}(a)\cos(b) - H_0^{(1)}(a)\sin(b))}{(H_0^{(1)}(a)\cos(b) + H_1^{(1)}(a)\sin(b))} \quad (82)$$

where, $H_1^{(1)}$ and $H_0^{(1)}$ are the Hankel functions of the first and zeroth order respectively. The friction velocity is determined from the Mach number (M), the mean flow velocity (U) and speed of sound in the medium (c_0) as,

$$\frac{U}{v_*} = 2.44\ln\left(\frac{v_* R}{\upsilon}\right) + 0.2 \quad (83)$$

Solving for the above equation gives the attenuation of the sound pressure level of the acoustic wave in the pipe in dB. Whenever this attenuation is represented, it is normalized by the attenuation in the absence of flow. The attenuation in the absence of flow is determined by

$$\alpha_0 = \frac{\sqrt{2\omega}}{c_0 D_p}\left(\sqrt{\upsilon} + \frac{\beta {c_0}^2}{c_p}\sqrt{\chi}\right) \tag{84}$$

One reason for doing this to make sure that the attenuation in presence of flow formulation from equation 81 is correct. This can be done by making sure that for M=0, the attenuation values from equation 81 and 84 are equal.

The parameters used for solving equations 82, 83 and 84 are given in table 5.

Table 5: Parameter values used to determine the attenuation of sound in pipe with turbulent flow and in the absence of flow.

Parameter Value	**Value**
ω	88Hz
M	0:0.01:0.12
c_0	343m/s
R	1.5cm
l	0.1524m
υ	0.15cm/s
χ	0.2cm/s
P_t	0.7
κ	0.41
T	293.15K
c_p	29130J/(kg*K)
δ_v	$(6.5^* \upsilon)/ v_*$

On observing the attenuation result from equation 91, it is observed that the attenuation increases with increase in the flow Mach number. Using the parameters of the pipe dimensions, Mach number, mean flow velocity, medium properties, the COMSOL flow model was built and simulated. The attenuation was determined by calculating the difference between the SPL observed in the pipe and the SPL of the source generating the acoustic wave in the pipe. Comparison between the simulated and analytical result shows good correlation. There is some difference in the two values mainly because of the difference between the friction velocity and boundary layer values generated in the COMSOL model and those calculated by the analytical equations. With this comparison, the COMSOL flow model of the coaxial CNT speaker was developed and simulated.

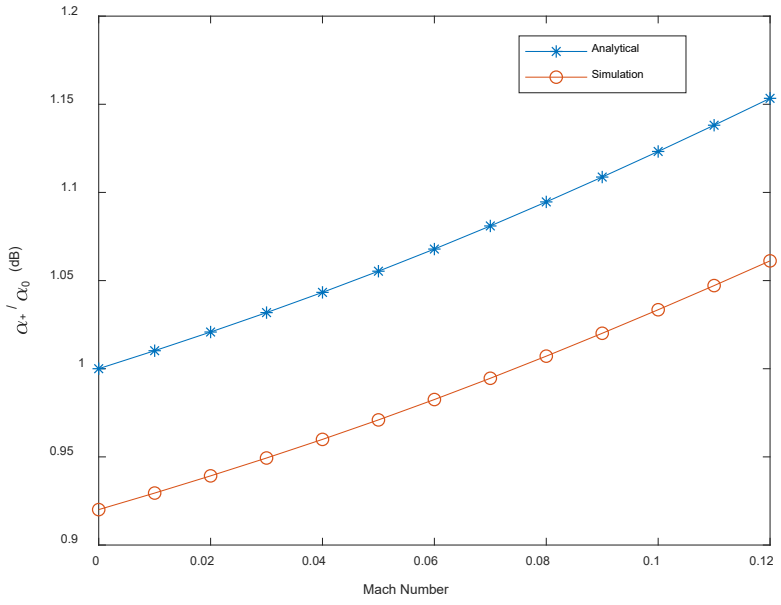

Figure 63: Comparison between the normalized attenuation by the analytical equation and the COMSOL flow model. The difference in the values is due to difference in the boundary layer parameters between the COMSOL model and analytical equation calculations.

5.6.2 COMSOL Coaxial CNT Speaker Flow Model Results

The CFD module computed the flow velocity and dynamic viscosity for flow through the coaxial CNT speaker (figure 64). It can be seen from the results that the flow velocity along the boundary of the slotted pipe is higher than the velocity inside the outer cover chamber. One reason for this is that slots have a large area and so, the flow moves through the slots, there is reduction in the flow velocity. This effect is like the nozzle principle, where speed decreases when cross-sectional area increases. For the dynamic viscosity result, it can be observed that the viscosity change is more prominent closer to the inlet, and it gradually stabilizes towards the outlet. Also, the change in the value is more prominent in the outer cover chamber than in the slotted pipe. The reason for this is that dynamic viscosity is expressed in terms of Pa*s. So, in the presence of higher pressure in the outer cover chamber, the dynamic viscosity also experiences a higher change as compared to slotted pipe where the pressure change is not significantly high.

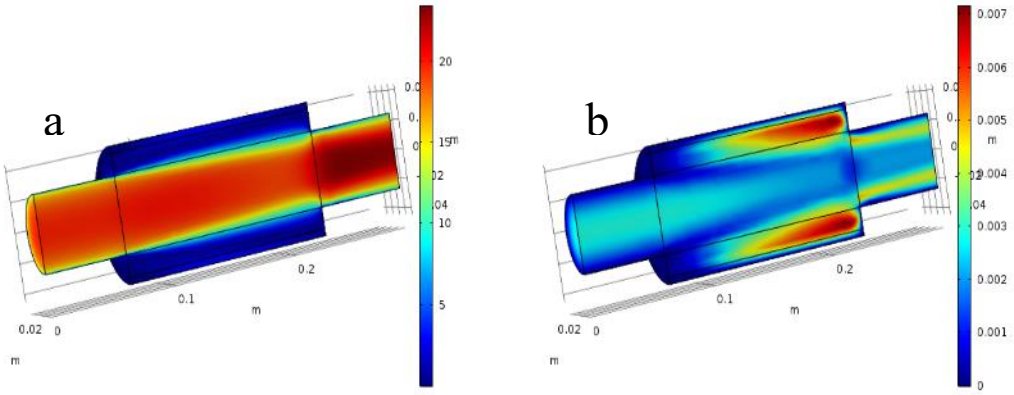

Figure 64: The flow velocity as simulated by the COMSOL model (a). It can be observed that we have reduced flow velocity in the outer chamber. The dynamic viscosity as simulated by the COMSOL model (b). Higher change in the dynamic viscosity is observed in the outer chamber.

The acoustic simulation results were obtained after mesh mapping the CFD computed parameters – flow velocity and dynamic viscosity (figure 64). The simulation was performed for a Mach number of 0.05 for a frequency of 300Hz. It can be observed from the result that sound field and the SPL value observed inside the speaker is significantly different from the condition when no flow is present through the coaxial speaker. One of the reasons for this is the effect of flow on the acoustic particle velocity and correspondingly the SPL. The attenuation of the SPL in the CNT speaker is mainly due to the generation of the thermal, viscous and thermoviscous boundary layers in the presence of fully developed turbulent flow. The sound field which was planar for no flow is changed to a more distorted field. It will be very difficult to cancel noise in the presence of a non-planar field. One of the ways in which the sound field can be made to remain as planar as

possible is to modify the slotted pipe geometry and area so that the flow velocity does not undergo a high level of change in its value. This will make sure that flow pressure and velocity inside the speaker will not have a large effect on the acoustic field.

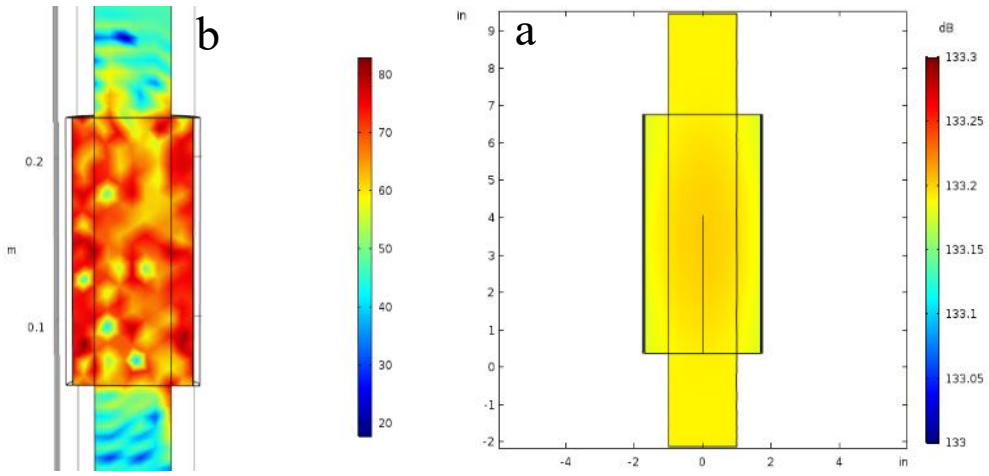

Figure 65: The acoustic field and the SPL generated inside the coaxial speaker in the presence of flow (a). The acoustic field and the SPL generated inside coaxial speaker in the absence of flow (b). Flow has a significant effect on the acoustic field.

From the results seen above, it is evident that the sound field generated in the absence of flow is different from that generated in the presence of flow. For applications where medium flow is present (example: automotive exhaust noise cancellation, HVAC noise cancellation, etc.), it becomes important to characterize the effect of flow on the enclosed, coaxial CNT speaker sound field. Understanding the flow profile of the medium, mainly its Mach number and either laminar or turbulent helps to determine the operating conditions of the CNT speaker. In addition, flow analysis can be linked to the axial, cross-sectional and radiated SPL of the coaxial CNT speaker. The results presented in section 5.4 are for no medium flow and planar sound field in the pipe conditions. As the sound field becomes

distorted, the SPL along the longitudinal axis is no longer uniform. This could result in significant changes in the sound radiated from the ends of the coaxial speaker. One effect might be further reduction in the radiated SPL compared to in-pipe SPL. Simulating the sound generation in different flow conditions will help to tune the speaker to achieve maximum performance and increase SPL. In addition, the flow simulations would help to estimate the coaxial speaker performance in situations where physical testing of all design iterations and all flow conditions is difficult or not possible.

5.7 Optimization of the CNT speaker model using COMSOL

5.7.1 Expansion Chamber Optimization

The transmission loss profile of a simple expansion chamber is well known. So, it was easy to verify the validity of the optimization process as well the optimized model. The transmission loss profile of a simple expansion chamber with equal area inlet and outlet tubes depends on the area of the central chamber, area of the side tube and the frequency of the sound passing through the chamber. So, for this optimization, the control variables chosen were the length and the diameter of the central chamber. These control variables were bound using a lower and upper limit to reduce the time required for computation and keep the control variable values within the reasonable range. The figure below shows the expansion chamber model in COMSOL. The initial values of the expansion chamber dimensions are listed in table.

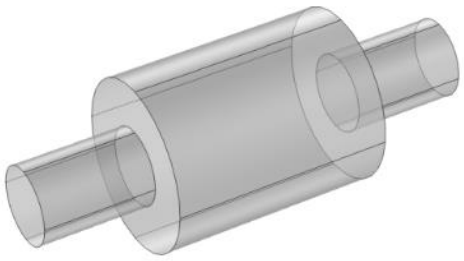

Figure 66: Expansion chamber model in COMSOL used for optimization. The model has the same dimension inlet and outlet pipe.

Table 6: Original dimensions of the expansion chamber model

Expansion Chamber Component	Length (m)	Diameter (m)
Central Chamber	0.2032	0.15328
Inlet Pipe	0.1048	0.0349
Outlet Pipe	0.1048	0.0349

The most important part of any optimization problem is the definition of the optimization variable. The goal of this optimization is to increase the transmission loss of the expansion chamber. With the original dimensions, the highest transmission loss value was 8dB. The target transmission loss was set at 20dB. The optimization function was defined as the

difference between the simulated transmission loss and the target value of 20dB. This difference was then minimized to get the dimensions that would give the transmission loss closest to the target value. The optimization algorithm used for this was the BOBYQA algorithm. The frequency range of optimization was from 10Hz to 1500Hz.

The result of the optimization and the corresponding transmission loss is shown in figure below.

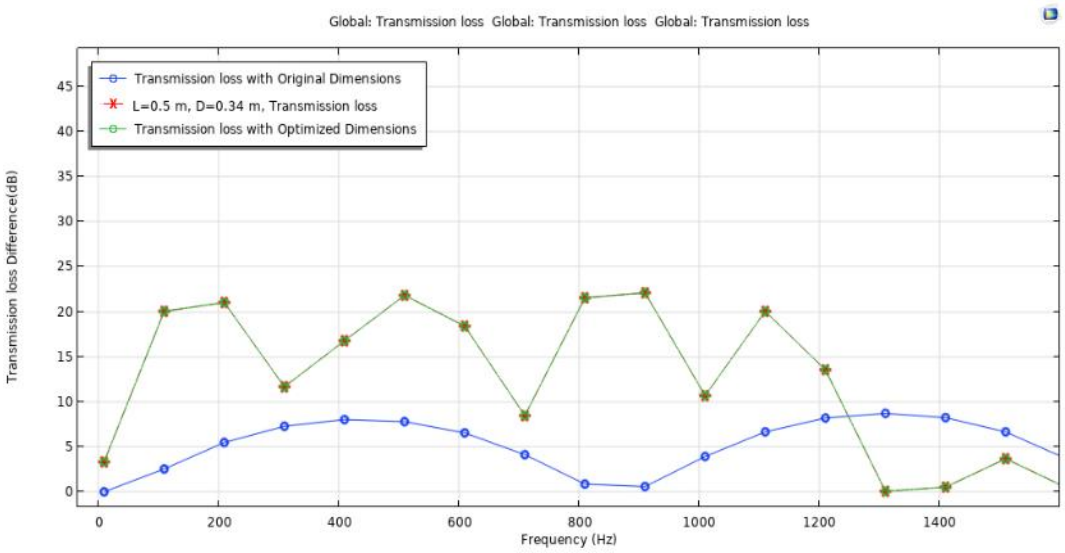

Figure 67: Transmission loss comparison between the original and optimized expansion chamber design. The target transmission loss of 20dB was met with this optimization.

From the above figure, it is evident that the transmission loss of the optimized design is higher than the original design expansion chamber and is close to 20dB in value. The optimized length and diameter of the central chamber are 0.5m and 0.34m respectively. These values are in the specified range of length (0.1m and 0.7m) and diameter (0.14m and 0.6m). Thus, the goal of the optimization has been met.

There is one important point to remember during multiple frequency optimization. The optimizer does not use the objective value at all frequencies during optimization. During the first sweep, the optimizer determines the frequency at which the objective function is closest to the specified objective. The remaining iterations are then performed at that frequency to satisfy the objective function requirement. The objective for this type of optimization is called as a min-max objective. Due to this, it is possible that we might not have the highest objective value at all frequencies used in the simulation. This is evident from the optimization result for the expansion chamber. For frequencies above 1200Hz, the transmission loss is lower than the original chamber transmission loss. It can be inferred from this that optimization has a tradeoff focusing on the most important frequencies. So, care must be taken to pinpoint the frequencies that are of most interest and then perform the optimization targeted at those frequencies.

The optimization of the transmission loss of the expansion chamber provided a validation of the optimization method – definition of objective function, selection of control variables and the optimization algorithm. Based on this, optimization was performed on the coaxial CNT speaker.

5.7.2 Coaxial CNT Speaker Optimization

The main goal of optimization of the coaxial CNT speaker is to achieve the desired SPL while keeping the dimensions of the speaker, particularly the length and diameter of the coaxial speaker within the required dimension limits. There are two main reasons for choosing these as the control variables. First, the SPL generated by an enclosed CNT speaker is dependent on its volume. So, changing the length and the diameter of the coaxial

speaker would have effect on the SPL of the speaker. Second, CNT speakers are known for being able to be designed smaller than conventional speaker systems. Optimizing the dimensions of the CNT speaker will help to select the best possible dimension within the desired range while maximizing the SPL from the speaker.

The optimization model setup of the coaxial CNT speaker is complicated compared to the expansion chamber. The basic goal of the optimization is the same – increase the SPL while maintaining the desired dimensions. The setup of the objective function is different compared to the expansion chamber. The coaxial CNT speaker should generate plane waves in the desired frequencies of interest for effective noise cancellation. During optimization, it is necessary to make sure that the final dimensions generate a plane wave along the CNT speaker. For this purpose, probes are defined along the longitudinal axis of the CNT speaker (figure 68). These probes measure the SPL generated inside the speaker during the simulation. Having multiple probes ensures that the SPL is uniform along the CNT speaker and thus a plane wave is generated for all the optimization steps. For each of the probe, the measured quantity is the SPL generated. When compared to reality, these probes can be assumed as microphones that measure the axial SPL of the CNT speaker.

Figure 68: Probe location in the coaxial CNT speaker optimization model. The red dots are the locations of the probes used to define the objective function.

As mentioned previously, maximizing the SPL is the target of the optimization. So, the objective of the optimization is like the expansion chamber optimization. The difference the SPLs measured by the probes and the target SPL is to be minimized to achieve optimized dimensions. The differences between all the probes and the target SPL are added and defined as the optimization objective. The objective is then minimized to determine the minimum difference between the mic SPLs and the target SPL. The addition of the difference in SPL is interpreted by the optimizer as the requirement for a flat response from the CNT speaker along its axis. Another advantage of defining the objective function in this fashion is that the optimizer will try to flat out the SPL response of the CNT speaker.

Choosing a high target SPL will make sure that the SPL at multiple frequencies will be closer to that value and increase the overall SPL response of the speaker. The optimizer identifies the frequency at which the objective function is the closest to the objective and then performs the remaining iterations at that frequency. So, it is expected that the SPL at

all frequencies might not be uniformly close to the target SPL due to optimizer behavior and the acoustic modes of the coaxial speaker.

The setup of the physics involved in the coaxial CNT speaker optimization involves thermoviscous acoustics and pressure acoustics. These two physics will simulate the model to determine the SPL generated by the speaker. For every single optimization iteration, the SPL is simulated using these physics and the objective value is compared with the previous value to determine the minimum objective value. The BOBQYA solver is used as it is a gradient free solver.

The original dimensions of the coaxial speaker model are listed in the table below:

CNT Speaker Component	Original Dimension Value (m)	Optimization Range (m)
Length of Outer Cover	0.16256	0.1524 – 0.2032
Diameter of Outer Cover	0.0889	0.0762 – 0.127

Two separate studies were setup – first study computes the SPL generated at the original dimensions and the second computed the optimized dimensions. The optimization was performed at three frequencies: 100Hz, 125Hz, and 160Hz. Only three frequencies were chosen because the complexity of the model and the time required for the simulation. The target SPL chosen was 2dB above the highest original SPL of the coaxial CNT speaker

which was 115.3dB. The small difference chosen between the original and target SPL was to reduce the range of the control variables. If the optimized dimensions SPL meet the 2dB increase requirement, it demonstrates the performance of the optimized model.

The comparison between the original SPL, optimized dimension SPL is shown in the figure below.

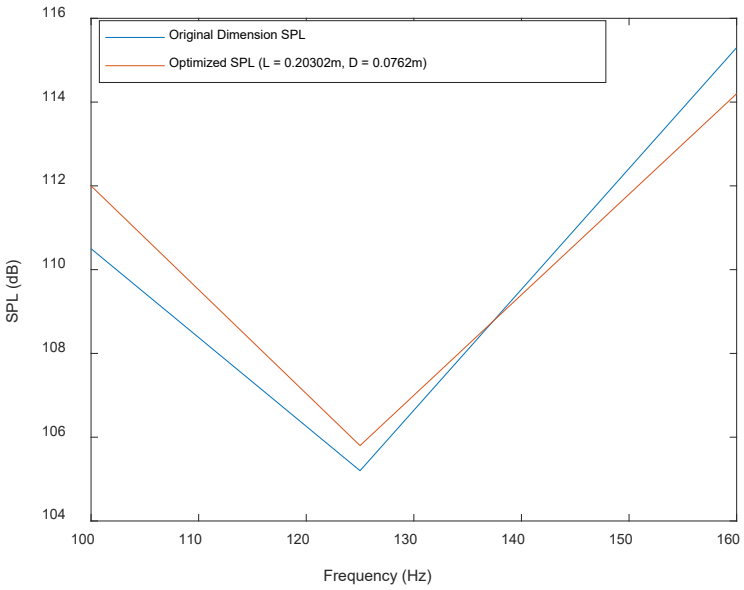

Figure 69: SPL comparison between the original dimension and optimized dimension coaxial CNT speaker. The optimization was performed at 125Hz frequency as the difference between the probe and target SPL was the minimum.

The optimized length and diameter of the outer cover of the coaxial CNT speaker is 0.2032m and 0.0762m respectively. The optimized values are within the specified control variable range and reasonable from manufacturing point of view. As regards to the SPL, optimized SPL is closer to the target SPL of 117dB. From the above graph, the optimized

SPL profile is following the original SPL profile, maintaining the reasoning that the acoustic modes of the coaxial speaker affect the SPL generated. In an ideal optimization, the SPL at all the frequencies would be close to the target SPL, thus generating a flat sensitivity of the CNT speaker.

The above-described procedure optimizing the CNT speaker should work for both open and enclosed CNT speakers. The main difference between the two models would be location of the probes, the value measured by the probes and control variables. For example, in the optimization model of an open CNT speaker, the probes would be in the near field and then the far-field values would be extrapolated using the measured SPL and the relation between distance and SPL. The control variables would still be length and the width of the CNT film but in this case, it is the area of the film that would be important.

Optimization is extremely beneficial in any design process, particularly in the case of CNT speakers. As mentioned in the previous sections, it is difficult, time consuming and expensive to manufacture and wrap every single design iteration of the CNT speaker. In addition, there can be several combinations of the speaker dimensions that could be possible when designing the CNT speaker. Identifying the perfect dimensions that would give the best performance in different operating conditions and applications is difficult without optimization. Optimizing the dimensions to achieve the desired performance (example: maximum SPL, minimum input power, small size, etc.) saves valuable time, money, and effort. It also provides a good approximation of the performance to expect from the CNT speaker. Comparison between the optimized speaker simulations and actual measurements can further help in fine tuning the CNT speaker and get the best possible

result for its performance and size. Optimization can also combine the flow, SPL and any other physics involved in the simulation of the CNT speaker to provide a complete analysis of the speaker performance in the desired operating conditions. The optimization procedure discussed in this research is the first step in perfecting a process to better analyze and design CNT speaker, both open as well as closed.

6 Conclusion

6.1 Contribution and Summary

The enclosed, coaxial CNT speaker developed for the automotive noise cancellation application is the first such design of its type for CNT speakers. It is a novel design for any speaker that allows the medium to flow through it without damaging the speaker. In addition, the speaker design is unique as it allows for in-line connection with the automotive tailpipe, like a muffler. Due to no obstruction to the exhaust gas flow, it generates little-to-no backpressure in the vehicle. This is an improvement not only on the current active control systems but also on mufflers as they generate backpressure. For the first time, a noise control element for automotive noise control was proposed, designed, and validated in lab that was small and whose size did not depend on the frequency of the sound that is being controlled or generated.

COMSOL Multiphysics is a powerful tool to model the behavior of the CNT speaker. In this research, the first 3D simulation model of an enclosed, coaxial CNT speaker is developed using COMSOL Multiphysics. This model is a powerful tool to simulate the SPL performance of the speaker. The surface temperature of the CNT film and the SPL generated were obtained using COMSOL model and validated by the experimental and analytical results. The model is the first 3D model to be applied for the enclosed CNT speaker to approximate its performance and the first to incorporate flow modeling in the acoustics of the CNT speakers and can be expanded to any enclosed design of the CNT speaker.

With respect to the SPL performance of the coaxial speaker, it was observed that there were peaks and valleys in the SPL with respect to frequency. The presence of acoustic modes of the speaker chamber is the reason behind this. On the determination of the acoustic modes both experimentally and by simulation, it was observed that the acoustic modes had constructive as well as destructive interference effect on the SPL generated by the CNT speaker. Performing acoustic modal analysis will aid in the design of the enclosed CNT speaker to improve performance at target frequencies for the selected design of the CNT speaker.

Three types of SPL characterization of an enclosed, coaxial CNT speaker were performed: axial, cross-sectional and industry standard. The axial SPL measurement is important to ensure that the SPL is uniform along the speaker axis, validating the generation of plane waves from the coaxial speaker. The enclosed, coaxial CNT speaker discussed in this research demonstrated plane wave generation from both experimental and simulation results. Secondly, when sound is transmitted along a pipe, the SPL profile at different frequencies across the pipe cross-section depends on the acoustic pipe modes. It is important to analyze these profiles if the sound radiated from the speaker emits into the ambient environment is of primary concern. Simulation and experimental results, in good agreement with each other showed that at high frequencies, the sound profile tends to be less uniform when compared to low frequencies. In the automotive industry, SPL from active control system speaker is measured at 500mm and 45^{o} from the outlet of the tailpipe. The SPL radiated from the enclosed, coaxial CNT speaker was measured at the above-mentioned distance and angle. On comparing the SPL at the center of the speaker with the radiated SPL, similar sound profile was observed with a reduction of 30dB in SPL. The

main recommendation is to use in-pipe SPL as a standard measurement method as opposed to the industry standard method (500mm and 45^{o} from the speaker outlet). This is because the coaxial CNT speaker inputs plane wave directly into the tailpipe which is important for good active cancellation.

In the real world, particularly for noise control application, there is almost always flow present in the medium in which the enclosed, coaxial CNT speaker will be operated. For example, in the automotive exhaust, there is flow of exhaust gases at high speeds. The effect of flow on the SPL generated by the CNT speaker was determined with the help of flow model in COMSOL. The flow model developed was the first model to simulate the effect of flow on the coaxial CNT speaker operation. It was observed that turbulent flow has a significant effect on the acoustic field generated inside the coaxial speaker, primarily in making it non-planar. In addition, the SPL was also reduced compared to the absence of flow in the medium. This model gave an idea of how the presence of flow affected the SPL and the acoustic field inside the coaxial speaker. The results were important from a noise cancellation point of view as it is very difficult to cancel non-planar sound. All said, this analysis provides a new aspect of CNT speaker design to improve its performance by iterating the speaker design for different mediums and flow parameters that was not done previously.

Optimization is a useful tool in any design process as it reduces the effort required to manufacture and test every single design iteration to assess system performance. CNT speakers are difficult to wrap manually making it a tiring and painstaking process to wrap and build every single design of the speaker. The optimization model developed in this

research is the first 3D model of the enclosed, coaxial CNT speaker that helps to approximate the best speaker dimension combination within the required dimensions limit. The COMSOL model described in this research has the objective of SPL maximization while setting limits on the control variables of length and diameter of the outer chamber. One important point to remember is to make sure the optimized dimensions of the speaker yield uniform SPL along the longitudinal speaker axis. This was achieved by using probes along the speaker axis and maximizing the sum of the SPLs at all the probes. In addition, the optimization model developed can be extrapolated to any CNT speaker design – open or closed to increase the speaker performance, especially the generated SPL.

In addition, during the research, literary contributions have been made in the form of two peer reviewed journal publications and five conference papers. The Acoustical Society of America presentations were abstract and presentation only, whereas the INTER-NOISE and NOISE-CON proceedings included an archival paper. The journal publications are:

1. Prabhu, S. M., & Barnard, A. (2020). Design and characterization of an enclosed coaxial carbon nanotube speaker. *The Journal of the Acoustical Society of America, 147*, EL333-EL338. http://doi.org/10.1121/10.0001029

2. Prabhu, S., Barnard, A., and Senczyszyn, S., "Multi-Physics and CFD Analysis of an Enclosed Coaxial Carbon Nanotube Speaker for Automotive Exhaust Noise Cancellation," *SAE Int. J. Adv. & Curr. Prac. in Mobility* 1(4):1808-1816, 2019, https://doi.org/10.4271/2019-01-1569.

The conference papers are:

1. Prabhu, S. M., & Barnard, A. Performance Analysis of an Enclosed, Coaxial Carbon Nanotube (CNT) Speaker in the presence of flow using COMSOL Multiphysics. The Journal of the Acoustical Society of America 148, 179th Virtual Meeting of the Acoustical Society of America. https://doi.org/10.1121/1.5147464.

2. Prabhu, S. M., & Barnard, A. COMSOL Model of an Enclosed Coaxial Carbon Nanotube (CNT) Speaker with Perforate Analysis. *Inter-Noise and Noise-Con Proceedings,* NoiseCon 19, San Diego, CA, pp. 218-226.

3. Prabhu, S. M., & Barnard, A. COMSOL Model for an Enclosed Coaxial Carbon Nanotube Speaker. *Inter-Noise and Noise-Con Proceedings,* InterNoise 18, Chicago, IL, pp. 1057-1065.

4. Prabhu, S. M., & Barnard, A. Active Control of Automotive Exhaust Noise using Carbon Nanotube Speakers. *Inter-Noise and Noise-Con Proceedings,* NoiseCon 17, Grand Rapids, MI, pp. 505-511.

5. Prabhu, S. M., & Barnard, A. Carbon Nanotube Coaxial Thermophone for Automotive Exhaust Noise Cancellation. *The Journal of the Acoustical Society of America 142,* 174th Meeting of the Acoustical Society of America, New Orleans, LA. https://doi.org/10.1121/1.5014277.

6.2 Simulation Model Setup Recommendations

A certain procedure must be followed to setup the four models developed in this research. The procedure relates to the definition of the CNT film material properties, domain definitions, number of mesh elements used, mesh element size, etc. The following sections identify the key recommendations based on this research.

6.2.1 Joule Heating and Thermoviscous Acoustics Model Setup

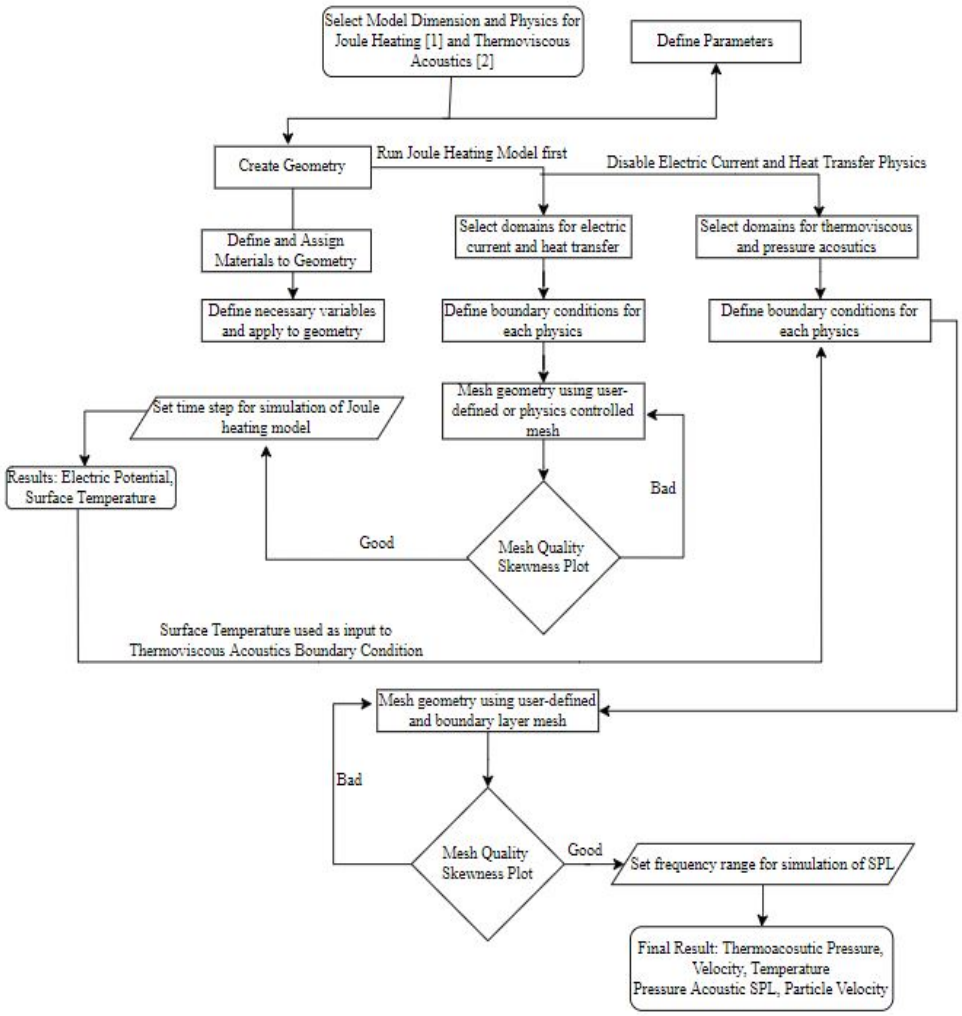

Figure 70: Flow chart for Joule Heating and Thermoviscous Acoustics model setup

[1] Joule Heating Model Recommendations

- The electrical conductivity of a metal can undergo change with increase in its temperature due to internal heat generation. This must be used in the material property using the appropriate equation that defines the relation between

conductivity and temperature change for that material. For copper electrodes, this value change is small as it acts as a heat sink.

- Electric current follows a path defined by the conducting and non-conducting boundaries. The definition of the non-conducting boundaries must be done by defining the potential (V) along them as zero, $V = 0$.
- Input electrical signal must be correctly defined to ensure proper replication of the actual operating signal. For example, the time used to define the AC input must be the same as the time specified for the simulation.
- In heat transfer physics, the heat flux of the boundaries defines the heat transfer, and its form is dependent on the material and the heat transfer mechanism. The correct heat transfer mechanism (conduction, convection, or radiation) must be selected, and the corresponding heat transfer coefficient of the material must be defined to get accurate results.
- The medium in which the model is simulated can experience a change in its material, electrical and thermal properties due to heat transfer from the model boundary. It is important to incorporate this, and it can be done by defining the properties using equations that relate the property and the variable affecting its change. For example, the density of the air medium can be related to temperature change using the ideal gas law equation, $pV = nRT$.

[2] Thermoviscous Acoustics

- The thermal expansion coefficient and isothermal compressibility coefficient of the medium are important variables in thermoviscous acoustics. They are dependent on

the temperature and the pressure developed in the medium. The model must account for changes in these variables by using the appropriate equations defining their dependence on temperature and pressure for the selected medium material. One form of equation is $\rho = \rho_0(\beta_T p - \alpha_0 T)$

- The thermal and viscous boundary layer thickness are frequency dependent and decrease exponentially with respect to the frequency. In multi frequency simulation, the maximum and minimum mesh element size must be the thickest and thinnest value of the boundary layers.
- The thermoviscous acoustic domain thickness must account for the thermal and viscous boundary layer thicknesses for the frequency range being simulated. So, the domain thickness should be the thickest value of the boundary layers that are generated. For smaller boundary layer thicknesses, it can result in error in the acoustic sound wave generation amplitude, but this error is small compared to the error generated when the domain thickness is smaller than the thermal and viscous boundary layer thicknesses.
- The boundary layer mesh is important to model the thermal and viscous boundary layers in the thermoviscous acoustics simulation. Mapped mesh elements are used to the boundary layer mesh. Boundary layer profile is parallel to the surface next to which it is developed, and mapped mesh elements make sure the mesh element sides next to the boundary follow the profile of the boundary.
- Higher order shape functions must be used when meshing the thermoviscous boundary. This results in a more accurate evaluation of the boundary behavior as

the distribution of the thermoviscous variables over the boundary is not liner. Generally, a fourth order shape function works best for these boundaries.

6.2.2 Flow and Optimization Model Setup

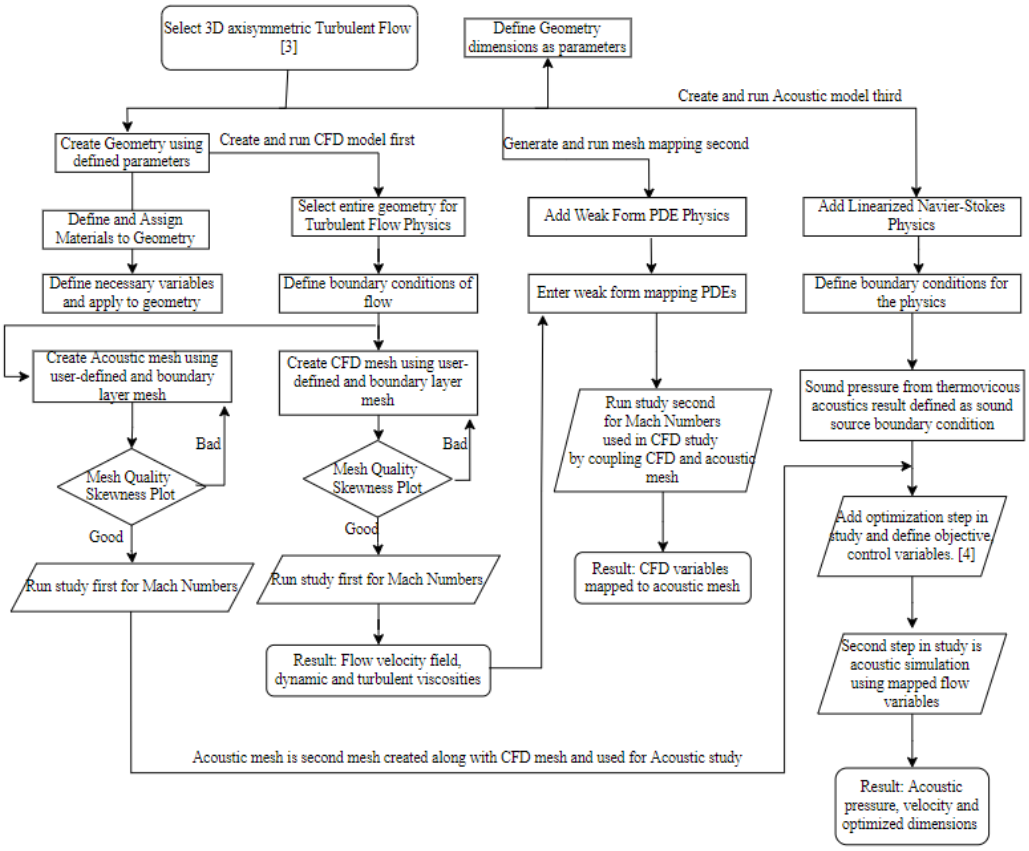

Figure 71: Flow chart for Flow and Optimization model setup

[3] Flow Model Recommendations

- The geometry profile is important for flow model accuracy. The geometry must be checked for missing faces, overlapping faces, gaps, free edges, and sharp angles. Before meshing the geometry, it must be checked for these points, and they must

be fixed. This can be done by modifying the geometry to fill gaps, add missing faces, removing the free edges by connecting or deleting the free edge.

- Large area changes result in more drastic medium flow variable changes. To model the flow variables accurately, finer mesh must be used at these parts in the model. The size of the mesh element must be smaller than the dimension of the boundaries at which there is large area change to get good resolution at those locations.
- The proper definition of the physical, thermal, and fluid properties of the medium can change during the simulation. For example, the automotive exhaust gases can undergo a change in their composition and properties based on the operating condition of the engine. So, identifying the change in the properties and modifying the material properties accordingly in important for accurate simulation.
- Boundary layer mesh is important in flow model. Based on the boundaries present in the geometry where boundary layers are generated, the boundary layer mesh made of mapped mesh elements must be used to accurately resolve the boundary layers for fully developed flows.
- Flow in a system can be laminar, turbulent or a combination of both. Each flow type has its own governing equations, model operating and boundary conditions. It is important to identify the correct flow type and then use the correct governing equations and boundary conditions to set up the flow model. For example, for a pipe, based on the diameter of the pipe, the Reynolds number (Re) is less than 2100 for fully developed laminar flow, greater than 4100 for fully developed turbulent flow. The medium material properties and Re number used must match the flow type being simulated.

- All boundary conditions must be defined for the geometry of the flow model. For example, the pipe walls are either no-slip, adiabatic or both relative to the flow medium. So, the correct boundary conditions must be used to simulate their behavior in the simulation model. This can be done by using the defining equation with respect to the variable (e.g.: adiabatic – $Q = 0$, no slip = $V_{normal} = 0$ and $V_{tangential} = V_{wall}$) and assigning it to the boundary.

[4] Optimization Model Recommendations

- The objective function selected must be based on the variable that has to be improved. For example, CNT speakers are evaluated by their generated SPL. The objective function should be defined as a value that is calculated by the model for every iteration or an equation whose solution is evaluated by the model for the iterations it performs. The definition of the PDE objective must include variables that are iterated by the optimizer. For example, if the temperature of a surface with heat flux is being optimized, the PDE for heat transfer can be optimized and the control variables will be the coefficient of heat transfer and surrounding medium temperature (equation 33).
- Control variables are the key to an optimization process. These variables are iterated, and the optimized results are obtained. The selection and definition of the control variables is important, and they must be related to the optimization objective. For example, the SPL generated in an enclosed CNT speaker depends on its volume (equation 23). The control variables in this case, must be the dimensions of the enclosure so that during the optimization process, every

iteration will result in change in the volume of the enclosure and the objective function value will change accordingly.

- Constraints to the control variables are important based on the optimization being performed. If they are not defined when required, it will result in free optimization that can continue for a very long time and provide results that are not feasible. For example, if the dimension control variables of the CNT speaker enclosure are not constrained, it might result in a shape that is not feasible in the real world.
- Depending on the type of optimization being performed, the correct optimizer must be selected. For a design optimization that changes the shape of the geometry in every iteration, derivative free solver must be used. This optimizer handles the geometry and corresponding finite element mesh change efficiently, without taking a long time to optimize the model.

The above-mentioned recommendations are important to successfully setup the CNT speaker models and can be used as a general recommendation when the models are used for other applications. These recommendations must be followed to make sure that the material properties, boundary conditions and meshing is done correctly to maintain the accuracy and repeatability of the models.

6.3 Model Limitations

The governing equations for the physics that are used to develop the modeling method for CNT speakers have limitations with respect to the operating conditions.

For effective resolution with frequency, it is a general rule of thumb that the minimum element size must be equal to at least 6 elements per wavelength for meshing the model. For low frequencies, it is a very small number, and it increases the number of elements required as well as reduces the size of the elements for proper frequency resolution. In region with extremely small thickness, sharp changing areas, boundaries with small dimensions, it becomes very difficult to maintain the size of the elements small to satisfy the frequency resolution condition as well as keep the element size smaller than the boundary dimensions. In addition, for multi frequency simulation, using an uniform mesh developed at one frequency will not provide a good resolution at other frequencies in the simulation. The models developed for the CNT speaker used uniform mesh size based on a single frequency. The frequency chosen for this was 250 Hz and required mesh elements within the range of 100000 to 300000 elements. This allowed the boundary layer mesh and the thermoviscous acoustic mesh to remain small with respect to the CNT film boundary. However, it affected the frequency resolution at lower frequencies, and it is possible that, this is one of the reasons why there is amplitude difference between the simulated and experimental SPL results. An adaptive mesh can be used but it takes significantly longer to simulate the model when multiple physics are involved, irrespective of the type of computer used for simulation.

The SPL model uses standard pressure acoustics equations that include the wave and Helmholtz equations to solve for the specified boundary conditions. Non-linear acoustics at high SPL requires full set of fluid dynamics and elasticity governing equations that are used to determine the sound wave behavior in liquids and gases. The model used to simulate the SPL of the CNT speaker cannot handle non-linear acoustics because the

physics does not incorporate the required governing equation. In addition, the system is highly non-linear, and the corresponding sound wave is distorted. The meshing process required for non-linear acoustics simulation is more complex and additional variables are required to define the element size. This is not defined in the developed model.

The Thermoviscous acoustics model uses Full Linearized Navier Stokes (FLNS) equations to solve the model. The FLNS equations are widely applicable but computationally costly and inefficient. For the 3D model of the enclosed, coaxial CNT speaker, it took the MTU supercomputer, Superior, almost 5 hours to run the model with 12 cores and the model had more than 5,000,000 elements. This simulation was done to estimate the time required to run the model with the finest mesh quality relative to the simulating conditions. One of the reasons for requiring a large number of mesh elements is that the mesh size must be extremely fine near the thermoviscous boundary to accurately resolve the viscous and thermal boundary layers. Second, the FLNS equations contain five coupled fields (velocity, temperature, and pressure) out of which four are quadratic in nature and the pressure field is linear. This makes it necessary to define appropriate order shape functions for the respective fields and this results in increased computation cost. Generating a very fine mesh becomes difficult when the thermoviscous domain is extremely thin and the geometry is complex, with sharp changes in profile. This is the case with carbon nanotube films, because their thickness is many orders of magnitude smaller than their other dimensions.

The flow model for turbulent flow can replicate the flow profile with only a high degree of approximation. This is because it is very difficult to accurately reproduce the fully developed turbulent flow using the governing equations. This limits the model response in

predicting the flow field and the corresponding effect on the sound field generated in the presence of turbulent flow. So, the model has limited capability and accuracy in determining the SPL and sound field generated. More developed the turbulent flow, more is the error in the calculation of the flow variables, and more is the error in the prediction of the sound field. The flow model as described in this research cannot simulate situations where the fluid is not always present in the domain or if the fluid is changing. In addition, the Navier Stokes equations require higher numerical approach to be solved efficiently. This is mainly due to the presence of a convective term that is highly non-linear. So, using the FEM as used in this model is not an efficient method. Instead, the FVM is more suitable to get a more accurate development of the turbulent flow.

6.4 MATLAB Model Limitations

The main goal of the MATLAB model was to understand the formulation of the Finite Element matrix equation and to verify the COMSOL model results by comparing them with the self-developed FE model results. For these reasons, the FE model developed was not a high-fidelity model. So, the modeling procedure and the FE model has many limitations.

First, four triangular elements were used to the discretize the model in Joule Heating and twelve rectangular elements were used to discretize the model in Heat Transfer physics. The number of elements used to discretize the domain are small for the described simplified CNT speaker model. This will result in what is known as discretization error. Discretization error occurs when transforming the physical continuous domain into a finite element discrete domain. The nodes of the elements discretize the domain and the unknown

variables are calculated primarily at the nodal points. The four elements selected can result in spatial aliasing of the solution over the target boundary. The value of the variables calculated over the desired domain can be different from the actual distribution due to absence of a well-defined mesh grid. This can result in an incorrect distribution of the selected variable over the domain. The generated error can propagate when the calculated variable is used as input in the further FE models.

Second, the shape function used to interpolate the data between the nodal points is linear for the FE models. However, this can create error in the resolution of the variable over the domain. Higher order shape functions like quadratic or cubic provide a higher resolution interpolation of the variable over the specified domain. In the FE model developed in this research, the linear shape function will result in error because the temperature, electric potential and thermoacoustic variables vary in a complex fashion over the CNT film surface. This limits the model's ability to accurately predict the variation of these variables.

Third, the mesh convergence was not checked for the FE models. Mesh convergence is a very important step that determines the number of elements required to correctly discretize and resolve the variable variation over the domain. It also serves as a check that the solution of the FE model is remains the same even after changing the size of the mesh. Performing mesh convergence makes the model more robust when simulation is performed at multiple frequencies. If this FE model is to be used in the future, the mesh convergence must be verified. The FE model was solved for two frequencies: 100Hz and 160Hz. Even though the results at those frequencies were in correlation with the COMSOL model results, it

cannot be said with certainty that the model would give comparable results at other frequencies.

6.5 COMSOL Limitations

The COMSOL models for simulating the SPL, flow and optimization have been validated using experimental and analytical results. However, all the models have certain limitations. They must be identified and kept in mind when attempting to simulate the performance of the CNT speaker. The limitations of the models are as follows:

1. In the Joule Heating model, the Terminal boundary condition is available only for the domain and not for the boundary. This limits the model when the electrodes need to be modeled as a boundary and not domain.
2. There is no way to define the resistance of the CNT film in the Joule Heating model. The resistance is calculated based on the electrical material properties defined for the CNT film. This limits the model as the CNT film resistance is dependent on the area of the film.
3. In the Thermoviscous Acoustics model, mesh element size required for the simulating the thermal and viscous boundary layers are dependent on their thickness. An adaptive mesh is required for this purpose. Adaptive mesh is effective, but it increases the simulation time significantly compared to standard mesh. The adaptive mesh algorithm used in COMSOL is not computationally efficient.

4. The Joule Heating and Thermoviscous Acoustics models cannot be coupled together, and two separate models are required. Using two models is fine but it really limits the modeling process as the two models cannot be run simultaneously.
5. In the Thermoviscous Acoustics model, the procedure to model the CNT film as an acoustically transparent material is not known. This a big limitation as the model is no longer the same as the actual prototype. Even after providing double input power, there is some error as the actual CNT film area is not exactly replicated in the model.
6. In the flow model, the SPL generated by the CNT film, which is radial in nature must be modeled from the Thermoviscous Acoustic model result. There is no way to couple the Thermoviscous Acoustic and flow models and this a major limitation. The conversion of the sound field generated by the CNT speaker as an acoustic source in the flow model introduces some error in the amplitude and phase.
7. In the optimization model, the solver checks the estimated error with the relative tolerance, or the number of iterations specified. When either condition is satisfied, the solver stops and gives the last iteration as the desired solution. This is a limitation because more combinations of the control variables might be possible that give a better performance of the CNT speaker.

6.6 Future Work Recommendations

The COMSOL model for simulating the SPL of the CNT speaker is a preliminary baseline model. It will help to improve the performance of the CNT speaker without having to

manufacture and test every single design iteration. More work can be done to improve the COMSOL model.

There is scope for making this model more accurate in terms of the CNT film representation. CNT films are acoustically transparent, and this property needs to be modeled in COMSOL. This will make sure that the total CNT film area used in the actual prototype is the same in the COMSOL model.

Another point of improvement is the definition of material properties of the CNT film – heat loss due to conduction, convection and radiation and the heat capacity per unit area. These properties are defined as variables in the model, and they can be defined more suitably as material properties in the model. Finding a way to link these material properties to the physics in COMSOL will make sure their effect is accurately replicated as proved in analytical solutions.

The heat transfer mechanism of the CNT speakers is extremely important and must be set up accurately in COMSOL. The models developed in this research use the built-in physics to model this process. However, the accuracy, and reliability of these models can be improved by developing a method to model the heat transfer mechanism in a more defined way compared to the actual physical mechanism.

The models developed in this research are not limited to CNT speakers. CNT films are not the only materials that generate sound using the thermoacoustic effect. Graphene, a two-dimensional material is also capable of generating sound using the thermoacoustic effect. The Thermoviscous Acoustic model can be expanded to simulate the performance of a

speaker made using Graphene. It can be used to predict the performance of the Graphene based transducers using the coupling between the Thermoviscous and Pressure Acoustics.

The flow model can be used in different applications that involve medium flow. The CFD part of the model is focused on determination of the flow variables and can be applied to any system with flow, irrespective of the medium. Some examples are HVAC systems, flow-induced noise for pumps, high pressure release valves. The CFD modeling procedure developed in this research can be extrapolated with modifications to the geometry, boundary conditions, mesh elements and shape functions to simulate the flow variables in the above-mentioned systems. The flow variables can be mapped on the acoustic mesh and the acoustic performance of the noise control system can be simulated using the modeling procedure used for the CNT speaker.

The optimization model is not limited to the CNT speaker. It can be used for almost any type of transducer, irrespective of the sound generation principle. The only thing that would probably remain the same is the definition of the objective function. In the model developed in this research, the optimization objective is defined using the SPL values measured by probes placed at the desired location in the target domain. The same principle can be used irrespective of the transducer. The main point to remember is location at which the SPL is important and place the probes at those locations. For example, the tailpipe outlet dimensions of the automotive exhaust can be optimized to reduce the radiated SPL in the ambient environment. In this optimization model, the possible control variables would be diameter of the tailpipe outlet and the probes would be placed in air domain that is modeled

surrounding the tailpipe outlet. Another application of the optimization method would be the optimization of the tweeter waveguide to get a flat SPL response of the tweeter.

Finally, the coaxial design developed for the automotive exhaust noise cancellation is not fixed for usage with CNT film. This design can be used with other transducers such as piezo-electric in a similar way. A comparison can be made between the coaxial CNT speaker and other coaxial speakers to understand the performance difference, advantages, and shortcomings of those speakers. In addition to piezo-electric transducers, conventional loudspeakers (particularly micro drivers) can be used in the coaxial design for noise cancellation and sound generation.

7 Reference List

[1] M.R. Bai and H.N. Lin, "Comparison of Active Noise Control Structures in the presence of acoustical feedback by using the H_∞ synthesis technique", *Journal of Sound and Vibration* 206(4), 1997.

[2] Y.B. Zalte and M.J. Sature, "Transmission Losses in Simple Expansion Chamber of Reactive Muffler Analysis by Numerical & Experimental Method", *International Engineering Research Journal*, 1933-1939.

[3] A.I. El-Sharkawy and Ali H. Nayfeh, "Effect of an expansion chamber on the propagation of sound in circular ducts", *Journal of Acoustical Society of America* 63(3), doi: 10.1121/1.381792.

[4] Marehalli Prasad and B. Rajavel, *Acoustical and Noise Control Engineering for K-12*.

[5] Sujata Sushant Tambe and Prof. Lagdive, "Analysis of Reactive Muffler by Experimental and Numerical Method", *Journal of Emerging Technologies and Innovative Research",*4(08), August 2017.

[6] S. N.Y. Gerges, F. A. Thieme, J.L. Bento Coelho, J. P. Arenas, "Muffler Modeling by Transfer Matrix Method and Experimental Verification", *The Journal of the Acoustical Society of America",* XXVII(2), April 2005.

[10] Noise Reduction for Internal Combustion Engine, file:///D:/dissertation/dissertation_research_papers/10.htm.

[11] David Neighuk and Abhinav Prasad, "Effect of Length and Porosity on the Acoustic Performance of Concentric Tube Resonators", *COMSOL Conference Proceedings,* 2015.

[12] David Neighuk, Abhinav Prasad, M.L. Munjal, "Friction factor for perforated pipes", *COMSOL Conference Proceedings,* 2015.

[13] Orcun Saf and Haluk Erol, "On acoustics and flow behaviour of the perforated mufflers", *17th International Congress on Sound and Vibration*, ICSV 2010. 2, 2010.

[14] Ezzeddin Milad and Mohamed Jolgaf, "Acoustic Analysis of a Perforated-pipe Muffler using ANSYS", *Zawia University Bulletin*, 19, 2017.

[15] Jan Bräuer, "Acoustic modelling of perforations in automotive exhaust mufflers using 3D cells", *Diploma Thesis TU Graz,* 2011.

[16] F.D. Deniaa, A. Selamet, F.J. Fuenmayor, R. Kirby, "Acoustic attenuation performance of perforated dissipative mufflers with empty inlet/outlet extensions", *Journal of Sound and Vibration* 302, 2007.

[17] Sudarshan Dilip Pangavhane, Amol Bhimrao Ubale, Vikram A Tandon, Dilip R Pangavhane, "Experimental and CFD Analysis of a Perforated Inner Pipe Muffler for the Prediction of Backpressure", *International Journal of Engineering and Technology* 5(5), October 2013.

[18] David Neighuk, Abhinav Prasad, M.L. Munjal, "Pressure Drop Characteristics of Perforated Pipes with Particular Application to the Concentric Tube Resonator", 2015, 10.4271/2015-01-2309.

[19] Daniel Potente, "General design principles for an automotive muffler", *Proceedings of ACOUTICS Australian Acoustical Society,* November 2005.

[20] D.W. Herrin, "Design of Mufflers and Silencers", *Department of Mechanical Engineering – Noise and Vibration Short Course".*

[21] P.Siva Kumar, "Design and construction of a reactive type muffle for a formula student vehicle", *"International Journal of Mechanical Engineering and Technology"* 9(5), May 2018.

[22] Jie Yao, Zhao-Xiang Deng, Pei-Ran Li, and Liang Yang, "Research on Pressure Loss for the reverse-flow extended-tube muffler", *International Conference on Artificial Intelligence and Computational Intelligence,* 2011.

[23] Pradyumna Saripalli, K. Sankaranarayana, "CFD Analysis on Flow Through a Resistance Muffler of LCV Diesel Engine", *International Journal of Science, Technology and Society* 3(4), 2015.

[24] Yunshi Yao, Shaodong Wei, Jinpeng Zhao, Shibin Chen, Zhongxu Feng and Jinxi Yue, "Experiment and CFD Analysis of Reactive Muffler" *Research Journal of Applied Sciences, Engineering and Technology* 6(17), 2013.

[25] Yunshi Yao, Shaodong Wei, Jinpeng Zhao, Shibin Chen, Zhongxu Feng, Jinxi Yue, "Experiment and CFD Analysis of Reactive Muffler", *Research Journal of Applied Sciences, Engineering and Technology* 6, 2013.

[26] Suyog Mane, "CFD analysis of backpressure of reactive muffler", *International Journal of Innovations in Engineering Research and Technology* 3(12), 2016.

[27] Liu Lianyun, Zhi-yong Hao, Chi Liu, "CFD analysis of a transfer matrix of exhaust muffler with mean flow and prediction of exhaust noise", *Journal of Zhejiang University SCIENCE,* 2012.

[28] Sileshi Kore, Abudlkadir Aman and Eddesa Direbsa, “Performance evaluation of reactive muffler using CFD”, *Journal of EEA* 28, 2011.

[29] D. Tutunea, M.X. Calbureanu and M. Lung, “The computational fluid dynamics (CFD) study of fluid dynamics performances of a resistance muffler”, *International Journal of Mechanics* 4(7), 2013.

[30] Ira Dyer, “Noise Attenuation of Dissipative Mufflers”, *Noise Control* 2, 1956.

[31] Iljae Lee, “Acoustic characteristics of perforated dissipative and hybrid silencers”, *Doctoral Thesis – The Ohio State University,* 2005.

[32] Ray Kirby, “Transmission loss predictions for dissipative silencers of arbitrary cross section in the presence of mean flow”, *The Journal of the Acoustical Society of America* 114(200), 2003.

[33] Ujjal Kalita, Abhijeet Pratap, Sushil Kumar, “Absorption Materials Used in Muffler A Review”, *International Journal of Mechanical and Industrial Technology* 2(2), October 2014 – March 2015.

[34] Jorge P. Arenas and Malcolm J. Crocker, “Recent Trends in Porous Sound-Absorbing Materials”, *Sound and Vibration*, 2010.

[35] H. P. Tang, et al., “Sound Absorption Characters of Metal Fibrous Porous Material,” in Porous Metals and Metallic Forms, *L. P. Lefebvre, J. Banhart, and D. C. Dunand, Eds.), DEStech Publications, Lancaster*, 2007.

[36] M. Schaeffer, and P. Colombo, “Cellular Ceramics: Structure, Manufacturing, Properties and Applications”, *Wiley-VCH, Wenham*, 2005.

[37] ULTRAMET - Refractory Open-Cell Foams: Carbon, Ceramic, and Metal http://www.ultramet.com / refractoryopencells_noise.

[38] ERG: Duocel® - Silicon Carbide Foam Properties http://www.ergaerospace.com/SiC-properties.htm.

[39] Jigar H. Chaudhri, *Int. Journal of Engineering Research and Applications* Vol. 4, Issue 1(Version 2), www.ijera.com ISSN : 2248-9622, January 2014.

[40] Jayashri P. Chaudhari, Amol B. Kakade, “Design, Development and Analysis of Absorptive Muffler with Ammonia Pulsator for IC Engine”, *International Engineering Research Journal.*

[41] P. B. Bhadke, K. A. Mahajan, “Analysis of Absorptive Muffler for Inductive & Resistive Damping”, *IOSR Journal of Mechanical and Civil Engineering.*

[42] Pradyumna Saripalli, K. Sankaranarayana, "CFD Analysis on Flow Through a Resistance Muffler of LCV Diesel Engine", *International Journal of Science, Technology and Society* 3(4), 2015.

[43] Bhagat Shailender, A. Rajni Kanth, "Computational Fluid Dynamics Analysis Of A Resistance Muffler", *International Journal of Innovative Technology and Research* 5(3), April – May 2017.

[44] S.Rajadurai, Suraj Sukumaran, P. Madhusudhanan, "CFD Analysis for Flow through Glass Wool as Porous Domain in Exhaust Muffler", *International Journal of Innovative Science, Engineering & Technology* 1(7), September 2014.

[45] Sushovan Chatterjee, "Computational Fluid Dynamic Analysis of the exhaust gas fow through absorptive and reactive mufflers: some case studies", *Proc IMechE Part D: J Automobile Engineering* 231(11), 2017.

[46] Lian-yun LIU, Zhi-yong HAO, Chi LIU, "CFD analysis of a transfer matrix of exhaust muffler with mean flow and prediction of exhaust noise", *Journal of Zhejiang University-SCIENCE A (Applied Physics & Engineering)* 13(9), 2012.

[47] Yogesh, Anandkumar S Malipatil, "CFD Analysis of a Resistance Muffler", *International Journal for Research in Applied Science & Engineering Technology* 5(XII), December 2017.

[48] Sen M. Kuo and Dennis R Morgan, "Active Noise Control: A tutorial review", *Proceeding of the IEEE* 87(6), June 1999.

[49] Sensory Systems/Control Systems, https://en.wikibooks.org/wiki/Sensory_Systems/Control_Systems

[50] B. Chaplin, "The cancellation of repetitive noise and vibration," *Proc. Inter-noise,* 1980.

[51] Feed Forward Control, https://en.wikipedia.org/wiki/Feed_forward_(control)

[52] S.M. Kuo and D. Vijayan, "Adaptive feedback active noise control," *Proc. Noise-Con*, 1994.

[53] Bernard Widrow and Marcian E. Hoff, "Adaptive Switching Circuits", https://isl.stanford.edu/~widrow/papers/c1960adaptiveswitching.pdf.

[54] LMS Tutorials, http://homepages.cae.wisc.edu/~ece539/resources/tutorials/LMS.pdf.

[55] Xu Wang, "Method of Steepest Descent and its Applications" IEEE Microwave Wireless Components Lett. 12, 2008.

[56] Saurabh Prasad, and Bhalchandra Godbole, “Optimization of LMS Algorithm for System Identification”, 2017.

[57] B. Widrow, J. McCool and M. Ball, "The complex LMS algorithm," *Proceedings of the IEEE* 63(4), April 1975.

[58] R. H. Kwong and E. W. Johnston, "A variable step size LMS algorithm,” *IEEE Transactions on Signal Processing* 40(7), July 1992.

[59] S. J. Elliott and T. J. Sutton, "Performance of feedforward and feedback systems for active control," *IEEE Transactions on Speech and Audio Processing* 4(3), May 1996.

[60] Muhammad Akhtar, Masahide Abe, M. Kawamata, “On Active Noise Control Systems With Online Acoustic Feedback Path Modeling. Audio, Speech, and Language Processing”, *IEEE Transactions on. 15,* 2007.

[61] Muhammad Akhtar, Muhammad Tufail, M. Abe, M. Kawamata, “Acoustic feedback neutralization in active noise control systems” *IEICE Electronics Express. 4,* (2007).

[62] Suman Bala Behera, Debi Prasad Das, Nirmal Kumar Rout, “Nonlinear feedback active noise control for broadband chaotic noise”, *Applied Soft Computing* 15, 2014.

[63] Patra, J.C., Pal, R.N., Chatterji, B.N., Panda, G, “Identification of nonlinear dynamic systems using functional link artificial neural networks”, *IEEE Transactions on Systems, Man, and Cybernetics, Part B: Cybernetics* 29 (2), 1999.

[64] Fengyan An, Yin Cao, Ming Wu, Hongling Sun, Bilong Liu, and Jun Yang, “Robust Wiener controller design with acoustic feedback for active noise control systems”, *The Journal of the Acoustical Society of America* 145(EL291), 2019.

[65] Shuichi Adachi, Hisashi Sano, “Modeling, Control and Experiment of a Feedback Active Noise Control System for Free Sound Fields”, *JSME International Journal Series C Mechanical Systems, Machine Elements and Manufacturing* 45(2), June 25, 2004.

[66] Kambiz C. Zangi, “Optimal Feedback Control Formulation of the Active Noise Cancellation Problem: Pointwise and Distributed”, *RLE Technical Report, Research Laboratory of Electronics, Massachusetts Institute of Technology,* May 1994.

[67] Sen Kuo, Xuan Kong, Woon-Seng Gan, “Applications of adaptive feedback active noise control system”, *Control Systems Technology, IEEE Transactions on. 11,* 2003.

[68] Naitik Nakrani, Niteen Patel, “Feed-forward and Feedback active noise control system using FxLMS algorithm for narrowband and broadband noise”, *International Conference on Communication Systems and Network Technologies,* 2012.

[69] Lifu Wu, Xiaojun Qiu, Yecai Guo, “A simplified adaptive feedback active noise control system”, *Applied Acoustics* 81, 2014.

[70] Sigurd Skogestad and Ian Postlethwaite, “Multivariable Feedback Control – Analysis and Design”, *IEEE Control Systems Magazine,* February 2007.

[71] Jan Lunze, “Robust Multivariate Feedback Control”, *Prentice Hall Publications*, December 1989.

[72] Jinsiang Shaw, “Design and Control of Active Muffler In Engine Exhaust Systems”, *WSEAS Transactions on Mathematics. 1,* 2002.

[73] “Active exhaust noise cancellation”, *The Clemson University Vehicular Electronics Laboratory,*
https://cecas.clemson.edu/cvel/auto/systems/active_exhaust_noise_cancellation.html.

[74] K. Li, D. Yang, S. Zheng, X. Lian and T. Takeharu, "Active noise control for vehicle exhaust noise reduction," *Tsinghua Science and Technology* 8(5), Oct. 2003.

[75] “Acoustic Analysis of an Active Noise Control Exhaust System on HiL Test bench”, https://docplayer.net/42694765-Acoustic-analysis-of-an-active-noise-control-exhaust-system-on-hil-test-bench.html.

[76] R.R. Leitch and M.O. Tokhi, “Active noise control systems”, *IEE Proceedings A (Physical Science, Measurement and Instrumentation, Management and Education, Reviews)* 134(6), 1987.

[77] A. M. Alvarez and R. R. Leitch, "Active attenuation of acoustic noise using adaptive algorithms,” *IEEE International Symposium on Circuits and Systems, Espoo, Finland,* Vol. 1, 1988.

[78] A.M. Alvarez and P.M. Grant, “Comparison of frequency domain adaptive equalizer structures”, *IASTED* 85, 1985.

[79] M.D. Croker, “The active control of internal combustion engine exhaust noise”, *Inter-noise 83. Proceedings of 1983 International Conference on Noise Control* Vol. I, 1983.

[80] Tanaka Takeharu, Li Keqiang, “Development of an active muffler for medium-duty diesel vehicles considering thermal influence and control trackability” *Noise Control Engineering Journal* 51(2), 2003.

[81] Bai, M. R., and Lin, Z. (October 1, 1998). "Active Noise Cancellation for a Three-Dimensional Enclosure by Using Multiple-Channel Adaptive Control and H∞ Control", *ASME. J. Vib. Acoust* 120(4), October 1998.

[82] “Active noise cancellation applied to diesel exhaust”, *EDN,* https://www.edn.com/active-noise-cancellation-applied-to-diesel-exhaust/.

[83] Douglas R. Browning, Randolph N.J., Michael A. Zuniga, “Active noise cancellation system for automotive mufflers”, US Patent 5325438, Filed Feb 1, 1993, and issued June 28, 1994.

[84] KIM Heung-Seob, HONG Jin-Seok, OH Jae-Eung, “Active noise control system with the active muffler in automotive exhaust systems”, *JSME International Journal Series C Mechanical Systems, Machine Elements and Manufacturing* 41(2), 1998.

[85] R Boonen.; P Sas, “Development of an active exhaust silencer for internal combustion engines using feedback control”. *SAE*, 1999-107.

[86] J. Krueger, M. Pommerer, and R. Jebasinski, "Lightweight Active Exhaust Silencers for Passenger Vehicles," *SAE Technical Paper* 2010-01-1425, 2010.

[87] P. Krause, H. Weltens, and S. Hutchins, "Advanced Design of Automotive Exhaust Silencer Systems," *SAE Technical Paper* 922088, 1992.

[88] Jan Kruger, Michael Pommerer, Matthias Conrath, “Active exhaust silencers from noise level reduction to sound design”, *ATZ Worldw* 115, 2013.

[89] J. Shaw, “Adaptive control for sound and vibration attenuation: a comparative study”, *Journal of Sound and Vibration* 235(4), 2000.

[90] Jian Da-Wu and Mingsian R. Bai, “Digital signal processor implementation of active noise control systems for broadband noise cancellation in engine exhaust system”, *Jpn. Journal of Applied Physics* Vol 39, 2000.

[91] Advanced Exhaust Silencing, *Automotive Engineering,* February 1993.

[92] X. Yu, R. Rajamani, K.A. Stelson, T. Cui, “Carbon nanotube-based transparent thin film acoustic actuators and sensors”, *Sensors and Actuators A: Physical* 132(2), 2006.

[93] Lin Xiao, Zhuo Chen, Chen Feng, Liang Liu, Zai-Qiao Bai, Yang Wang, Li Qian, Yuying Zhang, Qunqing Li, Kaili Jiang, and Shoushan Fan, “Flexible, stretchable, transparent carbon nanotube thin film loudpseakers”, *Nano Letters* 8(12), 2008.

[94] H.D. Arnold and I.B. Crandall, “The thermophone as a precision source of sound” *American Physical Society,* 1917, https://doi.org/10.1103/PhysRev.10.22.

[95] Mikhail E. Kozlova, Carter S. Haines, Jiyoung Oh, Marcio D. Lima, and Shaoli Fang, “Sound of carbon nanotube assemblies”, *Journal of Applied Physics* 106, 2009, https://doi.org/10.1063/1.3272691

[96] Katsunori Suzuki, Shingo Sakakibara, Morihiro Okada, Yoichiro Neo, Hidenori Mimura, Yoku Inoue and Toshihiro Murata, "Study of carbon nanotube web thermoacoustic loudspeakers" *Jpn. J. of Appl. Phys.* 50, 2011.

[97] Andrew R. Barnard, Timothy A. Brungart, Timothy E. McDevitt, David M. Jenkins, Richard I. Scott, "Background and development of a high powered carbon nanotube thin film loudspeaker", *41st International Congress and Exposition on Noise Control Engineering 2012, INTER-NOISE,* 2012.

[98] Ali A. Aliev, Marcio D. Lima, Shaoli Fang and Ray H. Baughman, "Underwater sound generation using carbon nanotube projectors", *Nano Letters* 10(7), 2010.

[99] Lin Xiao, Peng Liu, Liang Liu, Qunqing Li, Zhenghe Feng, Shoushan Fan, and Kaili Jiang, "High frequency response of carbon nanotube thin film speaker in gases", *Journal of Applied Physics* 110, 2011.

[100] Ali E Aliev 1, Nathanael K Mayo, Ray H Baughman, Dragan Avirovik, Shashank Priya, Michael R Zarnetske, John B Blottman, "Thermal management of thermoacoustic sound projectors using a free-standing carbon nanotube aerogel sheet as a heat source", *Nanotechnology* 25(40), October 2014.

[101] Andrew R. Barnard, Timothy A. Brungart, Timothy E. McDevitt, Ali E. Aliev, David M. Jenkins, Brian L. Kline and Ray H. Baughmang, "Advancement toward a high-power, carbon nanotube thin-film loudspeaker", *Noise Control Engineering Journal* 62(5), September – October 2014.

[102] T. Bouman, A. Barnard, J.. Alexander, "Continued drive signal development for the carbon nanotube thermoacoustic loudspeaker using techniques derived from the hearing aid industry", *SAE Technical Paper*, 2017.

[103] M. Asgarisabet, A. Barnard, T. Bouman, "Near field acoustic holography measurements of carbon nanotube thin film speakers", *Journal of Acoustic Society of America* 140(6), 2016.

[104] Sumio Iijima, "Helical microtubules of graphite carbon", *Nature* Vol. 354, November 1991.

[105] R.H. Baughman, A.A. Zakhidov and W.A. de Heer, "Carbon nanotubes – the route toward application", *Science* Vol. 297, August 2002.

[106] Mei Zhang, Shaoli Fang, Anvar A. Zakhidov, Sergey B. Lee, Ali E. Aliev, Christopher D. Williams, Ken R. Atkinson, Ray H. Baughman, "Strong, transparent, multifunctional, carbon nanotube sheets", *Science* Vol. 239, August 2005.

[107] Ken R. Atkinsona, Stephen C. Hawkinsa, Chi Huynha, Chris Skourtisa, Jane Daia, Mei Zhangb, Shaoli Fangb, Anvar A. Zakhidovb, Sergey B. Leeb, Ali E. Alievb, Christopher D. Williamsb, Ray H. Baughmanb, "Multifunctional carbon nanotube yarns and transparent sheets: fabrication, properties and applications", *Physics B* Vol. 394, 2007.

[108] Ali E. Aliev, Csaba Guthy, Mei Zhang, Shaoli Fang, Anvar A. Zakhidov, John E. Fischer, Ray H. Baughman, "Thermal transport in MWCNT sheets and yarns", *Carbon* Vol. 45, 2007.

[109] P. Eklund, P. Ajayan, R. Blackmon, A. John Hart, J. Kong, B. Pradhan, A. Rao, A. Rinzler, "International assessment of research and development of carbon nanotube manufacturing and applications", *World Technology Evaluation Center.*

[110] Ali E. Aliev, Jiyoung Oh, Mikhail E. Kozlov, Alexander A. Kuznetsov, Shaoli Fang, Alexandre F. Fonseca, Raquel Ovalle, Márcio D. Lima, Mohammad H. Haque, Yuri N. Gartstein, Mei Zhang, Anvar A. Zakhidov, Ray H. Baughman, "Giant-Stroke, Superelastic carbon nanotube aerogel muscles", *Science* Vol. 323, March 2009.

[111] Ali E Aliev, Marcio H Lima, Edward M Silverman and Ray H Baughman, "Thermal conductivity of multi-walled carbon nanotube sheets: radiation losses and quenching of phonon modes", *Nanotechnology* 21, 2010.

[112] Hao Chen, Ajit Roy, Jong-Beom Baek, Lin Zhu, Jia Qu, Liming Dai, "Controlled growth and modification of vertically-aligned carbon nanotubes for multifunctional applications", *Materials Science and Engineering: R: Reports* 70(3-6), 2010.

[113] Michael B. Jakubinek, Mary Anne White, Ge Li, Chaminda Jayasinghe, Wondong Cho, Mark J. Schulz, Vesselin Shanov, "Thermal and electrical conductivity of tall, vertically aligned carbon nanotube arrays", *Carbon* 48(13), 2010.

[114] M.S. Dresselhaus, "NT10: Recent Advances in Carbon Nanotube Science and Applications", *ACSNano* 4(8), 2010.

[115] Michael B. Jakubinek, Michel B. Johnson, Mary Anne White, Chaminda Jayasinghe, Ge Li, Wondong Cho, Mark J. Schulz, Vesselin Shanov, "Thermal and electrical conductivity of array-spun multi-walled carbon nanotube yarns", *Carbon* 50(1), 2012.

[116] Kaili Jiang , Jiaping Wang , Qunqing Li , Liang Liu , Changhong Liu , and Shoushan Fan, "Superaligned carbon nanotube arrays, films, and yarns: a road to applications", *Adv. Materials* Vol. 23, 2011.

[117] Albert G. Nasibulin, Antti Kaskela Kimmo Mustonen, Anton S. Anisimov, Virginia Ruiz, Samuli Kivisto, Simas Rackauskas, Marina Y. Timmermans, Marko Pudas, Brad Aitchison, Marko Kauppinen, David P. Brown, Oleg G. Okhotnikov, and Esko I. Kauppinen, "Multifunctional free-standing single-walled carbon nanotube films", *ACSNano* 5(4), 2011.

[118] Carlo Rainieri, G. Fabbrocino, Yi Song, V. Shanov, "CNT composites for SHM: A literature review", *International Workshop Smart Materials, Structures and NDT in Aerospace Conference,* November 2011.

[119] Jan-Hendrik Pöhls, Michel B. Johnson, Mary Anne White, Rachit Malik, Brad Ruff, Chaminda Jayasinghe, Mark J. Schulz, Vesselin Shanov, "Physical properties of carbon nanotube sheets drawn from nanotube arrays", *Carbon* 50(11), 2012.

[120] S. Kessler, G. Thomas, M. Borgen, C.T. Dunn, "Performance analysis for CNT-based SHM in composite structures", 2013.

[121] Vesselin Shanov, Wondong Cho, Rachit Malik, Noe Alvarez, Mark Haase, Brad Ruff, Nicholas Kienzle, Timothy Ochmann, David Mast, Mark Schulz, "CVD growth, characterization and applications of carbon nanostructured materials", *Surface and Coatings Technology* Vol. 230, 2013.

[122] Jonghoon Bin, William S. Oates, and Kunihiko Tairac, "Thermoacoustic modeling and uncertainty analysis of two-dimensional conductive membranes", *Journal of Applied Physics* Vol. 117, 2015.

[123] Seyram Gbordzoe, Rachit Malik, Noe Alvarez, Robert Wolf and Vesselin Shanov, "Flexible low-voltage carbon nanotube heaters and their applications", *Advances in Carbon Nanostructures* October 2016.

[124] M.M. Thiery, "Advanced uses for carbon nanotubes: a spherical sound source and hot-films as microphones", *Master's Thesis Michigan Technological University,* 2017.

[125] Lin Xiao, Zhuo Chen, Chen Feng, Liang Liu, Zai-Qiao Bai, Yang Wang, Li Qian, Yuying Zhang, Qunqing Li, Kaili Jiang, and Shoushan Fan, "Flexible, stretchable, transparent carbon nanotube thin film loudpseakers", *Nano Letters* 8(12), 2008.

[126] Finite Element Method, https://en.wikipedia.org/wiki/Finite_element_method.

[127] Introduction to finite element analysis (FEA) or finite element method (FEM), https://www.engr.uvic.ca/~mech410/lectures/FEA_Theory.pdf.

[128] O. Vasile and G-R Gillich, "Finite Element Analysis of acoustic pressure levels and transmission loss of a muffler", 2013.

[129] Abdullah A. Dhaiban, M-Emad S. Soliman, and M.G. ElSebaie, “Finite element simulation of acoustic attenuation performance of elliptical muffler chambers”, *Journal of Engineering Sciences* 39(6), November 2011.

[130] Jun Fu, Minghui Xu, Zengfeng Zhang, Wenjie Kang and Yong He, “Muffler structure improvement based on acoustic finite element analysis”, *Journal of Low Frequency, Noise, Vibration and Active Control* 38(2), 2019.

[131] A.G. Antebas, F.D. Denia, A.M. Pedrosa, F.J. Fuenmayor, “A finite element approach for the acoustic modeling of perforated dissipative mufflers with non-homogeneous properties”, *Mathematical and Computer Modelling* 57(7-8), 2013.

[132] A. Patil, P. Sajanpawar and V. Masurekar, “Acosutic three dimensional finite analysis of a muffler”, *SAE Transactions Journal of Passenger Cars* 105(6), 1996.

[133] F.D. Denia, J. Albelda, and F.J. Fuenmayor, “Acoustic Behaviour of Elliptical Chamber Mufflers,” *Journal of Sound and Vibration*, Vol. 241, 2001.

[134] E. Bécache, A.S. Bonnet-Bendhia, R. Ben Fatma, D. Drissi, N. Gmati, “Numerical simulation of exhaust muffler: a homogenized finite element method”, https://www.cari-info.org/actes2006/78.pdf.

[135] Xiaodong Li, Xintan Ma, “Mathematical Model and Finite Element Analysis of Acoustics Performance of Composite Exhaust Muffler”, *Applied Mechanics and Materials* Vol. 651-653, 2014.

[136] D. F. ROSS, "A finite element analysis of perforated component acoustic system", *Journal of Sound and Vibration* Vol. 79, 1981.

[137] Boundary Element Method, https://en.wikipedia.org/wiki/Boundary_element_method.

[138] Y. Liu, “An introduction to the Boundary Element Method and its applications in engineering”, http://www.yijunliu.com/Research/BEM_Introduction.pdf.

[139] M. Costabel, “Principles of Boundary Element Methods”, *Technische Hochschule Darmstadt Lectures in Finite Element in Physics*, September 1986.

[140] A. Doijode O. Gadre, “Transmission losses in reactive muffler analysis by boundary element method, numerical method and experimental method”, *IJRSI* II(VII), July 2015.

[141] T.W. Wu and C.Y.R. Cheng, “Boundary Element Analysis of Reactive Mufflers and packed silencers with catalyst converters”, *Electronic Journal of Boundary Elements* 1(2), 2003.

[142] T.W. Wu and P. Zhang and C.Y.R. Cheng, “Boundary Element Analysis of Mufflers with an improved method for deriving the four-pole parameters”, *Journal of Sound and Vibration* 217(4), 1998.

[143] Chao-Nan Wang, Chuan-Cheung Tse and Yih-Nan Chen, “Analysis of three dimensional mufflers with boundary element method”, *Applied Acoustics* 40(2), 1993.

[144] Zhe Cui and Yun Huang, “Boundary Element Analysis of Muffler Transmission Loss with LS-Dyna”, *12th International LS-Dyna User Conference.*

[145] T.W. Wu, P. Zhang, C.Y.R. Cheng, “Boundary element analysis of mufflers with an improved four-pole method” Vol. 24, 1997.

[146] T. W. Wu, G. C. Wan, “Muffler performance studies using a direct mixed-body boundary element method and a three-point method for evaluating transmission loss”, *Journal of Vibration and Acoustics, ASME Transactions,* 1996.

[147] T. Tanaka, T. Fujikawa, T. Abe and H. Utsuno. “A method for the analytical prediction of insertion losses of a two-dimensional muffler model based on the transfer matrix derived from the boundary element method*”*, *Trans. ASME*, **107**, 1985.

[148] A.F. Seybert, C.Y.R. Cheng, “Application of the boundary element method to acoustic cavity response and muffler analysis”, *J. Vib. Acoust. Stress, and Reliab.* 109(1), January 1987.

[149] J.C. Park, S.M. Wang, J.H. Kang, D. Kwon, “Boundary element analysis of the muffler for the noise reduction of the compressors”, *International Compressor Engineering Conference Purdue University,* 2004.

[150] M. Asgarisabet, A. Barnard, “Multi-physics simulation of ultra-lightweight carbon nanotube speakers”, *INTER-NOISE and NOISE-CON Congress and Conference Proceedings* 254(2), 2017.

[151] M. Asgarisabet, A. Barnard, S. Prabhu, “An experimentally validated electrical-thermal-acoustic model of non-planar carbon nanotube thermophones”, *The Journal of the Acoustical Society of America* 142(4), 2017.

[152] M. Asgarisabet, A. Barnard, “Multi-physics modeling of conformal, solid state, and thin-film thermophones”, *The Journal of the Acoustical Society of America* 140(4), 2016.

[153] Muffler Transmission Loss – A Simple Expansion Chamber, http://ansol.us/Products/Coustyx/Validation/MultiDomain/Muffler/SimpleExpansionChamber/Downloads/dataset_description.pdf.

[154] A. Pratap, U. Kalita, S. Kumar, "Effect of perforated tube on transmission loss of muffler – a review", *International Journal of Engineering Research and General Science* 3(3), May-June 2015.

[155] Standing Wave Patterns, https://www.physicsclassroom.com/class/sound/Lesson-4/Standing-Wave-Patterns.

[156] Robert Bernhard, "Acoustic finite element analysis of duct boundaries", *Dissertation Iowa State University*, 1982.

[157] Ali A. Aliev, Marcio D. Lima, Shaoli Fang and Ray H. Baughman, "Underwater sound generation using carbon nanotube projectors", *Nano Letters* 10(7), 2010.

[158] Lin Xiao, Zhuo Chen, Chen Feng, Liang Liu, Zai-Qiao Bai, Yang Wang, Li Qian, Yuying Zhang, Qunqing Li, Kaili Jiang, and Shoushan Fan, "Supporting Online Materials for Flexible Stretchable Transparent Magnet-Free Carbon Nanotube Thin Film Loudpseakers".

[159] S. Prabhu, A. Barnard, "Design and Characterization of an enclosed coaxial carbon nanotube speaker", *JASA Express Letters* 147(4), 2020.

[160] S. Prabhu, A. Barnard, S. Senczyszyn, "Multi-Physics and CFD Analysis of an enclosed coaxial carbon nanotube speaker for automotive exhaust noise cancellation", *SAE Int. J. Adv. & Curr. Prac. in Mobility* 1(4), 2019.

[161] S. Prabhu, A. Barnard, "Active noise control of automotive exhaust noise using carbon nanotube speakers", *INTER-NOISE and NOISE-CON Proceedings,* 2017.

[162] S. Prabhu, A. Barnard, "COMSOL Model for an enclosed coaxial carbon nanotube speaker", *INTER-NOISE and NOISE-CON Proceedings,* 2018.

[164] M.S. Howe, "The damping of sound by wall turbulent shear layers", *J. Acoust. Soc. Am.* 98(3), September 1995.

[165] Lord Rayleigh, "Theory of Sound", *Dover New York* Vol. 2, 1945.

[166] A.D. Pierce, "Acoustics: an introduction to its principles and applications", *American Institute of Physics, New York,* 1989.

[167] J.N. Reddy, "An Introduction to the Finite Element Method", *McGraw Hill International Editions*, 2nd Edition, 1993.

[168] Nicolas Joly, "Finite Element Modeling of Thermoviscous Acoustics on Adapted Anisotropic Meshes: Implementation of Particle Velocity and Temperature Variation Formulation", *Acta Acustica United with Acustica,* Vol. 96, 2010.